NTNU

Norwegian University of
Science and Technology

Controllability Analysis of Ammonia Synthesis Loops

Rebecca Maria Brigitte Gullberg

Chemical Engineering and Biotechnology
Submission date: June 2018
Supervisor: Sigurd Skogestad, IKP
Co-supervisor: Vidar Alstad, Yara International ASA

Norwegian University of Science and Technology
Department of Chemical Engineering

Abstract

Present ammonia synthesis loops normally operate under stationary conditions. Generally, ammonia synthesis loops can be slow to ramp up and down due to manual mode operation. Furthermore, load disturbances are not rejected efficiently. The aim of this thesis is to study possible control strategies that can increase the flexibility of ammonia synthesis loops with respect to load changes.

A simplified model of the ammonia synthesis loop was developed with CasADi in MATLAB. The model captures the main dynamics associated with load variations. Dynamic open-loop simulations of the model were conducted to analyze when load reduction leads to instability. Instability, in the form of temperature oscillations in the reactor, was visible after a reduction in makeup gas of around 7 % from nominal operation.

Based on a dynamic step-response analysis, several control schemes were proposed. The two main control strategies investigated distinguish between operating the system at an open-loop (1) unstable or (2) stable operating point. Both control strategies are able to handle a load range of 30-100 % of nominal capacity. The first strategy only needs temperature control for stabilization. The latter strategy requires a more complex control scheme, with pressure control in addition to temperature control. The drawbacks associated with a more complex control scheme are considered to be outweighed by the benefits of operating at an open-loop stable operating point.

Sammendrag

Nåværende ammoniakksynteseanlegg opererer normalt under stasjonære forhold. Vanligvis foregår endringer i produksjonslast sakte på grunn av manuell regulering. Videre blir forstyrrelser i last ikke avvist effektivt. Formålet med denne oppgaven er å studere mulige reguleringsstrategier som kan øke fleksibiliteten til ammoniakksyntesen med hensyn til lastendringer.

En forenklet modell av ammoniakksyntesen ble utviklet med CasADi i MATLAB. Modellen fanger den viktigste dynamikken knyttet til lastningsvariasjoner. Dynamiske simuleringer av modellen ble utført for å analysere når lastningsreduksjon fører til ustabilitet. Ustabilitet, i form av temperaturoscillasjoner i reaktoren, var synlig etter en reduksjon i tilførsel av syntesegass på rundt 7 % fra nominell drift.

Basert på en dynamisk sensitivitetsanalyse ble flere reguleringsstrukturer foreslått. De to hovedstrategiene som ble undersøkt skiller mellom drift av systemet ved et åpen-sløyfe (1) ustabilt eller (2) stabilt driftspunkt. Begge reguleringsstrategier er i stand til å håndtere et lastningsområde på 30-100 % av nominell kapasitet. Den første strategien trenger bare temperaturregulering for stabilisering. Den sistnevnte strategien krever et mer komplekst reguleringsskjema, med trykkregulering i tillegg til temperaturregulering. Ulempene forbundet med et mer komplekst reguleringsskjema anses å være oppveid av fordelene ved drift ved et åpen-sløyfe stabilt driftspunkt.

Preface

This thesis concludes the master's degree program in Chemical Engineering at the Norwegian University of Science and Technology (NTNU). The work presented in this thesis was conducted during spring 2018 as a collaboration project between NTNU and Yara International ASA.

Acknowledgements are directed towards NTNU and Yara International ASA for the possibility to work on this project. First of all, I would like to my superviser Dr.Ing. Vidar Alstad[1] for his helpful guidance and for always being available whenever I needed advise. Further, I would like to thank Professor Sigurd Skogestad for his valuable insight and helpful discussions. I would also like to thank PhD candidate Julian Straus for his highly appreciated help and support during the model development process.

[1] Yara Technology Centre in Porsgrunn, Norway

Contents

List of Tables

List of Figures

List of Symbols

Symbol	Description	Unit
A	Heat transfer area	m^2
C^*	Heat capacity ratio	
$C_{p,cat}$	Heat capacity of gas	J/kg cat
$C_{p,gas}$	Heat capacity of gas	J/kmol gas
H_i	Henry's law coefficient	atm
K_c	Controller gain	
K_i	Vapor-liquid equilibrium constant	
K_{HX3}	Heat exchanger flow resistance	kmol/(s $\sqrt{\text{bar}}$)
K_{VLV1}	Valve flow resistance	kmol/(s $\sqrt{\text{bar}}$)
K_{eq}	Chemical equilibrium constant	
Q	Heat transfer duty	W
Q_{HX1}	HX1 heat duty	W
Q_{HX3}	HX3 heat duty	W
Q_{max}	Maximum possible heat transfer duty	W
R	Gas constant in reactor	J/(K mol)

Symbol	Description	Unit
R	Gas constant in separator	m^3 bar/(kmol K)
R	Gas constant in compressor	J/(K kmol)
SV	Space Velocity	h^{-1}
T	Temperature	°C
T_{sep}	Separator temperature	K
U	Heat transfer coefficient	W/(m^2 K)
V_{bed}	Volume of catalyst bed	m^3
V_{sep}	Separator volume	m^3
W	Compressor duty	W
W_{C1}	Compressor C1 power	W
W_{C2}	Compressor C2 power	W
X_{N_2}	Converison of nitrogen	
$\bar{u}$	Steady-state controller output	
$\boldsymbol{v}$	Process stream variable vector	
$\dot{n}$	Molar flow	kmol/s
$e(t)$	Error signal	
f	Catalyst activity factor	
k_1	Forward reaction rate constant	
k_{-1}	Reverse reaction rate constant	
m_{cat}	Mass of catalyst	kg
n_{sep}	Separator mass accumulation	kmol
ns	Number of reactor compartments	
p	Pressure	bar
p_i	Partial pressure	bar
p_i^{sat}	Saturation pressure	bar

Symbol	Description	Unit
p_{purge}	Purge pressure	bar
$p_{reactor}$	Reactor pressure	bar
p_{sep}	Separator pressure	bar
r_j	Reaction rate	kmol N_2/(kg cat h)
$r_{N_2,tot}$	Total reaction rate	kmol N_2/s
r_{N_2}	Reaction rate	kmol N_2/(kg cat s)
s	Separation coefficient	
t	Time	s
u	Controller output	
u_1	Split ratio, quench 1	
u_2	Split ratio, quench 2	
v_0	Volumetric flow rate	m^3/h
x_i	Mole fraction	
y_i	Mole fraction in vapor phase	
$y_m(t)$	Measured controlled value	
$y_{sp}(t)$	Set point	
z	Axial position along the reactor	
Greek letters		
ΔH_{rx}	Heat of reaction	J/kmol N_2
$\Delta H_{vap,NH_3}$	Heat of vaporization of ammonia	J/kmol
Δt	Sampling period	s
Γ	Dispersion coefficient	
$\boldsymbol{\nu}$	Stochiometric coefficient vector	
ϵ	Preheater effectiveness	
η_c	Isentropic efficency	

Symbol	Description	Unit
ν_i	Stochiometric coefficient	
ρ_{cat}	Catalyst bulk density	kg/m^3
τ_I	Integral time	s
Subscripts		
c	Cold stream	
h	Hot stream	
i	Chemical species index	
in	Inlet stream	
j	Reactor compartment index	
k	Sampling instant	
$makeup$	Makeup stream	
out	Outlet stream	
$preheat$	Stream sent to preheater	
$product$	Product stream	
$purge$	Purge stream	
$quench$	Cold quench stream	

Abbreviations

DAE Differential-Algebraic Equations

NMPC Nonlinear Model Predictive Control

NTU Number of Transfer Units

VPC Valve Position Controller

Chapter 1

Introduction

This chapter gives the background for this thesis. Previous work on this topic is introduced, followed by the scope of this work. Furthermore, the main structure of this thesis is explained.

1.1 Background

In current ammonia synthesis plants, safe operation of ammonia reactors proceeds at steady-state. Normally, ammonia synthesis loops are partially operated in manual mode, without an automatic control scheme that can reject disturbances in the feed stream. To avoid instability related to feed disturbances, ammonia reactors operate at higher temperatures than the optimal operating point. The optimal operating point is close to the limit of instability, whereas a higher reactor temperature provides a larger back-off from instability. Dynamic operation of industrial ammonia reactors is associated with the risk of reactor extinction and temperature oscillations (limit cycles). Reactor extinction can appear after a sudden drop in temperature, which results in low conversion rates and external heat is required in order to resume normal operation. Moreover, limit cycle behavior has been reported in ammonia reactors as a response to pressure and temperature disturbances, characterized by temperature oscillations that

can cause material damage to the reactor and the catalyst [1].

Optimizing ammonia production with respect to varying capacity will require a more flexible design than what is traditionally applied. The possible future transition to a higher degree of automatic control of ammonia synthesis reactors, opens up the opportunity for more flexible operation of ammonia synthesis loops. There has been an increased interest for small-scale ammonia plants that can periodically produce ammonia, depending on the availability of raw materials and the local demand. For example, a recent study by Reese et al. [2] investigates a small-scale ammonia plant driven by wind power.

1.2 Previous Work

Van Heerden [3] analyzed the steady-state stability of autothermal reactors and found that ammonia reactors have three steady-state operating points. The upper operating point has the highest inlet temperature and corresponds to the highest conversion of ammonia. The middle operating point is unstable, while the lowest operating point results in reactor extinction.

Stephens [4] further investigated van Heerden's findings, with both steady-state and dynamic simulations. His dynamic model includes both accumulation of heat in the catalyst and accumulation of synthesis gas in the loop. The steady-state stability margin was introduced as the distance between the upper and middle steady-state operating point. Based on the steady-state analysis, one would expect that the system is at the limit of instability when these operating points coincide. However, the dynamic simulations showed that the system becomes unstable even if the steady-state solution indicates that there is a stability margin. This result suggests that the steady-state analysis is insufficient.

An incident in an industrial ammonia synthesis reactor, where limit cycle behavior was observed, prompted further investigations of the system dynamics. The studied reactor design consists of three catalyst beds and an external heat exchanger. Part of the synthesis gas is preheated with the hot reactor effluent, while the rest is injected as cold quench flows in between the adiabatic catalyst beds. Several dynamic models have been

developed that are able to reproduce the temperature oscillations observed. Morud and Skogestad [1] developed a model for the given converter design. The reactor beds are described by mass and energy balances in the form of two partial differential equations. These equations are converted into a system of algebraic and ordinary differential equations by spatial discretization of the beds into 10 segments. The simulation results focus on the oscillatory behavior caused by disturbances in the reactor pressure. Naess et al. [5] were also able to reproduce the limit cycle phenomenon with the same reactor model in combination with a complete synthesis loop of heat exchangers, compressors and separators. Both Naess et al. and Morud and Skogestad suggested that feedback control should be implemented to manipulate the cold quench flows, in order to keep the reactor inlet temperature stable.

Moreover, Rabchuk et al. [6] [7] developed a model, which can be used to find the margin to instability with respect to current load, pressure and temperature. The model consists of a single dynamic catalyst bed and a static heat exchanger unit. In the reactor model, the mole balance and the energy balance are combined and discretized in space, which gives a set of ordinary differential equations. The mole balance is combined with the ideal gas law, eliminating temperatures along the reactor as states. Instead, the number of moles of the different species and the heat flow through the heat exchangers are kept as states. A similar model is found in the work of Jinasena et al. [8] [9], except that the reactor model consists of three reactor beds with explicit equations for the heat exchanger temperatures. Furthermore, Jinasena [9] investigated temperature dependent heat capacities and heat of reaction. The study shows that the oscillatory behavior is seen faster when temperature dependency is included. In both these models, the reactor pressure is assumed to be perfectly controlled and the simulations focus on the behavior of the system when there is a change in the inlet temperature.

In the study by Rovaglio et al. [10], two dynamic reactor beds are modeled in combination with a synthesis loop consisting of steady-state heat exchangers and separation units. Compared to previous work, a more complex catalyst bed model with radial flow was investigated. In addition, the ammonia converter configuration stands out from the other studies since only one quench flow can be manipulated. The simulation results showed that a more complete layout with mass recycle increases the systems sensitivity

to disturbances. The main recycle stream introduces the snowball effect, where small disturbances in the inlet stream leads to large deviations in the reactor conditions. Limit cycle behavior was detected for temperature, pressure and H_2/N_2 ratio variations. A control strategy for the considered synthesis loop configuration is suggested, which is able to prevent both snowball effects and undesirable oscillations. The inlet temperatures to the catalyst beds are pointed out as the most important controlled variables for safe operation, which are controlled by manipulating the amount of cold synthesis gas sent directly to the converter. The heat duty of a heat exchanger downstream the reactor is also adjusted to help maintain stable inlet temperatures. Furthermore, the recycle flow is controlled in order to avoid snowball effects. Finally, dynamic simulations demonstrate that the proposed control scheme is able to reject disturbances in the makeup gas composition, makeup gas temperature, loop pressure and loop temperature.

Several other studies in literature have suggested complete control schemes for the ammonia synthesis loop [11] [12] [13]. These plant-wide control schemes optimize the ammonia synthesis process with respect to steady-state economics for different operating conditions, without paying much attention to the possibility of instability in the ammonia converter. Optimization of the ammonia synthesis reactor is usually performed at steady-state. A recent article by Straus and Skogestad [14] showed that steady-state optimization of a three-bed reactor with quench cooling improves the ammonia conversion. The performance is improved by adjusting the split ratios of the quench flows. However, dynamic simulations show that the optimized ammonia reactor is more sensitive to disturbances that can lead to reactor extinction or limit cycle behavior. The proposed control scheme of Economical Nonlinear Model Predictive Control (NMPC) is implemented, which is able to both increase the conversion and rapidly reject disturbances.

The article by Reese et al. [2] investigates a small-scale ammonia plant driven by wind power, which can produce small amounts of ammonia for local demand. A simple steady-state model of this plant was developed to analyze experimental data. The analysis indicates that the plant mainly operates at steady-state, even though large variation in the supply of synthesis gas was observed.

1.3 Scope of Work

In normal industry practice, ammonia synthesis plants are designed for constant operation, whereas rapid load variation is related to the risk of reactor extinction and temperature oscillations. From an economical point of view, it can be desirable to periodically change the production rate of ammonia. However, optimization of production rate is limited by the low flexibility of the large-scale conventional plants. This thesis explores the possible application of automatic control for dynamic operation of a small-scale ammonia synthesis loop. The objective of this thesis is to develop a simplified mathematical model of the ammonia synthesis loop, which captures the main dynamics with respect to load variations. The model should be developed in MATLAB with CasADi [15]. Model simulation with the numerical integrator IDAS, available in the open-source software SUNDIALS suite [16], can thereafter be used to evaluate the controllability of the process. The main goal is to suggest a control structure that can increase the flexibility of the ammonia synthesis loop with respect to load variations.

1.4 Structure of the Thesis

The following chapter of this thesis (Chapter 2) introduces the key aspects of ammonia synthesis technology, focusing on operating conditions and design. Subsequently, Chapter 3 presents the development of the model. Open-loop simulations results are introduced in Chapter 4. The controllability analysis can be found in Chapter 5. Finally, conclusions and suggestions for further work are given in Chapter 6.

Chapter 2

Ammonia Production

In this chapter, a brief history of the ammonia synthesis technology is introduced. Thereafter a description of the ammonia process and the fundamental concepts of operating an ammonia synthesis plant are presented.

2.1 Historical Development

Toward the end of the 19^{th} century, there was a growing concern that the world's food supply would be insufficient for a growing global population. It had long been known that fixed nitrogen is essential for plant growth. At the time, nitrogen for fertilizers was recovered as a byproduct in the process of converting coal to coke. Another source of nitrogen was the natural reserves of nitrates in the desert regions of Chile, which were mainly exported to European countries. In addition to nitrogen fertilizers, there was also an increasing demand for nitrogen related to the use of industrial and military explosives [17].

Although nitrogen is available in excess in the atmosphere, the challenge lies in breaking the bond of the nitrogen molecule N_2 due to its strength. At the beginning of the twentieth century, three main methods to fix nitrogen from the atmosphere were investigated: the electric arc process, the calcium cyanamide process and the catalytic

ammonia synthesis [18].

In Norway, Christian Birkeland and Sam Eyde collaborated to develop the electric arc method, called the Birkeland Eyde method (1903). This method combines nitrogen and oxygen from air to nitric oxide by passing air through an electric arc at a high temperature. A large amount of electrical energy is required, about 60,000 kWh per tonne of fixed nitrogen. However, inexpensive hydroelectric power in Norway made it possible to use this method on an industrial scale but had limited success in other parts of the world [19].

The cyanamide process (1898), also called the Frank–Caro process, is able to fix nitrogen in the compound calcium cyanamide. It only consumes a quarter of the electric power compared to the electric arc method. The first commercial plant was built in 1910 and this process was the major production method of nitrogen before the First World War [19].

The great breakthrough in large-scale ammonia production came with the Haber-Bosch process in 1909, which was a lot more energy efficient compared to the other methods. Fritz Haber realized the importance of high pressure in combination with a catalyst and material recycle of unconverted reactants. Carl Bosch further adopted the discovery of Haber on an industrial scale. Today, the Haber-Bosch process is the leading industrial procedure. The process has also laid the basis for other high-pressure production processes and contributed to the fundamental knowledge about industrial catalysts [17].

2.2 Synthesis Gas Generation

In the Haber-Bosch process, a synthesis gas consisting of nitrogen and hydrogen reacts over a catalyst at high temperature and pressure. A major part of the ammonia process is the production of synthesis gas, consisting of hydrogen and nitrogen of stochiometric ratio 3:1. For economic reasons, synthesis gas is nowadays mostly prepared from steam reforming of natural gas [17].

The first step in steam reforming involves converting hydrocarbons into hydrogen

and carbon oxides. The following endothermic reforming reaction takes place

$$C_nH_{(2^n+2)} + nH_2O \rightleftharpoons nCO + (2n+1)H_2 \quad \Delta H_{rx} > 0 \tag{2.1}$$

The water-gas shift reaction also proceeds simultaneously.

$$CO + H_2O \rightleftharpoons CO_2 + H_2 \tag{2.2}$$

In order to achieve the desired H_2/N_2 ratio, the procedure is split into two steps. In the primary reformer, catalytic steam partially converts the hydrocarbons. In the following secondary reformer, combustion with air takes place to produce heat for the highly endothermic reforming reaction and introduce nitrogen to the mixture. Thereafter CO is shifted to CO_2 through the water-gas shift reaction, which can be removed. The last step involves removing the last traces of carbon oxides, since they are poisonous to the synthesis catalyst, by converting them to methane. The final product consists of hydrogen and nitrogen, with small amounts of methane and argon (from air) [17]. Impurities such as water, oxygen and carbon monoxide should be kept to a minimum since they are poisonous to the catalyst [20]. Subsequently, the synthesis gas is compressed before it enters the ammonia synthesis loop.

2.3 Ammonia Synthesis Process

Fritz Haber discovered that both high pressure and temperature are required in order to increase the production of ammonia. However, the single-pass conversion of synthesis gas through a converter with catalyst is only around 20-30% [17]. Haber therefore came to the realization that a recycle stream with unconverted reactants is necessary. The basic configuration of the ammonia loop consists of mixing fresh make-up gas with a recycle stream. The exothermic ammonia conversion makes it possible to preheat the synthesis gas by using the hot exhaust gas. Ammonia product is separated out from the gas by cooling and condensing under high pressure. To avoid accumulation of inerts, a purge stream is employed, but this is at the expense of losing unconverted synthesis

gas. The remaining part of the gas is recycled by a circulation compressor [17]. Clearly, there are a number of design variables in the synthesis loop that have a major influence on the process. The following sections include the fundamental factors which have to be taken into account when choosing the operating conditions.

2.3.1 Ammonia Synthesis Reaction

The exothermic reaction occurring over the catalyst in ammonia converters is the following

$$N_2 + 3H_2 \rightleftharpoons 2NH_3 \quad \Delta H_{rx} = -92.44\text{kJ/mol N}_2 \tag{2.3}$$

with a highly negative reaction enthalpy ΔH_{rx} under normal operating conditions in ammonia converters [17]. When choosing the operating conditions for the ammonia converter, two important considerations are the reaction rate and chemical equilibrium.

The reversible reaction has the following equilibrium constant K_{eq}:

$$K_{eq} = \frac{p_{NH_3}}{p_{N_2}^{1/2} p_{H_2}^{3/2}} \tag{2.4}$$

which is a function of the partial pressures p_i of the different species. Because there is a decrease in the number of moles in the reaction, the reaction shifts to the right with increasing pressure according to Le Chatelier's principle. Today's plants operate at a pressure between 150-250 bar. Considering the negative reaction enthalpy, the chemical equilibrium favors production of ammonia at lower temperatures [20]. However, the reaction kinetics also plays a role in finding the optimum reactor temperature.

High activation energy is needed to break the nitrogen N-N bond, but high temperatures are unfavorable from the perspective of chemical equilibrium. A catalyst is therefore used to reduce the activation energy, thus allowing the reaction to precede at a lower temperature. The dominating catalyst used is iron based. The reactants bond to the iron catalyst, which reduces their translational degrees of freedom and makes it easier to dissociate the H_2 and N_2 bond. A sufficiently high temperature is still needed, between 250-400 °C, to accelerate the reaction [17].

In 1940, Temkin and Pyzhev [21] developed the widely used rate equation for

ammonia synthesis over an iron catalyst

$$r = k_1 p_{N_2} \left(\frac{p_{H_2}^{3/2}}{p_{NH_3}} \right) - k_{-1} \left(\frac{p_{NH_3}}{p_{H_2}^{3/2}} \right) \tag{2.5}$$

in which k_1 and k_{-1} are rate constants. The first term represents the forward rate of ammonia formation, while the second term represents the reverse rate of ammonia decomposition.

In summary, the two opposing effects are that higher temperatures accelerate the reaction rate but shift the chemical equilibrium to the left. To begin with, the conversion increases with rising temperature, but at a certain temperature the shift in chemical equilibrium starts to dominate. This means that there is a true optimum where the maximum amount of ammonia is obtained. Furthermore, the optimal operating temperature is also closely related to the ammonia concentration profile along the converter. In order to sustain a high conversion rate, the temperature should decrease with increasing ammonia concentration [17].

2.3.2 Space Velocity

Space velocity, SV, through the reactor is defined as

$$SV = \frac{v_0}{V_{bed}} \tag{2.6}$$

where v_0 is the entering volumetric flow rate and V_{bed} is the reactor volume. Typical space velocities in industrial plants vary from 12 000h^{-1} (low pressure) to 35 000h^{-1}(high pressure) [17]. At low space velocities, the process approaches thermodynamic equilibrium, which increases the conversion per pass. Higher space velocities cause lower conversion per pass, which result in a larger recycle stream. Furthermore, increasing the space velocity causes the pressure drop to rise. One often observes that even though the conversion per pass decreases with increased space velocity, the increased flow rate makes up for the drop in conversion. Hence, the total production flow of ammonia increases. However, the increased space velocity comes at the expense

of a higher compressor duty, due to a larger recycle stream and increased pressure drop [19].

2.3.3 Gas Composition

The optimal stochiometric ratio H_2/N_2 depends on the space velocity. When the process is close to equilibrium at low space velocities, the ideal ratio is 3, equivalent to the stoichiometric ratio in Equation 2.3. The ideal ratio drops down to 2 at higher velocities because the thermodynamic equilibrium is of less importance [17].

Furthermore, the H_2/N_2 ratio also depends on the temperature. At low temperatures, H_2 blocks the catalyst surface, which inhibits the catalyst activity. Thus, a lower H_2:N_2 ratio is suitable at lower temperatures, while at temperatures above 380 °C the ideal ratio is between 2.5-3. Generally, the ratio in ammonia synthesis plants are close to 3 since the process is usually close to equilibrium and the converters operate at elevated temperatures [22].

The performance of ammonia converters are affected by the reactor feed inert and ammonia contents since they both dilute the synthesis gas. The effect is a reduction in reaction rate. Moreover, the inerts reduce the catalyst quality. Generally, the purge stream maintains the content of the inerts in the range of 0-10 mol%. The content of ammonia in the converter feed depends on the efficiency of the separation system and usually lies in the range 2-4 mol% [19].

2.3.4 Ammonia Converters

As previously mentioned, the optimal converter temperature should decrease with increasing ammonia concentration along the converter. The reaction kinetics requires that the synthesis gas enters the converter at an elevated temperature. Thereafter, cooling is needed in the exothermic ammonia converter in order to maintain a satisfactory operating temperature. A number of converter designs have been developed with different flow pattern and operating conditions. The basic design of an ammonia converter consists of preheating part of the synthesis gas with the hot reactor effluent for heat recovery. Cooling along the reactor can be achieved by internal cooling with

reactor feed or by dividing the catalyst into multiple adiabatic beds with injections of cold synthesis gas in between [17].

2.3.5 Limit Cycle Behavior

As previously mentioned, temperature oscillations were observed at an ammonia synthesis plant, due to a sudden drop in reactor pressure. The system was brought back to stability when the reactor pressure returned to its nominal value [5]. Limit cycle behavior can be understood by studying the difference in dynamics of the temperature and composition in the ammonia converter. First, a drop in converter feed temperature or pressure can result, due to equilibrium and kinetic effects, in a lower conversion at the inlet of the reactor. Next, as the fast concentration wave with more reactants moves along the reactor, more of the exothermic reaction proceeds closer to the reactor outlet. Thus, the inverse temperature response is observed at the reactor outlet. The slow temperature wave eventually travels down the reactor, hence the reactor outlet temperature decreases. When the inverse response of reactor outlet temperature is coupled with the positive feedback from the preheater, limit cycles occurs. This phenomenon is explained in greater detailed in the work of Morud and Skogestad [1] with a linear analysis of the reactor system.

2.3.6 Ammonia Separation

Following the converter, the reactor effluent is cooled by a refrigeration cycle to condense ammonia at a high pressure. Ammonia can thereafter be removed by adiabatic high-pressure flash. The performance of the flash increases with falling temperature, hence a lower ammonia concentration in the loop is achieved. A lower ammonia concentration has a positive effect on the power consumption of the recycle compressor and the converter performance. Furthermore, the efficiency of the adiabatic flash is higher when the outlet stream from the converter has a high content of ammonia, while inerts reduce the performance of the ammonia recovery [19].

2.3.6.1 Vapor-Liquid Equilibrium for the Multicomponent System

The vapor-liquid equilibrium for a species i in a multicomponent mixture can be described by the constant K_i, as follows

$$K_i = \frac{y_i}{x_i} \tag{2.7}$$

where y_i and x_i are the mole fractions in the vapor phase and liquids phase, respectively. In ideal solutions, the equilibrium relationship between the partial pressure in gas phase p_i and x_i can be approximated by Raoult's law

$$p_i = x_i p_i^{sat}(T) \tag{2.8}$$

in which p_i^{sat} is the saturation pressure. There exists a critical temperature which at and above the pure component i no longer occur in liquid phase. Raoult's law is not appropriate to use for these *supercritical* species, since $p_i^{sat}(T)$ is not possible to obtain. Instead, Henry's law for dilute species can be used

$$p_i = H_i x_i \tag{2.9}$$

where H_i is Henry's law coefficient. This linear relationship is only valid when a small amount of species is dissolved in the liquid phase [23].

In the multicomponent mixture in the ammonia synthesis loop, the vapor-liquid equilibrium of ammonia can be approximated by Raoult's law. The other supercritical species are only present in small amounts in the liquid phase, hence they follow Henry's law for dilute species [24]. In [25] the vapor-liquid equilibrium for the multicomponent system found in the ammonia synthesis loop was investigated. The system consists of hydrogen, nitrogen, ammonia and inerts (methane and argon). Henry's constant as a function of temperature for the components H_2, N_2, CH_4 and Ar were calculated up to 400 atm and for temperatures in the range of -20 °C to 100 °C.

Chapter 3

Model Development

In this chapter, the development of the model is described. The developed model has a nominal capacity of 20,000 tonne NH_3 per year, when assuming a plant uptime of 91 %. The species included in the model are i = [H_2, N_2, NH_3, $inert$], where $inert$ is the sum of possible inert species in the system. A set of process stream variables were selected to describe the system, which are the total molar flow $\dot{n}$, the temperature T, the pressure p and the mole fractions of each species x_i. Each process stream is described by a process stream variable vector $\boldsymbol{v}$, denoted as $\boldsymbol{v}$ = [$\dot{n}$, T, p, x_{H_2}, x_{N_2}, x_{NH_3}, x_{inert}]. CasADi [15] in MATLAB was used for symbolic modeling. Simulations of the Differential-Algebraic Equations (DAE) were performed with the numerical integrator IDAS, available in the open-source software SUNDIALS suite [16]. A fixed time interval of one second was used in all simulations. The MATLAB code can be found in Appendix D.

3.1 Flowsheet

The flowsheet of the considered ammonia synthesis loop can be seen in Figure 3.1. The makeup gas is compressed in the compressor C1 before entering the synthesis loop. In the loop, the gas is mixed with the recycle stream and heated in the heat exchanger HX1. Thereafter, the gas is sent to the ammonia converter, which consists of two adiabatic reactor beds. Part of the stream fed to the reactor is preheated by the reactor effluent in the heat exchanger HX2, while two quench flows are injected before the beds without preheating. The reactor effluent thereafter condenses in the cooler HX3 before a single separation unit S1 recovers the product stream from the recycle steam. A purge stream is necessary in order to avoid accumulation of inerts in the system. Subsequently, the recycled stream passes through the recycle compressor C2 before the gas mixes with the compressed make-up gas.

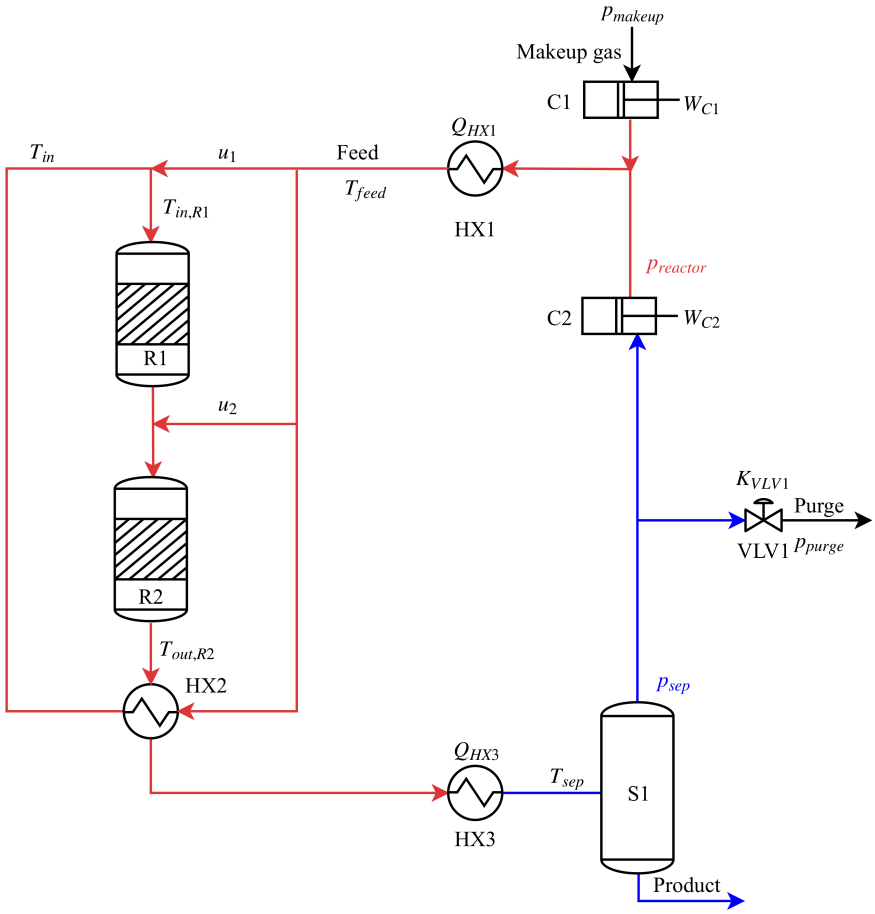

Figure 3.1: Flowsheet of the ammonia synthesis loop.

The flowsheet in Figure 3.1 depicts the degrees of freedom of the synthesis loop, which are:

- power W_{C1} to the makeup gas compressor C1;
- power W_{C2} to the recycle compressor C2;
- split ratios u_1 and u_2 for the quench flows;
- valve opening for the purge flow K_{VLV1};
- heat duty Q_{HX1} in the heat exchange HX1;
- heat duty Q_{HX3} in the heat exchanger HX3.

To ensure flexibility of the developed model, the different unit operations have been modeled independently, such that the model can be used for other synthesis loop configurations as well. Design parameters used in the different unit operations can be found in Appendix A. Included in the model are the following individual process unit operations:

- reactor bed with heat accumulation in the catalyst;
- preheater;
- cooler with condensation;
- simple heater;
- separator with mass accumulation;
- compressor;
- flow splitter (quench flows);
- flow mixer.

For the investigated system, both accumulation of heat and mass in the loop have been considered, similar to the approach in [4]. The main heat accumulation is in the catalyst in the reactor beds, which are modeled with an axial temperature distribution. Heat accumulation is considered to be negligible in the other process units where the main process phase is gas, since it has a significantly smaller heat capacity compared to the catalyst.

Furthermore, all mass holdup has been modelled to take place in the separator, using a "pseudo-volume" that considers the total gas volume in the loop. A dynamic pressure state is included in the separator to account for the change in mass holdup, while the other units have steady-state mass balances. This simplification has been based on the assumption that the mass holdup is of importance for the pressure of the loop, while the redistribution of pressure in the loop is instantaneous.

The inlet pressure of the makeup gas and exit pressure of the purge stream are set to given values. A pressure drop is included in the cooler HX3 to account for the total pressure drop in the entire loop, hence the flowsheet can be divided into two pressure sections. The pressure p_{sep} (marked with blue in Figure 3.1) is defined by the dynamic pressure state in the separator. Furthermore, the pressure $p_{reactor}$ (marked with red in Figure 3.1) is given by the steady-state pressure drop in HX3. The flow through the compressors C1 and C2 vary with the compressor duties and the pressures inside the loop.

3.2 Reactor Bed

A single reactor bed is modelled as a separate process unit, similar to the model proposed by Morud and Skogestad [1]. However, the mass balance is replaced with a mole balance since molar flows $\dot{n}$ and molar fractions x_i are used to describe the process streams. The following assumptions are made to simplify the reactor model.

- The gas holdup is neglected since it changes on a faster time-scale than the temperature dynamics.
- The pressure drop is negligible.

- The heat capacity of gas is assumed to be small compared to the heat capacity of catalyst.
- Perfect mixing in each reactor compartment.
- Only axial flow.
- The heat capacity of catalyst and the heat of reaction are independent of temperature and gas composition.

3.2.1 Mole Balance

The mole balance for species i over the reactor bed can be written as the differential equation

$$\frac{\partial(\dot{n}x_i)}{\partial z} = m_{cat}\nu_i r_{N_2} \tag{3.1}$$

where ν_i is the stochiometric coefficient of species i, r_{N_2} is the reaction rate, m_{cat} is the mass of catalyst and z is the axial position in the reactor. In the equation above, the gas holdup $(\partial(\dot{n}x_i)/\partial dt)$ is neglected. Discretizing the mole balance into a number of cells along the trajectory of the fixed bed reactor, as depicted in Figure 3.2, the expression above becomes an algebraic equation. The discretized sections are treated as a sequence of stirred-tank reactors with perfect mixing in each section, which means that the process variables only vary in the axial direction. The mole balance over cell number j is

$$0 = \dot{n}_{j-1}x_{i,j-1} - \dot{n}_j x_{i,j} + m_{cat,j}\nu_i r_{N_2,j} \tag{3.2}$$

The mass of catalyst in each reactor compartment $m_{cat,j}$ is given by

$$m_{cat,j} = \frac{V_{bed}}{ns}\rho_{cat} \tag{3.3}$$

where V_{bed} is the total bed volume, ns is total number of reactor compartments in each bed and ρ_{cat} is the catalyst bulk density.

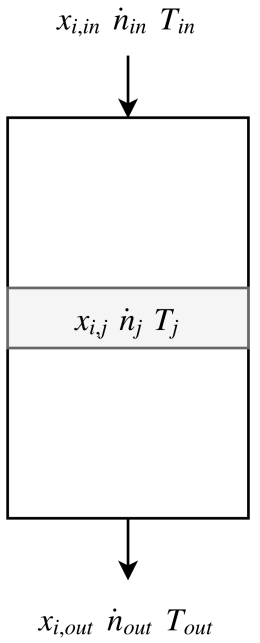

Figure 3.2: Schematic of a single reactor bed.

Furthermore, the change in molar flow is given by the equation

$$\dot{n}_j = \dot{n}_{j-1} + \sum_{i}^{species} m_{cat,j}\nu_i r_{N_2,j} \tag{3.4}$$

3.2.2 Energy Balance

The energy balance over the reactor bed is given by

$$m_{cat}C_{p,cat}\frac{\partial T}{\partial t} + C_{p,gas}\frac{\partial(\dot{n}T)}{\partial z} = m_{cat}r_{N_2}(-\Delta H_{rx}) + \Gamma m_{cat}C_{p,cat}\frac{\partial^2 T}{\partial z^2} \tag{3.5}$$

where t is time in seconds, $C_{p,cat}$ is the heat capacity of catalyst, $C_{p,gas}$ is the heat capacity of gas, ΔH_{rx} is the heat of reaction and Γ it the dispersion coefficient. In

the first term, the heat capacity of gas is considered to be negligible compared to heat capacity of catalyst. Likewise the mole balance, the energy balance is discretized in space, which transforms the partial differential equation to a ordinary differential equation, as follows

$$\frac{\partial T_j}{\partial t} = \frac{C_{p,gas}(\dot{n}_{j-1}T_{j-1} - \dot{n}_j T_j) + m_{cat,j} r_{N_2,j}(-\Delta H_{rx})}{m_{cat,j} C_{p,cat}} \tag{3.6}$$

Here the last term in Equation 3.5 is neglected. Because some numerical diffusion is introduced by the mixing in the discretized cells, the number of grid points ns can be selected in such a way that the numerical diffusion cancels out the dispersion term.

3.2.3 Rate of Reaction

The employed rate expression is given by the Temkin-Pyzhev equation [21]. A catalyst activity factor of f = 4.75 is added to account for the improvements of catalyst activity [1]. The reaction kinetics is a function of the partial pressures p_i, given as

$$r_j = \frac{f}{\rho_{cat}} \left(k_{1,j} p_{N_2,j} \frac{p_{H_2,j}^{3/2}}{p_{NH_3,j}} - k_{-1,j} \frac{p_{NH_3,j}}{p_{H_2,j}^{3/2}} \right) \tag{3.7}$$

where r_j is the reaction rate in kmol N_2/(kg cat, h). The reaction constants k_1 and k_{-1} are defined as

$$k_{1,j} = 1.79 \cdot 10^4 \text{exp}\left(-\frac{87,090}{RT_j} \right) \tag{3.8}$$

$$k_{-1,j} = 2.57 \cdot 10^{16} \text{exp}\left(-\frac{198,464}{RT_j} \right) \tag{3.9}$$

where R is the gas constant. The final rate equation becomes $r_{N_2,j}$ = r_j/3600 in kmol N_2/(kg cat s). The stochiometric coefficient vector $\boldsymbol{\nu}$ takes the form of [-3 -1 2 0] in the order H_2, N_2, NH_3 and $inert$.

3.3 Preheater

The preheater, called HX2 in Figure 3.1, is modeled as a steady-state counter-current heat exchanger using the Number of Transfer Units (NTU) method [26]. Both the heat capacity of the gas and the overall heat transfer coefficient are assumed to be constant. The heat capacity rate ratio, C^*, is given by

$$C^* = \frac{\dot{n}_c C_{p,gas,c}}{\dot{n}_h C_{p,gas,h}} \tag{3.10}$$

where subscripts c and h represent the hot and cold streams, respectively. The number of transfer units, NTU, is given by

$$NTU = \frac{UA}{\dot{n}_c C_{p,gas,c}} \tag{3.11}$$

where U is the overall heat transfer coefficient and A is the heat transfer area. The effectiveness, ϵ, can be calculated as

$$\epsilon = \frac{1 - e^{-NTU(1-C^*)}}{1 - C^* e^{-NTU(1-C^*)}} \tag{3.12}$$

The effectiveness factor represents the relationship between the actual heat transfer Q and the maximum possible heat Q_{max}, as follows

$$Q = \epsilon Q_{max} \tag{3.13}$$

The maximum possible heat transfer is given by

$$Q_{max} = \dot{n}_c C_{p,gas,c}(T_{in,h} - T_{in,c}) \tag{3.14}$$

where subscripts in and out represent the inlet and outlet streams, respectively. The heat transfer can also be expressed as

$$Q = \dot{n}_h C_{p,gas,h}(T_{in,h} - T_{out,h}) = \dot{n}_c C_{p,gas,c}(T_{out,c} - T_{in,c}) \tag{3.15}$$

By rewriting this expression, the outlet temperatures of the cold stream $T_{out,c}$ and hot stream $T_{out,h}$ is given by

$$T_{out,h} = T_{in,h} - \frac{Q}{\dot{n}_h C_{p,gas,h}} \tag{3.16}$$

$$T_{out,c} = T_{in,c} + \frac{Q}{\dot{n}_c C_{p,gas,c}} \tag{3.17}$$

3.4 Cooler

The gas entering the cooler is a gas mixture of ammonia and non-condensables (H_2, N_2 and $inert$). In the cooler, marked as HX3 in Figure 3.1, only a separation coefficient s of ammonia is assumed to be condensed. This separation factor is calculated in the separator based on the solubilities of the different species. Furthermore, the heat capacity of gas and the heat of vaporization are assumed to be independent of temperature. The duty of the cooler Q is set to a fixed value. The energy balance over the heat exchanger gives the outlet temperature, as follows

$$Q = \dot{n} C_{p,gas}(T_{out} - T_{in}) - s\dot{n}\Delta H_{vap,NH_3} \tag{3.18}$$

where $\Delta H_{vap,NH_3}$ is the heat of vaporization of ammonia.

3.5 Heater

A simple heat exchanger is included in the model to transfer heat to the synthesis gas in HX1 with the assumption constant heat capacity. The outlet temperature is calculated from the following equation.

$$Q = \dot{n} C_{p,gas}(T_{out} - T_{in}) \tag{3.19}$$

where the heat transfer duty Q is set to a fixed value.

3.6 Separator

With variable load, there is a change in the system's mass holdup, which is included in the separator unit. For simplicity, the entire section with pressure p_{sep} is lumped in this process unit. It is assumed that there are no temperature or pressure variations within the control volume. The mole balance over the control volume, shown in Figure 3.3, is

$$\frac{dn_{sep}}{dt} = \dot{n}_{in} - \dot{n}_{product} - \dot{n}_{purge} - \dot{n}_{out} \tag{3.20}$$

where n_{sep} is the number of moles in the separator, subscript in represents the inlet stream, $product$ represents the product stream, $purge$ represents the purge stream and out represents the stream to the recycle compressor.

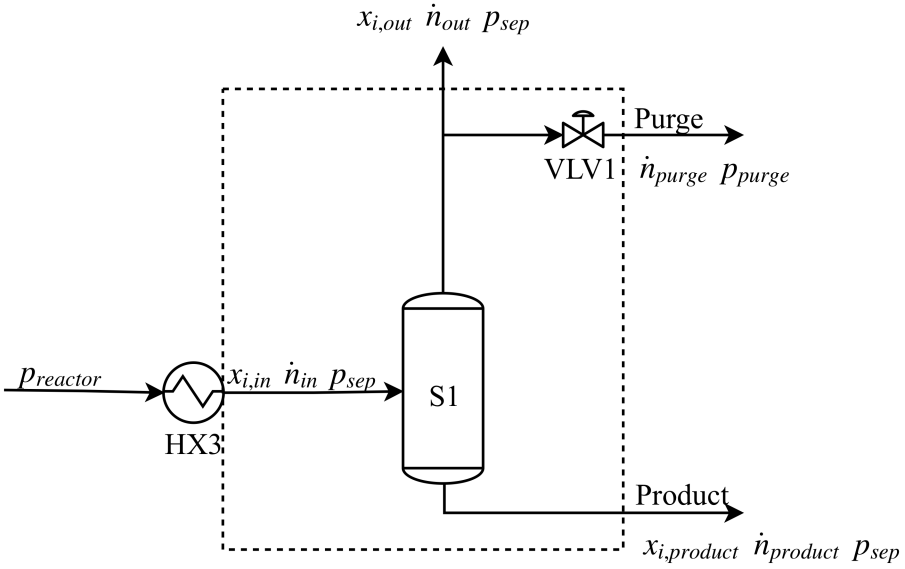

Figure 3.3: Schematic diagram of the separator. The control volume is marked with a dashed line.

Applying the ideal gas law, n_{sep} can be written as

$$n_{sep} = \frac{p_{sep} V_{sep}}{R T_{sep}} \tag{3.21}$$

where V_{sep} is a "pseudo-volume" of the total available gas volume in the loop, T_{sep} is the temperature in the control volume (calculated in the cooler) and R is the gas constant. Substituting the ideal gas law into the mole balance gives

$$\frac{V_{sep}}{R T_{sep}} \left(\frac{dp_{sep}}{dt} \right) = \dot{n}_{in} - \dot{n}_{prod} - \dot{n}_{purge} - \dot{n}_{out} \tag{3.22}$$

In this unit, the inlet flow is a function of pressure because of the pressure drop across the cooler HX3, given as

$$\dot{n}_{in} = K_{HX3} \sqrt{p_{reactor} - p_{sep}} \tag{3.23}$$

where K_{HX3} is the flow resistance in HX3. It is worth noting that the pressure drop across the heat exchanger increases with $\dot{n}_{in}$. Furthermore, a pressure dependent purge stream is extracted from the recycle stream. The purge stream is defined as

$$\dot{n}_{purge} = K_{VLV1} \sqrt{p_{sep} - p_{purge}} \tag{3.24}$$

where K_{VLV1} is the valve flow resistance for valve VLV1 and p_{purge} is the pressure of the purge stream. Here p_{purge} is set to a fixed value, hence $\dot{n}_{purge}$ vary with p_{sep}. Substituting Equation 3.23 and Equation 3.24 into Equation 3.22 gives

$$\begin{aligned} \frac{dp_{sep}}{dt} = \frac{R T_{sep}}{V_{sep}} (K_{HX3} \sqrt{p_{reactor} - p_{sep}} \\ - \dot{n}_{prod} - K_{VLV1} \sqrt{p_{sep} - p_{purge}} - \dot{n}_{out}) \end{aligned} \tag{3.25}$$

In the ammonia synthesis loop model, the steady-state Equation 3.23 calculates $p_{reactor}$, while the differential Equation 3.25 calculates p_{sep}. It is possible to run the model with the dynamic mass balance given above or with a steady-state mass balance, which

corresponds to leaving out the left-hand side of the equation above.

3.6.1 Vapor-liquid Equilibrium in the Separator

The separator recovers ammonia from the mixture based on vapor-liquid equilibrium of the multicomponent system, which is pressure and temperature dependent. The $inert$ component is considered to be argon from air. Ammonia is assumed to be separated out according to Raoult's law $p_{sep}x_{NH3,out} = p^{sat}_{NH_3}(T_{sep})x_{NH_3,product}$, where the out stream and $product$ streams are assumed to be in vapor and liquid phase, respectively. The saturation pressure in atm is expressed as a function of temperature according to [25]

$$p^{sat}_{NH_3}(T_{sep}) = A + BT_{sep} + CT^2_{sep} + DT^3_{sep} + ET^4_{sep} \tag{3.26}$$

where A-E are constants.

Henry's law $p_{sep}x_{i,out} = H_i x_{i,product}$ is used to calculate the amounts of H_2, N_2 and inert that are condensed to the product steam. Henry's constant, H_i in atm, is a function of temperature in the separator [25]

$$ln(H_i)(T_{sep}) = H_{1,i} + \frac{H_{2,i}}{T_{sep}} + \frac{H_{3,i}}{T^2_{sep}} \tag{3.27}$$

where $H_{1,i}$, $H_{2,i}$ and $H_{3,i}$ are constants. Note that both the saturation pressure and Henry's constants are converted from atm to bar in the model.

3.7 Compressor

Compressors can become unstable if the flow drops to the surge limit, which defines the minimum flow that is needed for stable operation. To avoid problems related to compressor surge, a type of positive-displacement compressor called piston compressor (or reciprocating compressor) is used for the compressors C1 and C2 in Figure 3.1. Piston compressors collect a volume of gas within a chamber and compress the gas by reducing the chamber volume. Usually, piston compressors are analyzed by an adiabatic reversible (isentropic) compressor model, assuming ideal gas and constant heat capacity

[27]. The ideal isentropic outlet temperature can be found by the following relationship

$$\frac{T_{out}}{T_{in}} = \left(\frac{P_{out}}{P_{in}}\right)^{\frac{R}{C_{p,gas}}} \tag{3.28}$$

where subscript in represents the inlet flow, subscript out represents the outlet flow from the compressor and R is the gas constant. For the given isentropic process, the ideal work W can be found by

$$W = \dot{n} C_p T_{in} \left[\left(\frac{P_{out}}{P_{in}}\right)^{\frac{R}{C_{p,gas}}} - 1\right] \tag{3.29}$$

The ratio of isentropic work to actual work, called the isentropic efficiency η_c, usually lies between 0.85-0.95 [27]. Taking into account the isentropic efficency, the outlet temperature of the compressor becomes

$$T_{out} = T_{in} + \left[1 + \frac{(P_{out}/P_{in})^{\frac{R}{C_{p,gas}}} - 1}{\eta_c}\right] \tag{3.30}$$

3.8 Splitter

At the split point, a single stream is divided into three quench streams with split fractions denoted as u_1 and u_2. The mole balance for the split where the inlet stream n_{in} is divided, is given by

$$\dot{n}_{quench,1} = u_1 \dot{n}_{in} \tag{3.31}$$

$$\dot{n}_{quench,2} = u_2 \dot{n}_{in} \tag{3.32}$$

$$\dot{n}_{preheat} = (1 - u_1 - u_2)\dot{n}_{in} \tag{3.33}$$

where subscripts $quench$ represents cold quench flows and $preheat$ represents the flow sent to the heat exchanger HX2 for preheating. Note that the inequality constraint for the split ratios is

$$u_1 + u_2 - 1 \leq 0 \tag{3.34}$$

3.9 Mixer

Assuming constant heat capacity when mixing two streams with temperatures T_{in1} and T_{in2}, the final outlet temperature of the mixed stream T_{out} can be expressed as

$$T_{out} = \frac{\dot{n}_{in1}}{\dot{n}_{in1} + \dot{n}_{in2}} T_{in1} + \frac{\dot{n}_{in2}}{\dot{n}_{in1} + \dot{n}_{in2}} T_{in2} \tag{3.35}$$

The following equation applies for the mole fraction of species i

$$x_{i,out} = \frac{\dot{n}_{in1}}{\dot{n}_{in1} + \dot{n}_{in2}} x_{i,in1} + \frac{\dot{n}_{in2}}{\dot{n}_{in1} + \dot{n}_{in2}} x_{i,in2} \tag{3.36}$$

3.10 Discrete PI Controller

In addition, a simple PI controller is included as a separate function. The control output u from a PI controller is given by

$$u(t) = \bar{u} + K_c \left[e(t) + \frac{1}{\tau_I} \int_0^t e(\tau) d\tau \right] \tag{3.37}$$

where $\bar{u}$ is the steady state control output, K_c is the controller gain and τ_I is the integral time. The purpose is to reduce the error $e(t)$ between the measured controlled variable $y_m(t)$ and the setpoint $y_{sp}(t)$, given as

$$e(t) = y_{sp}(t) - y_m(t) \tag{3.38}$$

Writing the discrete-time PI controller on the *velocity form* according to [28] at sampling instant k gives

$$u_k = u_{k-1} + K_c \left[(e_k - e_{k-1}) + \frac{\Delta t}{\tau_I} e_k \right] \tag{3.39}$$

where Δt is the sampling period.

Chapter 4

Open-loop Analysis

This chapter investigates the open-loop behavior of the ammonia synthesis loop. In the first two sections, simulations are performed with only the two reactor beds and the preheater HX2, in order to study reactor extinction and limit cycle behavior. Thereafter, the dynamic behavior of the entire synthesis loop is analyzed.

4.1 Number of Reactor Compartments

To begin with, the steady-state reactor temperature profile was studied by simulating the two reactor beds and the preheater. As can be seen in Figure 4.1, the number of reactor compartments ns had a small effect on the steady-state temperature profile along the reactor beds. However, the selection of ns was found to be important for the dynamic behavior. The model was initially simulated with 10 compartments in each reactor bed, the same number used by Morud and Skogestad [1]. As seen in Figure 4.2, the model did not show limit cycle behavior when there was a sudden decrease in the reactor pressure from 150 bar to 125 bar, but reactor extinction was observed when the pressure further decreased to 115 bar.

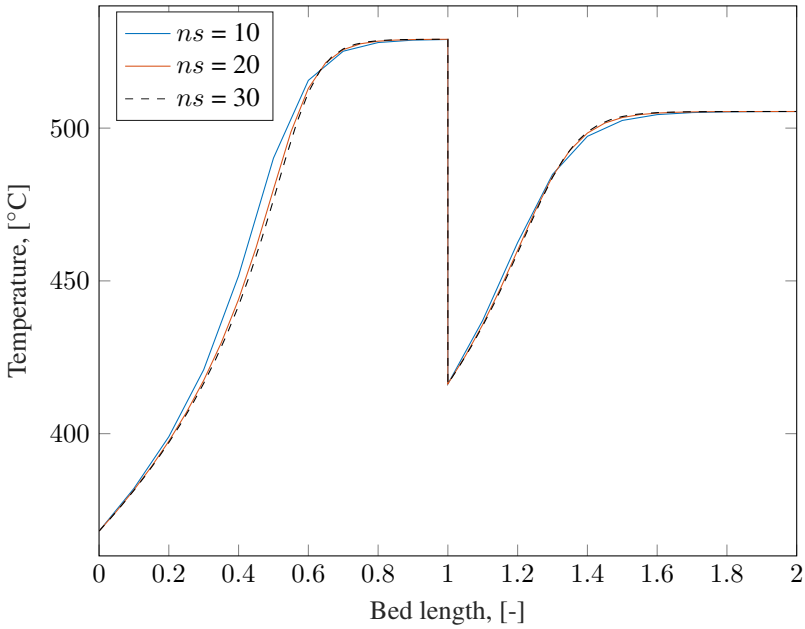

Figure 4.1: Reactor temperature profiles for different number of reactor sections (ns) per bed.

Limit cycle behavior first became apparent for a pressure reduction to 125 bar when ns in each reactor bed was increased to 20. The temperature oscillations ceased to happen when the pressure increased back to 150 bar after 5 h. Furthermore, reactor extinction was observed when the pressure fell to 115 bar after 10 h. A further increase to 30 reactor compartments in each bed displayed higher amplitude temperature oscillations even faster. However, the oscillations did not stop after the pressure returned back to 150 bar. Instead the oscillations entered another limit cycle with a smaller amplitude.

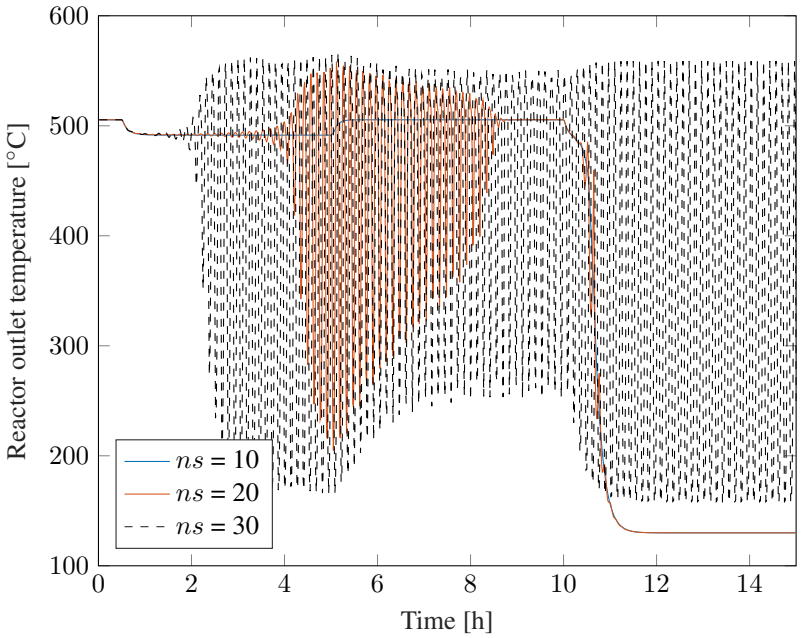

Figure 4.2: Reactor outlet temperature responses for different number of reactor sections (ns) per bed. The pressure decreased from 150 bar to 125 bar (t = 0.5 h), increased back to 150 bar (t = 5 h) and decreased to 115 bar (t = 10 h).

One can therefore conclude that the model with 20 reactor compartments in each bed gives a better match to industrial data, since the system returns to the starting point after the temperature oscillations. This behavior can be explained by the fact that the model with smaller reactor compartments does not include back-mixing inside the reactor, but only describes an idealized plug flow in the axial direction. However, some back-mixing is expected in the reactor due to diffusion. As previously mention in the chapter about model development, ns has to be selected in such a way that the numerical diffusion introduced by the discretization cancels out the diffusion term.

4.2 Steady-state Analysis of the Reactor

Steady-state analysis of the ammonia converter, consisting of the two reactor beds and the preheater, can be performed by studying the classical van Heerden plot in Figure 4.3.

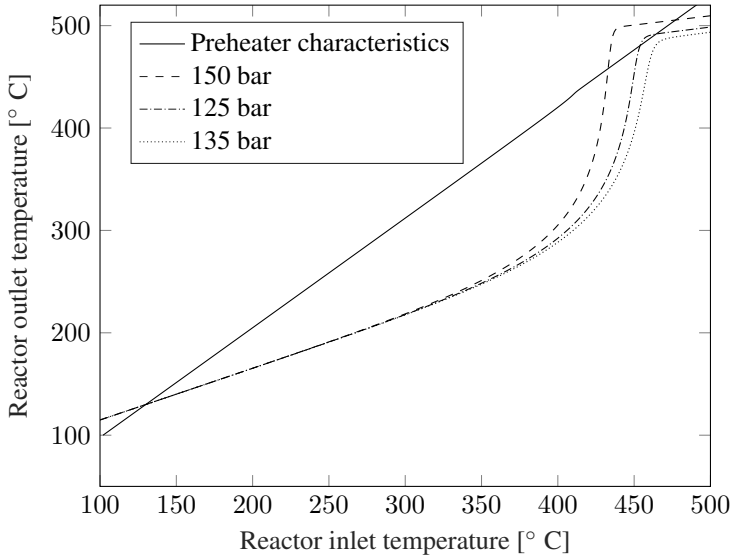

Figure 4.3: Steady-state van Heerden plot for different reactor pressures.

In this analysis, the s-shaped curved is found by varying the reactor inlet temperature T_{in} and plotting the reactor outlet temperature $T_{out,R2}$ along the y-axis (see Figure 3.1 for definitions). The preheater characteristics is found by varying the reactor outlet temperature $T_{out,R2}$ while plotting the straight-line relationship with the reactor inlet temperature T_{in} [1].

The analysis shows that the system has three stable operating points at the nominal pressure 150 bar. Lowering the pressure to 125 bar, the two upper operating points nearly intersect, but there are still three stable operating points based on this analysis. At a reactor pressure of 115 bar, the s-shaped curve no longer intersects with the preheater characteristics at higher temperatures. This means that only the lower operating point

exists, hence one can expect reactor extinction at this reactor pressure.

Based on this steady-state analysis, one would expect that the reactor is stable at 125 bar. However, the dynamic simulations in the previous section, with ns = 20, displayed oscillations at 125 bar. This result therefore emphasizes that the steady-state analysis is inefficient when ns = 20.

4.3 Dynamic Analysis of the Synthesis Loop

As could be seen in the last section, steady-state analysis is not sufficient for analyzing the stability of the ammonia converter. Hence, it is necessary to investigate the dynamic behaviour of the system. This is conducted through a sensitivity analysis of the entire synthesis loop with respect to changes in the load and the composition of the makeup gas. In addition, changes in the degrees of freedom are analyzed. The nominal process variables can be found in Appendix B.

4.3.1 Effect of Decrease in Load on Open-loop System

Initial simulations of the entire loop were performed with two models, one with the steady-state mass balance and one with the dynamic mass balance in the separator. The behavior of the loop was studied when there was a decrease in load which was applied to the system by reducing the duty of the makeup gas compressor W_{C1}.

As can be seen in Figure 4.4, the makeup flow decreases instantaneous with the compressor duty. When the pressure in the loop decreases (Figure 4.5), the makeup flow eventually rises to a new steady-state level. The pressure response has a time constant of around 6.6 minutes with the dynamic mass balance. It is evident that the dynamic pressure balance has an effect on the makeup flow response. The time it takes for the pressure in the loop to change is longer, thus it takes more time for the makeup flow to reach a new steady-state. Moreover, the product flow follows the same behavior as the makeup flow.

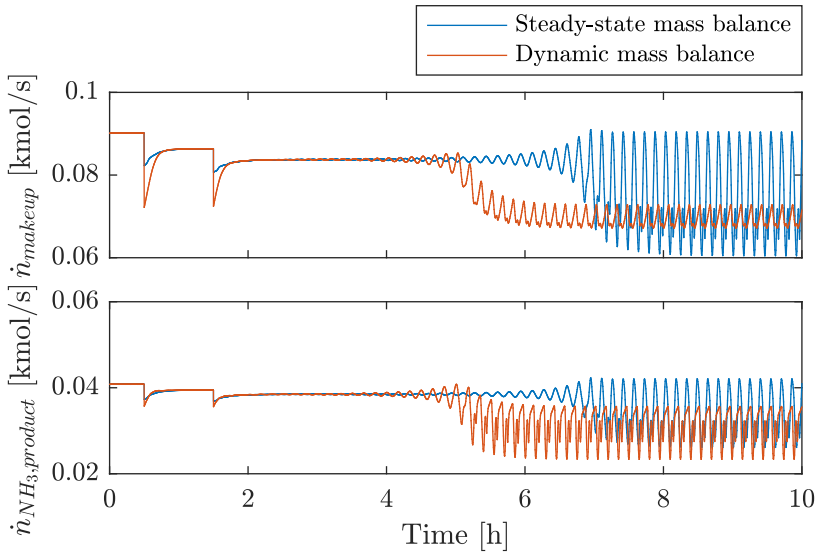

Figure 4.4: Open-loop responses of makeup flow $\dot{n}_{makeup}$ and product flow of NH_3 $\dot{n}_{NH_3,product}$ to input changes in W_{C1} of -20% (t = 0.5 h) and -33% (t = 1.5 h) from nominal value.

Figure 4.5 shows that the pressure in the loop decreases as a result of less mass in the loop. Furthermore, the outlet reactor temperature also decreases, which can be understood by studying the temperature response of the entire loop, as will be done in the next section. It seems as the decrease in both temperature and pressure reduces the stability of the system. Limit cycle behavior was apparent for both models when the compressor duty was reduced by 33 % from its nominal value. This corresponds to a change in the makeup flow of -6.9 % and the product flow of -5.8 %. It is worth noting that the models do not exhibit limit cycle behavior after the first step change, even though the pressure is reduced to 124 bar. This can seem surprising, since limit cycle behavior appeared at 125 bar when only the reactor model was studied. However, this can be explained by the fact that a number of operating variables are changing in the loop as the makeup flow is reduced, not only the pressure, which can have a stabilizing effect.

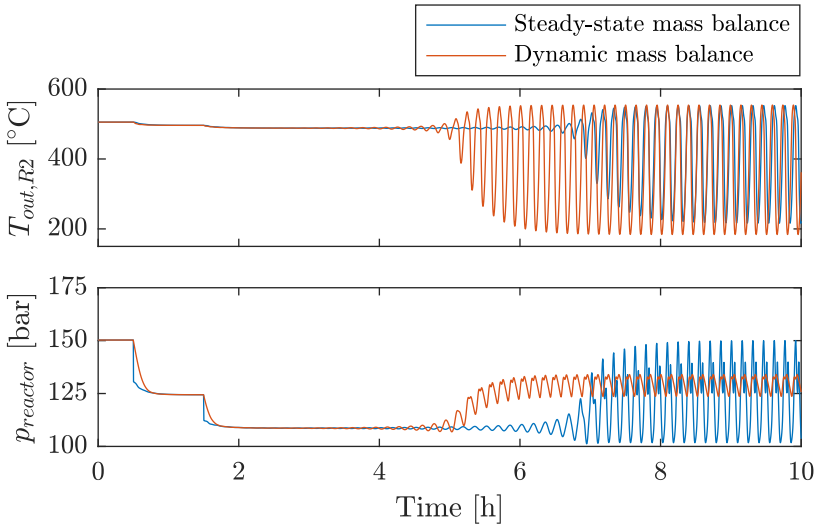

Figure 4.5: Open-loop responses of reactor outlet temperature $T_{out,R2}$ and reactor pressure $p_{reactor}$ to input changes in W_{C1} of -20% (t = 0.5 h) and -33% (t = 1.5 h) from nominal value.

The reactor pressure initially decreases to 109 bar when W_{C1} is reduced by 33 % from its nominal value. There is a clear difference between the limit cycle behavior of the two models. When the limit cycles start, the pressure responses of both models oscillate around 126 bar with periods of 9.1 min (steady-state mass balance) and 8.9 min (dynamic mass balance). However, the pressure amplitude of the case with a dynamic pressure balance is much smaller compared to the case with a steady-state mass balance. This effect is also evident in the makeup flow and product flow, which both depend on the pressure. Furthermore, these differences between the models affect the response of the reactor outlet temperature $T_{out,R2}$, which starts oscillating faster and with a larger amplitude with a dynamic mass balance. For the purpose of model verification, simulations in Appendix C show that the behavior of the model with the dynamic mass balance with a smaller V_{sep} approaches the model with the steady-state mass balance. As the volume of the separator V_{sep} becomes smaller, the dynamic response becomes faster and appears more like the steady-state response. From this

point on, the simulations are performed with the dynamic mass balance, since it is of interest to study the effect the system dynamics has on the stability.

4.3.2 Effect of Change in H_2/N_2 Ratio on Open-loop System

The snowball effect is apparent in Figure 4.6 after a disturbance in the stoichiometric ratio between H_2 and N_2, demonstrating that a small change in the composition of the makeup flow has a large impact on the composition inside the loop. Initially, the H_2/N_2 ratio of the makeup stream is 3, whereas it is slightly lower inside the loop because H_2 dissolves in the product stream.

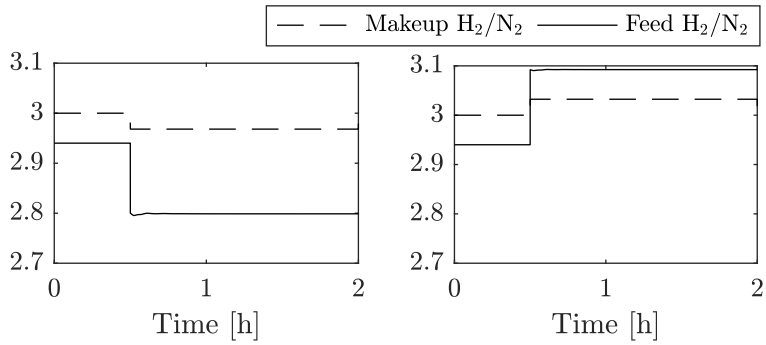

Figure 4.6: Effect of change in H_2/N_2 ratio on open-loop system.

Other process variables are also affected by the snowball phenomenon. As can be seen in Figure 4.7, the conversion of N_2 per pass X_{N_2} changes proportionally with the H_2/N_2 stochiometric ratio. It is well known that if the conversion is reduced to a certain level, the temperature in the rector decreases, which can result in reactor extinction. In addition, simulations in [10] showed that cyclic behavior can be induced this disturbance.

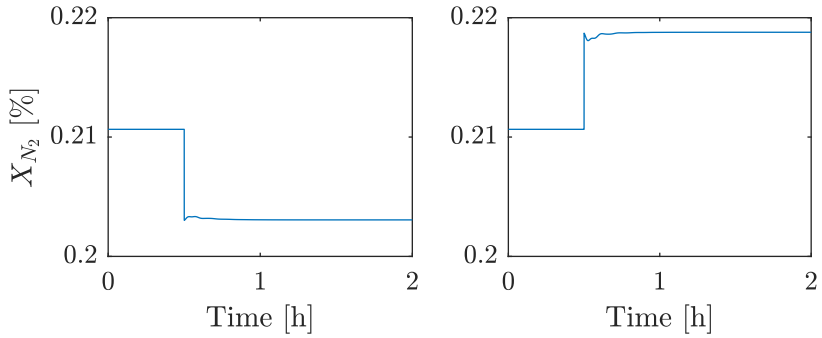

Figure 4.7: The effect a decrease (left) and an increase (right) in the H_2/N_2 ratio has on the conversion X_{N_2} of the open-loop system.

From Figure 4.8, it appears as the system exhibits oscillations when the H_2/N_2 stoichiometric ratio in the makeup stream was reduced to 2, while the ratio inside the loop approaches 0.7. A look at Figure 4.9 reveals that when the conversion decreases, the reactor pressure increases since less synthesis gas is converted to ammonia. This beneficial high pressure will help stabilize the converter, but eventually the reduction in reactor outlet temperature causes the system to enter limit cycle behavior.

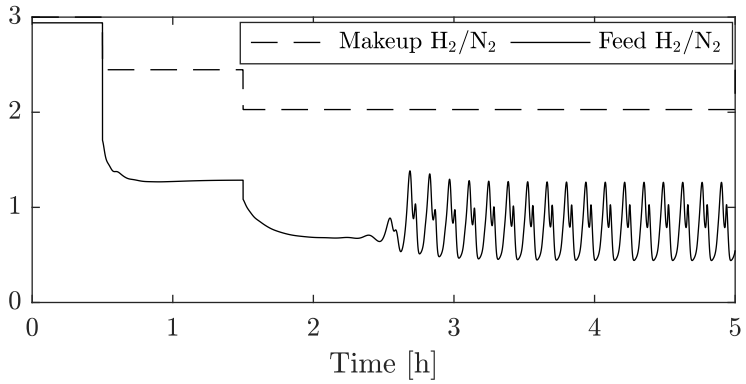

Figure 4.8: Limit cycles induced by change in H_2/N_2 ratio of open-loop system.

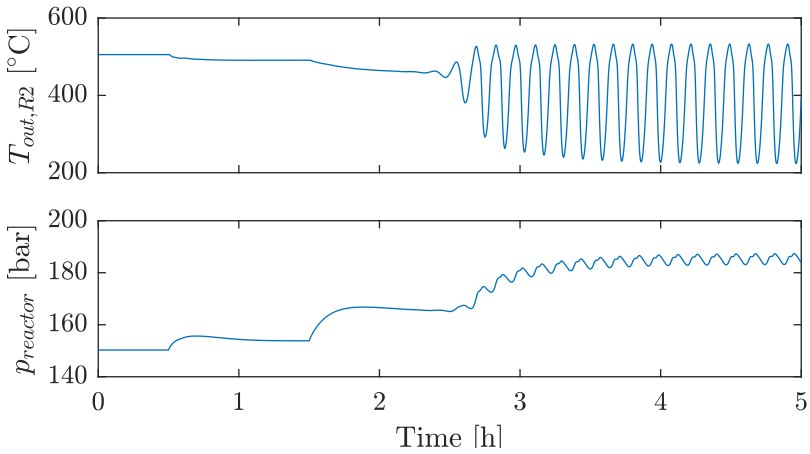

Figure 4.9: Open-loop responses of reactor outlet temperature $T_{out,R2}$ and reactor pressure $p_{reactor}$ to input changes in the H_2/N_2 ratio.

4.3.3 Step-response Analysis

To further broaden our understanding of the ammonia synthesis loop's dynamic response, a step-response analysis is performed to a selection of the degrees of freedom.

4.3.3.1 Step Changes in the Makeup Gas Compressor Power W_{C1}

The system's response when W_{C1} was both increased and decreased with 10% is shown in Figure 4.10.

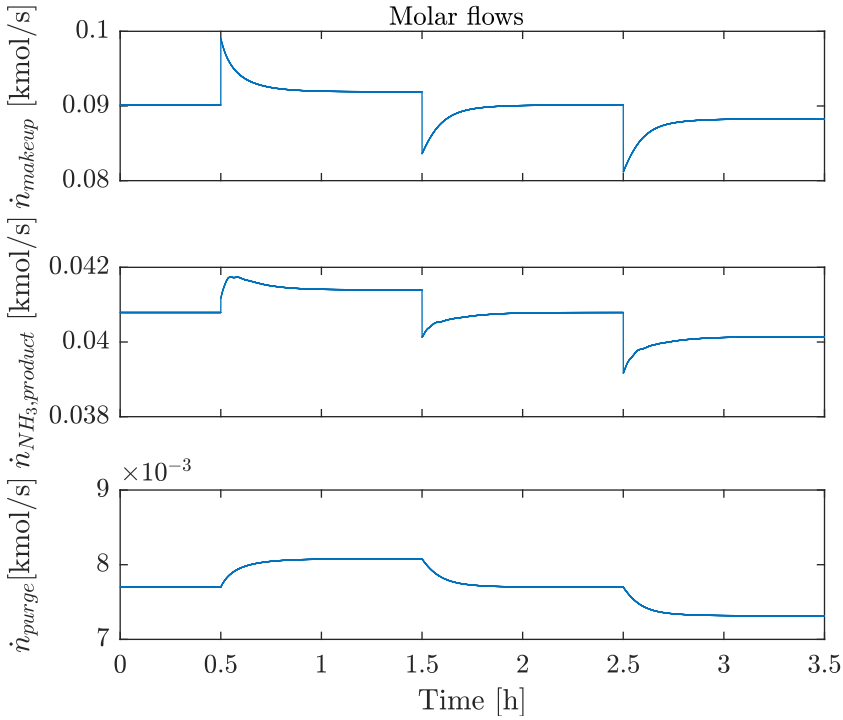

Figure 4.10: Flow responses to input changes in W_{C1} of +10% (t = 0.5 h), 0% (t = 1.5 h) and -10% (t = 2.5 h) from nominal value.

Figure 4.10 shows that all the flows increase with W_{C1} and the opposite response occurs when W_{C1} is reduced. This change in makeup flow (±2.1 %), product flow (±1.5 %) and purge flow (±4.9 %) has a direct impact on the mass accumulation in the loop, which is evident in the pressure responses in Figure 4.11.

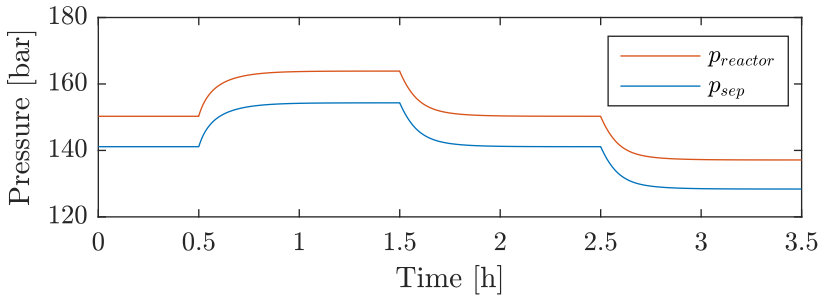

Figure 4.11: Pressure responses to input changes in W_{C1} of +10% (t = 0.5 h), 0% (t = 1.5 h) and -10% (t = 2.5 h) from nominal value.

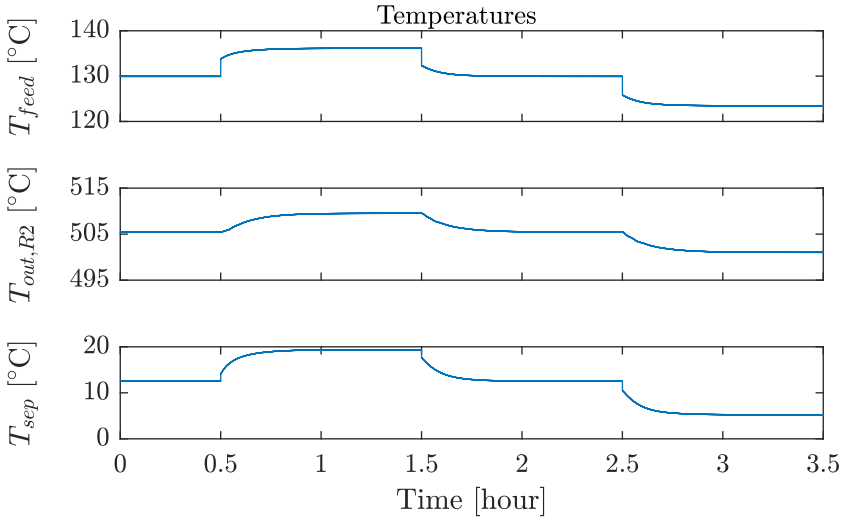

Figure 4.12: Temperature responses to input changes in W_{C1} of +10% (t = 0.5 h), 0% (t = 1.5 h) and -10% (t = 2.5 h) from nominal value.

All temperatures in the loop are affected by the change in W_{C1}. It appears as the feed temperature T_{feed} immediately increases with W_{C1} as the makeup gas enters at a elevated temperature (174 °C) compared to the recycled gas (53 °C). The outlet reactor temperature $T_{out,R2}$ eventually rises as well, but it takes more time for the temperature change to move through the reactor beds. The cooling duty before the separator is not efficient enough to keep T_{sep} at a constant value with more synthesis gas in the loop. The rise in T_{sep} further affects the purity of the product, as can be seen in Figure 4.13.

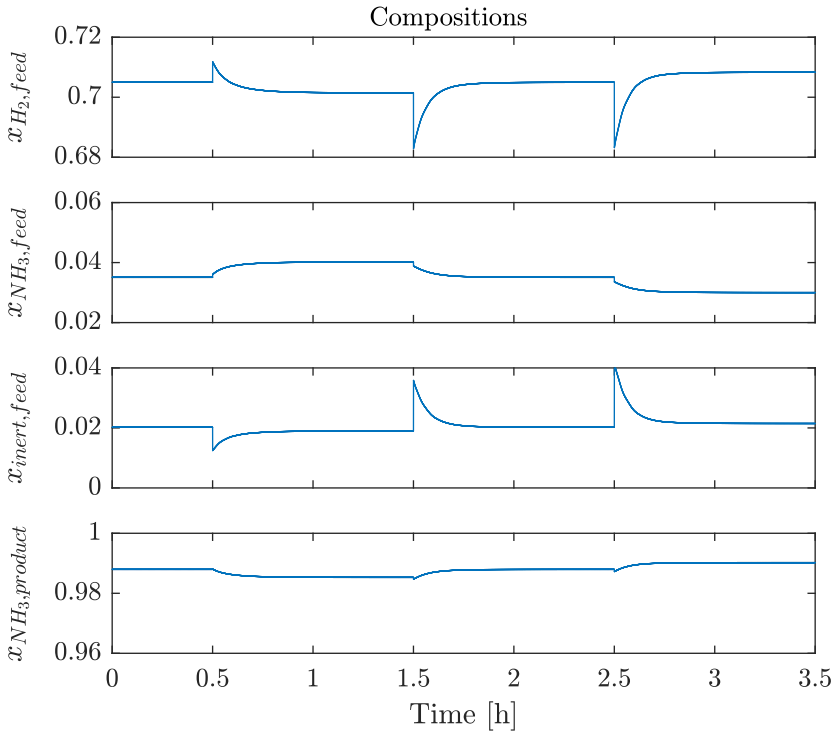

Figure 4.13: Composision responses to input changes in W_{C1} of +10% (t = 0.5 h), 0% (t = 1.5 h) and -10% (t = 2.5 h) from nominal value.

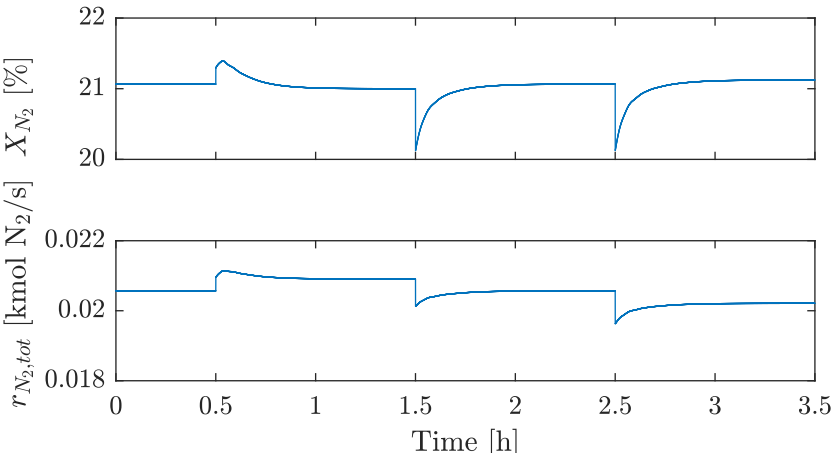

Figure 4.14: Responses of conversion,X_{N_2}, and total reaction rate, $r_{N_2,tot}$, to input changes in W_{C1} of +10% (t = 0.5 h), 0% (t = 1.5 h) and -10% (t = 2.5 h) from nominal value.

The mole fraction of ammonia in the product $x_{NH_3,product}$ is slightly reduced with a higher T_{sep}, while the amount of ammonia in the reactor feed $x_{NH_3,feed}$ increases. Furthermore, there is a slight decrease in $x_{inert,feed}$ as a result of an increase in the ratio between the purge flow and makeup flow.

From Figure 4.14 it appears as even though the steady-state value of overall conversion X_{N_2} seems to be unaffected by the step changes in W_{C1}. The overall reaction rate of N_2 in the converter, $r_{N_2,tot}$, follows the trend of the temperature and pressure in the reactor. Thus, more ammonia is produced at elevated temperatures and pressures.

4.3.3.2 Step Changes in the Split Ratio u_1

Step changes were applied to u_1 to investigate the effect it has on the temperatures in the loop, which can be seen in Figure 4.15.

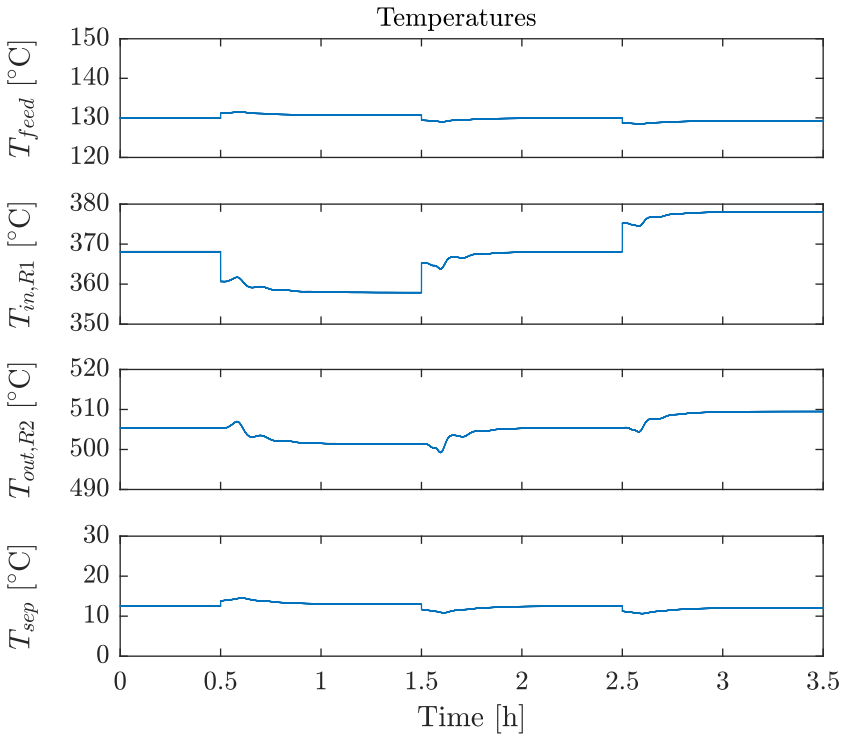

Figure 4.15: Temperature responses to input changes in u_1 of +10% (t = 0.5 h), 0% (t = 1.5 h) and -10% (t = 2.5 h) from nominal value.

As expected, variations in u_1 have a significant effect on the inlet temperature to the first reactor bed $T_{in,R1}$, while the other temperatures are less affected. The temperature $T_{in,R1}$ decreases as more synthesis gas is sent directly to the reactor bed R1, while it increases as more synthesis gas is sent to the preheater before entering the reactor.

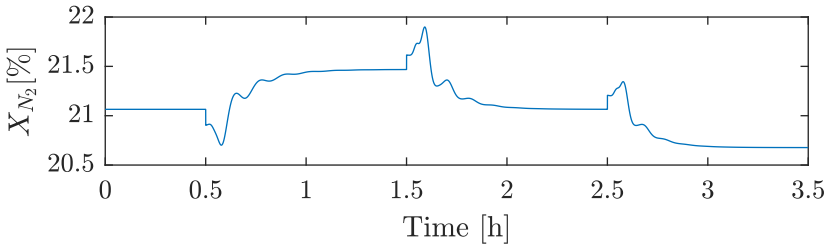

Figure 4.16: Conversion X_{N_2} response to input changes in u_1 of +10% (t = 0.5 h), 0% (t = 1.5 h) and -10% (t = 2.5 h) from nominal value.

It seems as a lower $T_{in,R1}$ leads to more favorable operating conditions in the reactor, as the steady-state conversion per pass increases (Figure 4.16) after an initial inverse response. When more ammonia is produced, more cooling duty is spent to condense ammonia, while less cooling duty is used to cool the gas. This clarifies why there is an increase in T_{sep}, which also affects T_{feed}. Another initial effect is the immediate increase in the reactor outlet temperature $T_{out,R2}$. The outlet temperature eventually decreases when the cold temperature wave travels through the reactor.

4.3.3.3 Step Changes in the Heater Duty Q_{HX1}

Step changes in the heater duty Q_{HX1} directly impacts T_{feed}, which changes proportionally with the heat duty, as can be seen in Figure 4.17.

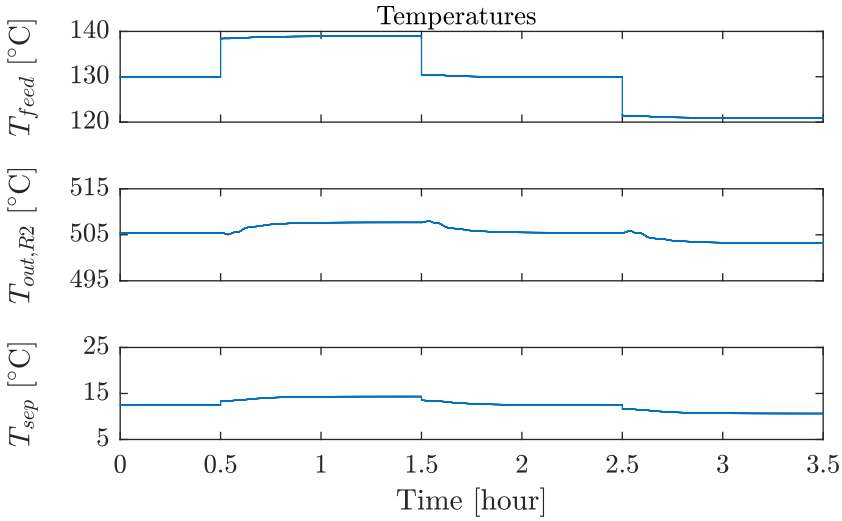

Figure 4.17: Temperature responses to input changes in Q_{HX1} of +10% (t = 0.5 h), 0% (t = 1.5 h) and -10% (t = 2.5 h) from nominal value.

The other temperatures in the the loop follow the same trend but are only affected to a small extent. Also in this case, $T_{out,R2}$ displays an initial inverse response.

4.3.3.4 Step Changes in the Cooler Duty Q_{HX3}

Figure 4.18 plots the variations in the temperatures in the loop as step changes are applied to the cooler duty Q_{HX3}. As expected, T_{sep} decreases with more cooling and increases with less cooling. Furthermore, T_{feed} follows the same trend.

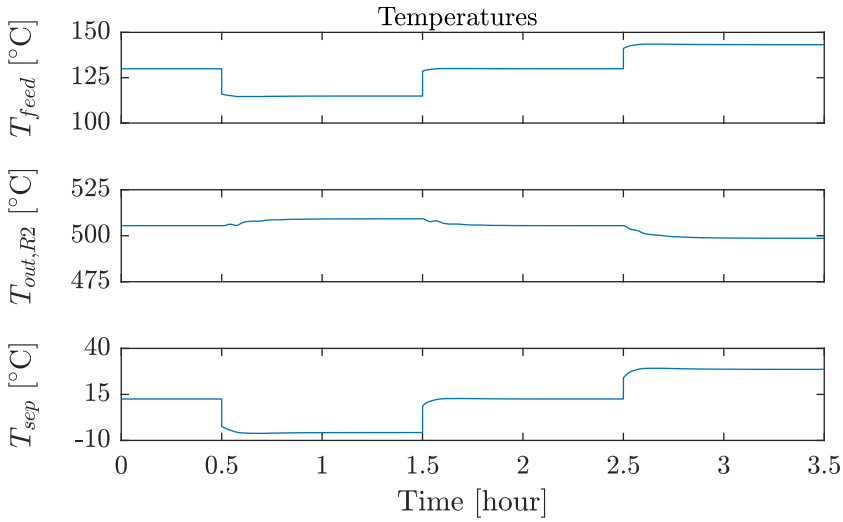

Figure 4.18: Temperature responses to input changes in Q_{HX3} of +10% (t = 0.5 h), 0% (t = 1.5 h) and -10% (t = 2.5 h) from nominal value.

In contrast to the analysis of the heat duty Q_{HX1}, the temperature $T_{out,R2}$ in this case increases when T_{feed} decreases. This demonstrates the complexity of the system's response as a number of operating conditions varies in the loop when changes are applied to a single input variable. It is apparent that $T_{out,R2}$ is highly dependent on what operating conditions favors the reaction rate. This result suggests that an improved separation efficiency leads to a more desirable gas feed composition, which gives a higher extent of the exothermic reaction.

4.3.3.5 Step Changes in Recycle Compressor Power W_{C2}

The step-response analysis performed with respect to the duty of the recycle compressor W_{C2} displayed an instantaneous change in $\dot{n}_{feed}$. As can be seen in Figure 4.19, $\dot{n}_{feed}$ increases with W_{C2}, thus the system exhibits a higher space velocity through the reactor. The makeup flow and the product flow, on the other hand, demonstrate a slow inverse response, which can be understood by studying the pressure responses shown in Figure 4.20.

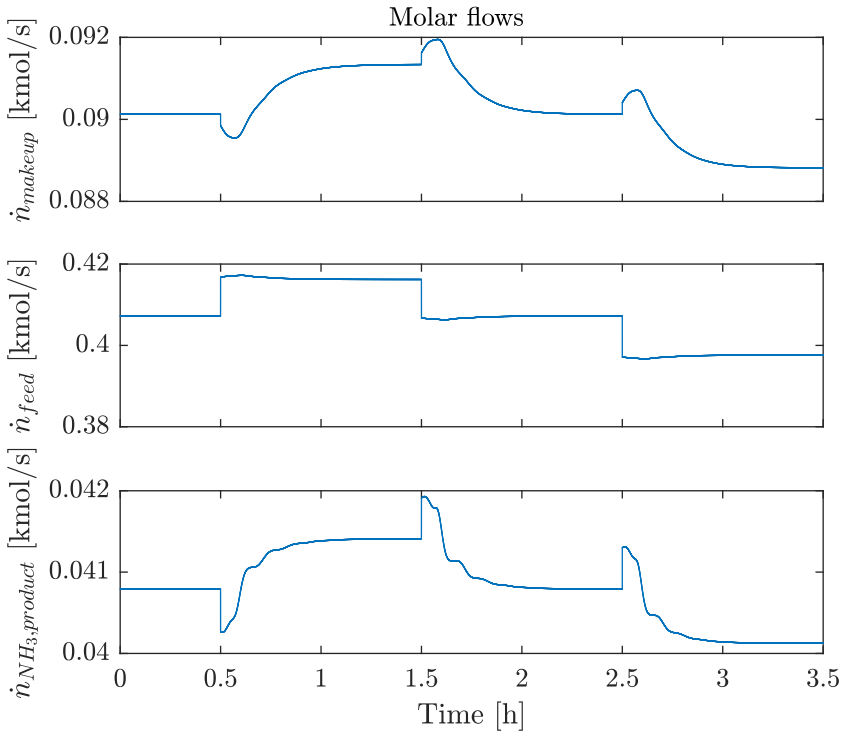

Figure 4.19: Flow responses to input changes in W_{C2} of +10% (t = 0.5 h), 0% (t = 1.5 h) and -10% (t = 2.5 h) from nominal value.

When W_{C2} is increased, there seems to be an initial increase in the pressure in the loop as a result of lower conversion per pass through the converter (less mole reduction), which can be seen in Figure 4.21. Despite the fact that the conversion per pass through the reactor decreases with a higher space velocity, the total reaction rate eventually rises, which furthermore leads to a higher product flow. The pressure in the loop eventually decreases to a lower value as more synthesis gas is converted to ammonia. The reduction in pressure is also a result of a higher pressure drop across HX3.

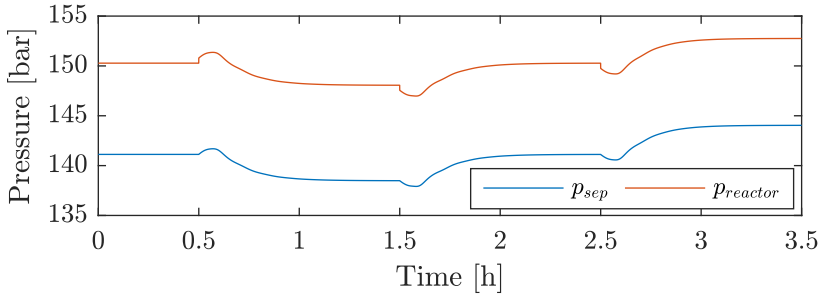

Figure 4.20: Pressure responses to input changes in W_{C2} of +10% (t = 0.5 h), 0% (t = 1.5 h) and -10% (t = 2.5 h) from nominal value.

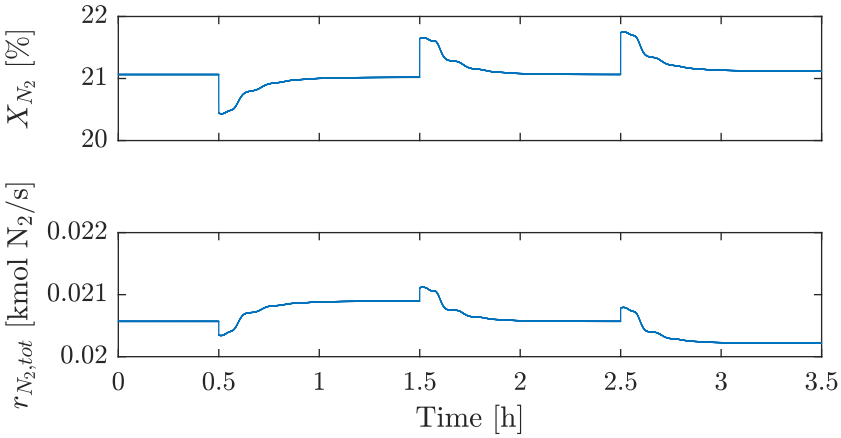

Figure 4.21: Responses of conversion, X_{N_2}, and total reaction rate, $r_{N_2,tot}$, to input changes in W_{C2} of +10% (t = 0.5 h), 0% (t = 1.5 h) and -10% (t = 2.5 h) from nominal value.

The opposite effect is seen when W_{C2} is reduced, which means that the pressure in the loop rises when the space velocity decreases. Although W_{C2} seems to have a large impact on the pressure in the loop, using W_{C2} to control the pressure could be difficult due to the inverse response.

4.4 Limitations of the Model

The studied model may differ from industrial standards in several ways. The reactor design has not been optimized for the nominal production load. In addition, the preheater HX2 is oversized compared to the reactor beds, in order to recover as much heat from the reactor effluent as possible. In a more realistic synthesis loop layout, it is more likely that a sequence of coolers would be implemented after the preheater to recover heat from the reactor effluent. The recovered heat can be utilized to produce high-pressure steam that can run the two compressors in the loop. The heater HX1 is added to avoid temperature cross-over in the preheater HX2. In an industrial ammonia synthesis loop, the heat duty Q_{HX1} comes from better utilizing the reactor effluent.

Furthermore, it is likely that the time constant of the dynamic pressure response is too long when considering the size of the synthesis loop. The actual time constant is difficult to estimate since an ammonia loop of this size does not exist. The time constant can be adjusted by varying the "pseudo-volume" of gas accumulated in the loop V_{sep}.

Chapter 5

Controllability Analysis

This chapter explores different control structures that stabilizes the process when ramping down the production load. In the previous chapter, it was observed that the open-loop system enters limit cycle behavior when the load is reduced. In addition, the simulations showed that there is a tight coupling between the process units. This leads to a complex dynamic behavior, which can be difficult to control. The dynamic step-response analysis in the previous chapter formed the foundation for the control structure assessment. The control loops were closed and tuned sequentially, using a trial and error procedure to obtain the tuning parameters found in Appendix A. In this chapter, the two main control strategies investigated are:

1. To operate at an open-loop unstable operating point.
2. To keep the system at an open-loop stable operating point.

Operating the system at an open-loop stable operating point, according to control strategy 2, is considered to be more desirable since it ensures stability even when the control structure fails or saturates.

A simple PI flow controller was implemented in all control structures to make it easier to control the makeup flow by manipulating W_{C1}. It is assumed that W_{C1} easily can be adjusted. Note that this assumption is not always applicable in industrial

compressors. Furthermore, perfect control of T_{sep} was assumed in order to maintain a stable efficiency of ammonia recovery, which is considered to be normal industrial practice. A good candidate for the manipulated variable is Q_{HX3} since it has a direct impact on T_{sep}. However, the simplified approach of perfect control was assumed since the model of the condensation process was already significantly simplified. With these two controllers implemented, the following control structures were evaluated:

Control Structure A: In this control structure, only the temperatures in the loop are controlled by feedback control. Because the pressure is reduced when there is a ramp down in makeup gas, the system operates at an unstable operating point, hence the control structure follows control strategy 1.

Control Structure B: Saturation of the manipulated variable in control structure A prompted the investigation of control structure B, which avoids saturation. Control structure B also operates at an unstable operating point according to control strategy 1.

Control Structure C: Adding a pressure controller to control structure A, ensures that the reactor pressure is maintained. This control structure follows control strategy 2, meaning that it operates at an open-loop stable operating point.

Optimized Control Structure: A final control structure was obtained by optimizing the energy efficiency performance of control structure C.

5.1 Control Structure A

Control structure A can be seen in Figure 5.1.

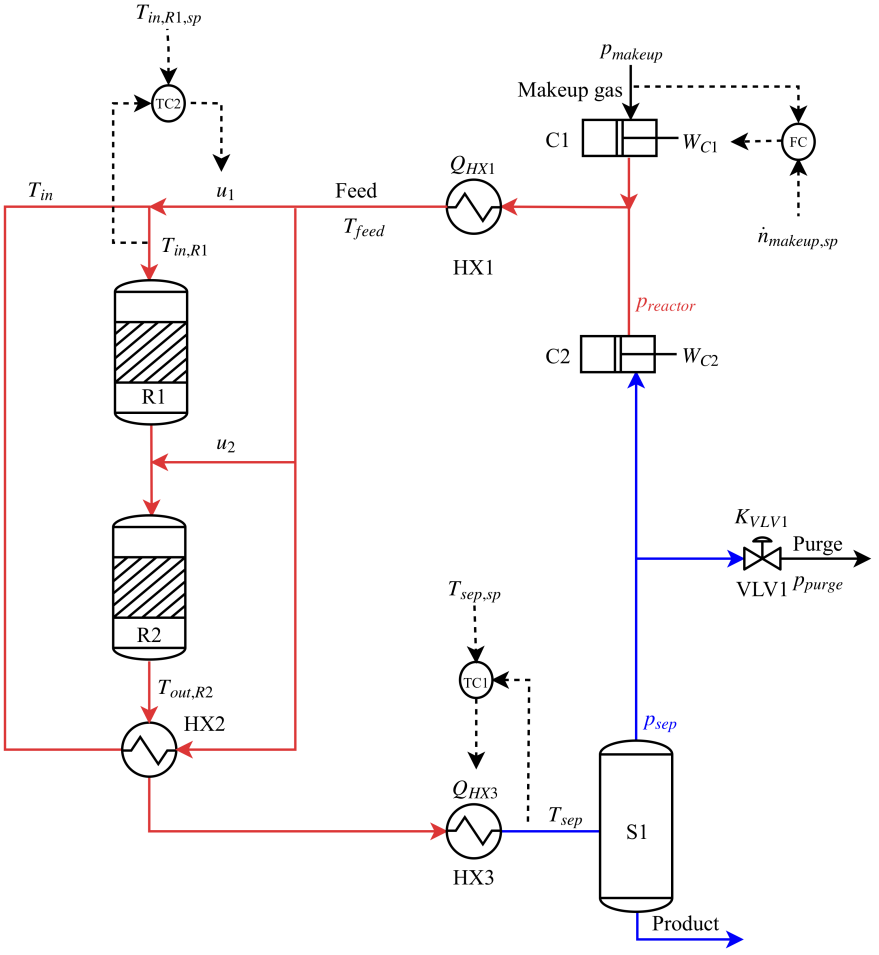

Figure 5.1: Flowsheet of the ammonia synthesis loop with control structure A installed.

Recognizing that the function of the control structure should be to increase the flexibility with respect to load variations, while considering the stability of the system's dependence on temperature, the temperature controller TC2 was implemented. The inlet temperature to the first reactor bed $T_{in,R1}$ was controlled with a PI controller by manipulating the split ratio u_1. The aim of this simple control structure is to counteract reductions in the reactor feed temperature by reducing the direct feed to the first bed. Similar control structures have been suggested in [1][5].

5.1.1 Effect of Decrease in Load

With the controllers implemented, the makeup flow was reduced in order to study when the system reaches the stability limit.

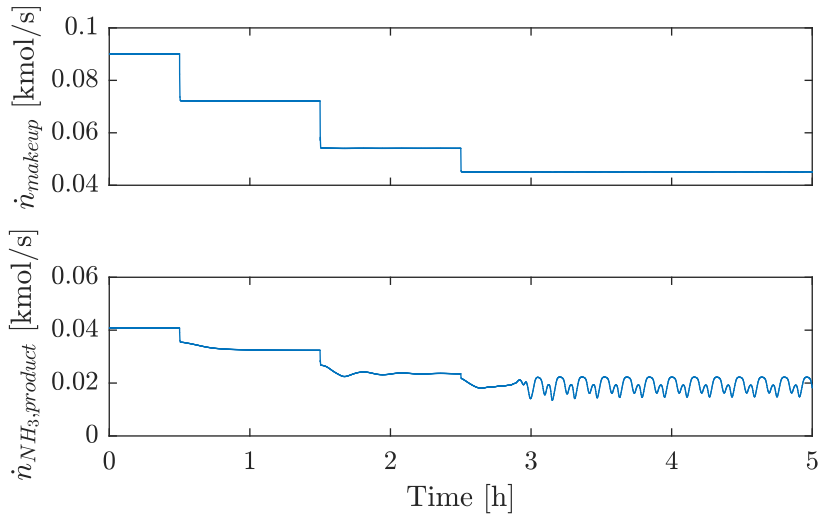

Figure 5.2: Responses of makeup flow $\dot{n}_{makeup}$ and product flow of NH_3 $\dot{n}_{NH_3,product}$ with control structure A to setpoint changes in $\dot{n}_{makeup}$ of -20 % (t = 0.5 h), -40 % (t = 1.5 h) and -50 % (t = 2.5 h) from nominal value.

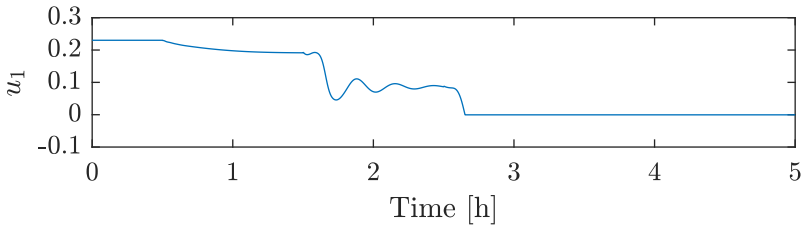

Figure 5.3: Response of the manipulated variable u_1 to setpoint changes in $\dot{n}_{makeup}$ of -20 % (t = 0.5 h), -40 % (t = 1.5 h) and -50 % (t = 2.5 h) from nominal value.

In this case, oscillatory behavior was apparent in the dynamic simulations when the pressure in the loop dropped to 106 bar (Figure 5.4). From Figure 5.2 it appears as the oscillation starts when $\dot{n}_{makeup}$ is reduced by 50 %, which is significantly lower compared to the open-loop system. The largest turn down in $\dot{n}_{makeup}$ that results in stable operation is estimated to be around -40 %, corresponding to a reduction in NH_3 product of 42.4 % from nominal value.

To compensate for the reduction in feed temperature when less hot makeup gas is added, as well as the reduction in $T_{out,R2}$, the split ratio u_1 moves to a lower value. Hence, more synthesis gas is sent through the heat exchanger HX2 for preheating. A look at Figure 5.3 reveals that the split ratio saturates when the oscillations starts after 2.5 h. Morud and Skogestad [1] addressed the issue of u_1 saturating and suggested a control structure that reduces the other quench flows as well. Naess et al. [5] also recommended a type of split-range controller to avoid saturation of u_1, even though specific implementation instructions and simulation results are missing. However, the split-range controller will only help to a certain degree. As also pointed out by [1], when feedback control of the quench flows becomes inefficient, additional heating of the reactor feed or an increase in pressure may be required.

For the open-loop system, the overall conversion was naturally maintained at a stable value until the stability limit was reached. This can be understood by considering that under lower pressure conditions, lower reactor temperatures are desirable from an equilibrium point of view. However, when $T_{in,R1}$ is controlled, the overall conversion is no longer constant when $\dot{n}_{makeup}$ is reduced (Figure 5.5), but instead decreases to a lower

value. This reduction in conversion causes less synthesis gas to be converted. Hence, a higher pressure is maintained when the flow of makeup gas is reduced compared to the open-loop system.

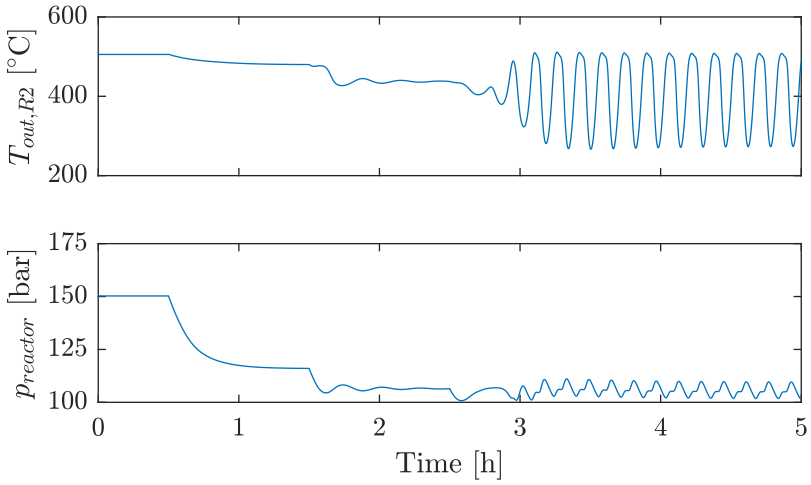

Figure 5.4: Responses of reactor outlet temperature $T_{out,R2}$ and reactor pressure $p_{reactor}$ with control structure A to setpoint changes in $\dot{n}_{makeup}$ of -20 % (t = 0.5 h), -40 % (t = 1.5 h) and -50 % (t = 2.5 h) from nominal value.

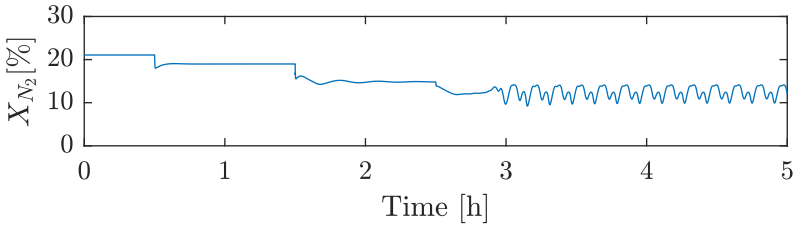

Figure 5.5: Response of conversion X_{N_2} with control structure A to setpoint changes in $\dot{n}_{makeup}$ of -20 % (t = 0.5 h), -40 % (t = 1.5 h) and -50 % (t = 2.5 h) from nominal value.

5.1.2 Analysis of Open-loop Stability

An analysis of the open-loop stability was performed by reducing the makeup flow by 40 % from its nominal value and then turning off the controller TC2 at t = 2 h. Figure 5.6 reveals that the system is operating at an open-loop unstable operating point and cyclic behavior is induced without applying any disturbances.

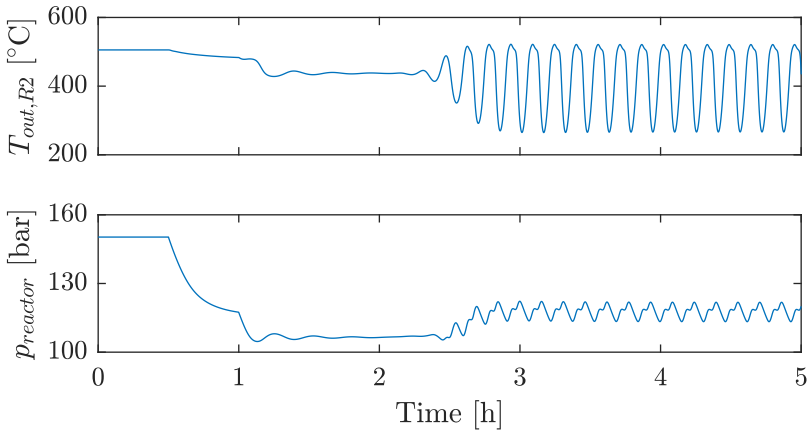

Figure 5.6: Analysis of open-loop stability after setpoint changes in $\dot{n}_{makeup}$ of -20 % (t = 0.5 h) ad -40 % (t = 1 h) from nominal value. Control structure A is turned off at t = 2 h.

5.2 Control Structure B

The motivation behind control structure B, as can be seen in Figure 5.7, is to avoid saturation of split ratio u_1. A Valve Position Controller (VPC) is implemented with the purpose to keep u_1 above 0.15 by increasing Q_{HX1}. The integral-only VPC is only activated when u_1 falls below 0.15. As previously mention in the section about limitations of the model, the heater HX1 is added to simplify the plant configuration. In an industrial application, the heat duty Q_{HX1} would be produced from the hot reactor effluent. It is therefore uncertain where the additional supply of heat required for this

control structure would come from.

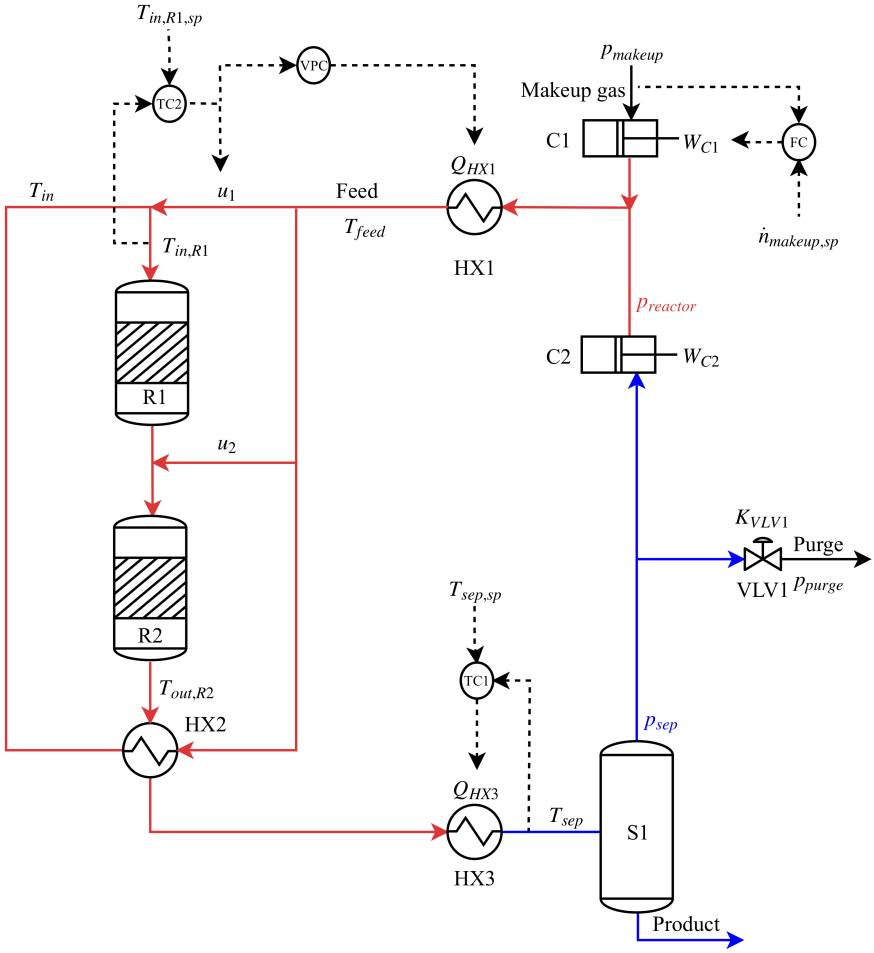

Figure 5.7: Flowsheet of the ammonia synthesis loop with control structure B installed.

5.2.1 Effect of Decrease in Load

With the VPC implemented, the system was able to handle a larger step down in load compared to control structure A, because saturation of u_1 was avoided. A look at Figure 5.8 shows that no oscillations are induced even though there is a turn down in makeup gas of 70 %, corresponding to a decrease in NH_3 product of 74.2 % from its nominal value. From Figure 5.9, it appears as oscillations are avoided even though $T_{out,R2}$ and $p_{reactor}$ both decrease considerably. However, Figure 5.10 shows that Q_{HX1} is more than doubled in order to keep u_1 from saturating. It seems as the addition of heat is able to prevent the system from oscillating, even at a surprisingly low pressure around 80 bar. The inlet temperature of the converter can therefore be considered the most critical condition to control. Although, one should keep in mind that the control structure is still operating in an open-loop unstable region since the reactor pressure is reduced.

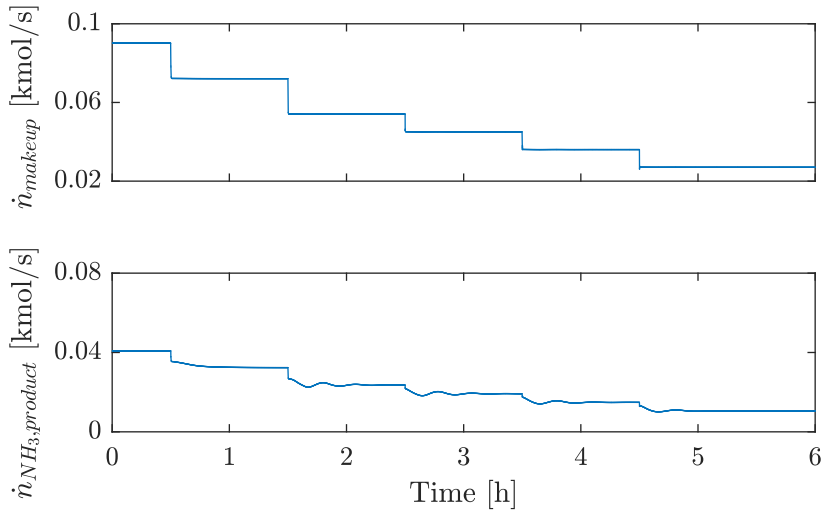

Figure 5.8: Responses of makeup flow $\dot{n}_{makeup}$ and product flow of NH_3 $\dot{n}_{NH_3,product}$ with control structure B to setpoint changes in $\dot{n}_{makeup}$ of -20 % (t = 0.5 h), -40 % (t = 1.5 h), -50 % (t = 2.5 h) -60 % (t = 3.5 h) and -70 % (t = 4.5 h).

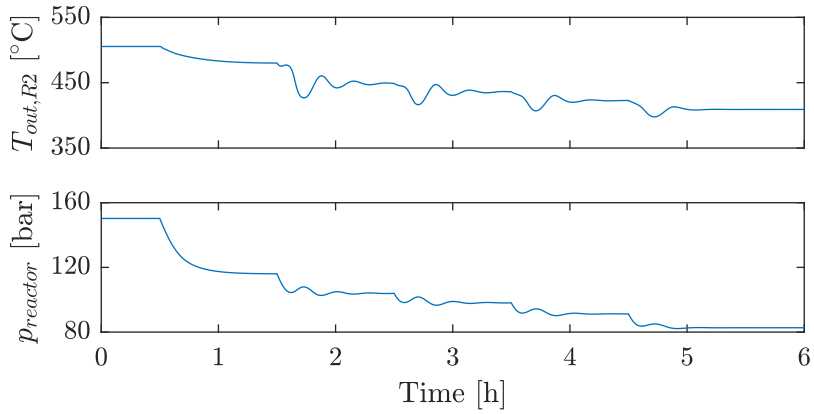

Figure 5.9: Responses of reactor outlet temperature $T_{out,R2}$ and reactor pressure $p_{reactor}$ with control structure B to setpoint changes in $\dot{n}_{makeup}$ of -20 % (t=0.5 h), -40 % (t=1.5 h), -50 % (t=2.5 h) -60 % (t=3.5 h) and -70 % (t=4.5 h).

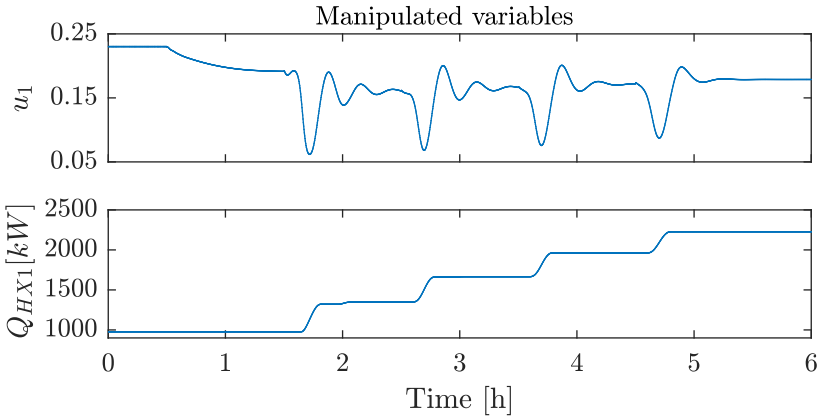

Figure 5.10: Responses of the manipulated variables in control structure B to setpoint changes in $\dot{n}_{makeup}$ of -20 % (t = 0.5 h), -40 % (t = 1.5 h), -50 % (t = 2.5 h) -60 % (t = 3.5 h) and -70 % (t = 4.5 h).

Another interesting effect of ramping down the makeup flow is the change in compositions in the loop, which can be seen in Figure 5.11. Most prominent is the increase in $x_{NH_3,feed}$ from 0.035 to 0.075. This can have a significant effect on the performance of the ammonia converter since the partial pressure of synthesis gas is reduced. On the other hand, the control structure is able to keep the steady-state $x_{inert,feed}$ at a constant value. Furthermore, $x_{NH_3,product}$ is maintained at a stable value since the control of T_{sep} ensures stable ammonia recovery.

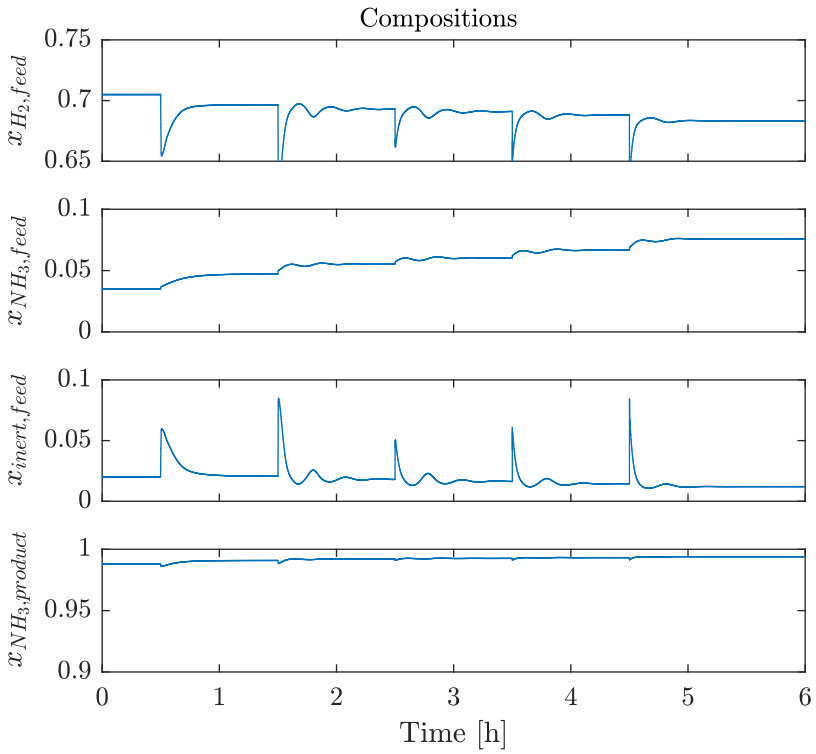

Figure 5.11: Responses of composition variables with control structure B to setpoint changes in $\dot{n}_{makeup}$ of -20 % (t = 0.5 h), -40 % (t = 1.5 h), -50 % (t = 2.5 h) -60 % (t = 3.5 h) and -70 % (t = 4.5 h).

5.3 Control Structure C

Control structure C can be seen in Figure 5.12.

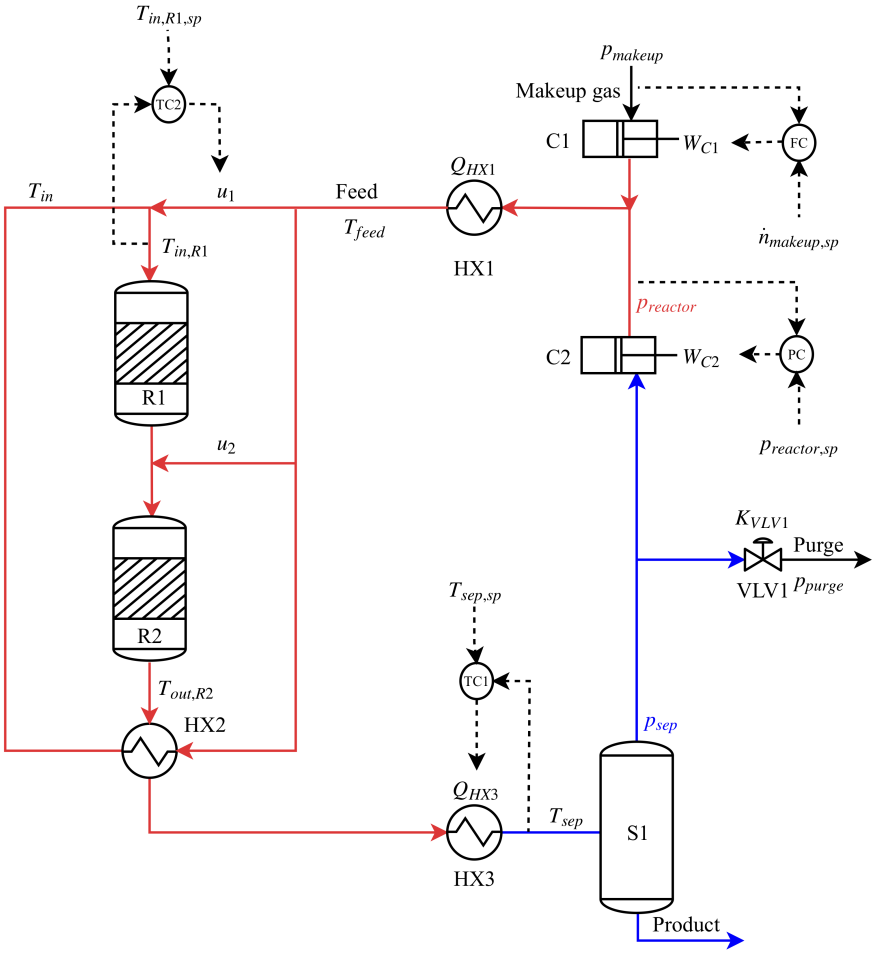

Figure 5.12: Flowsheet of the ammonia synthesis process with control structure C installed.

A PI controller was implemented to control $p_{reactor}$ by manipulating W_{C2}. The motivation behind this controller is to maintain the reactor pressure at 150 bar when decreasing $\dot{n}_{makeup}$ from its nominal value. Controlling $p_{reactor}$ will prevent the system from moving into an unstable region. It is important to note that W_{C2} can be difficult to manipulate in an industrial compressor.

5.3.1 Change in Recycle Compressor Power W_{C2} with Control Structure A

A new step-response analysis of W_{C2} was performed with control structure A implemented. As can be seen in Figure 5.13, the slow inverse response seen in the pressure responses in the previous step-response analysis is gone. The inverse response is completely eliminated from the p_{sep} response. There is still as small inverse response in $p_{reactor}$, but it is significantly faster compared to the open-loop response. This result suggests that the open-loop system vigorously respond to variations in the inlet temperature to the reactor, due to equilibrium and kinetic considerations, which indirectly affects the pressure. The small inverse response in $p_{reactor}$ can be understood as an instantaneous decrease/increase of synthesis gas in the reactor section, which does not appear to affect p_{sep} before the system settles to a new steady-state value.

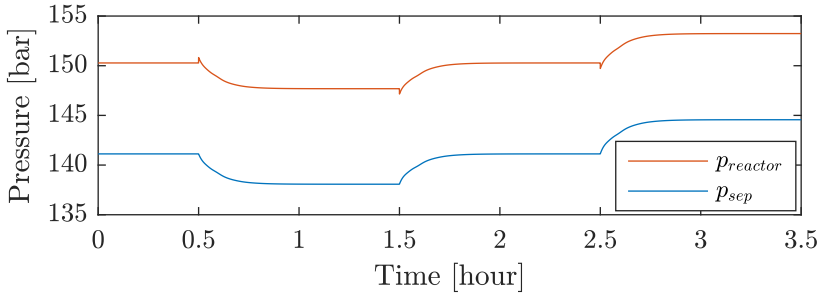

Figure 5.13: Pressure responses with control structure A to input changes in W_{C1} of +10% (t = 0.5 h), 0% (t = 1.5 h) and -10% (t = 2.5 h).

Based on this analysis, it was concluded that control of temperature leads to faster control of pressure. This is the reason why no simulations are performed with only pressure control. The reactor pressure was selected as a controlled variable, even though the small inverse response may introduce sluggish control performance.

5.3.2 Effect of Decrease in Load

From Figures 5.14-5.18, it appears as control structure C allows the production to proceed when decreasing $\dot{n}_{makeup}$ by 70 %, which corresponds to a decrease in $\dot{n}_{NH_3,product}$ of 77.2 % and an increase in $\dot{n}_{purge}$ of 3.3 % from nominal value. A lower flow rate of synthesis gas through the loop gives a smaller pressure drop through the heat exchanger HX3. That is the reason why p_{sep} rises when $p_{reactor}$ is controlled, which directly affects $\dot{n}_{purge}$. It is worth noting that the increase in $\dot{n}_{purge}$ is undesirable since unconverted synthesis gas is lost.

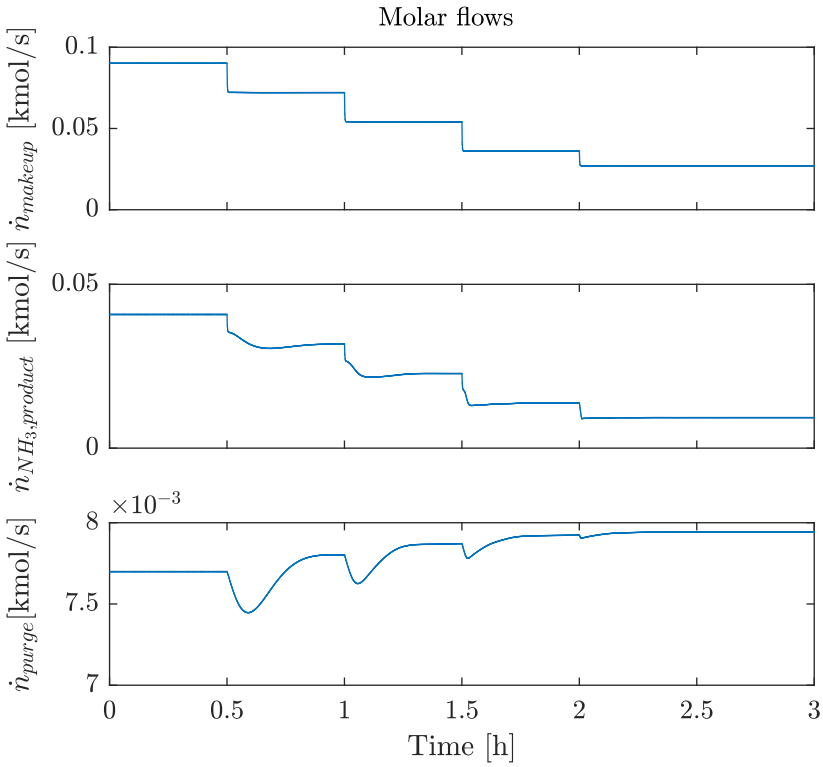

Figure 5.14: Flow responses with control structure C to step changes in $\dot{n}_{makeup}$ of -20 % (t = 0.5 h), -40 % (t = 1 h), -60 % (t = 1.5 h) and -70 % (t=2 h).

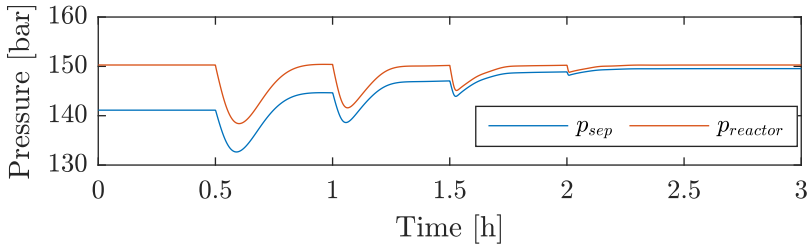

Figure 5.15: Pressure responses with control structure C to step changes in $\dot{n}_{makeup}$ of -20 % (t = 0.5 h), -40 % (t = 1 h), -60 % (t = 1.5 h) and -70 % (t = 2 h) from nominal value.

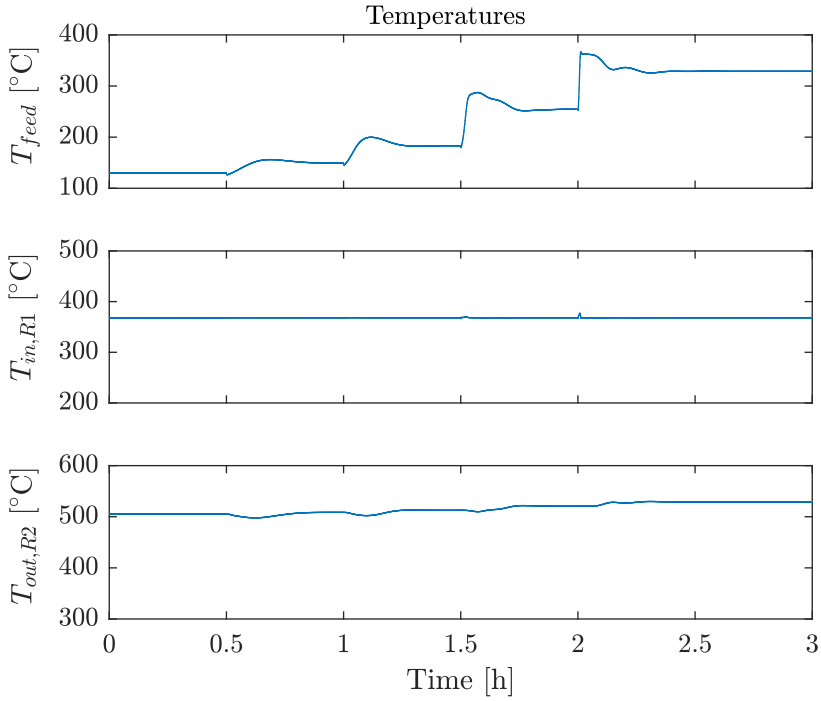

Figure 5.16: Temperature responses with control structure C to step changes in $\dot{n}_{makeup}$ of -20 % (t = 0.5 h), -40 % (t = 1 h), -60 % (t = 1.5 h) and -70 % (t = 2 h) from nominal value.

Figure 5.16 shows that there is a significant increase in T_{feed} of 200 °C, since less gas is passing through HX1. The temperature $T_{in,R1}$ is controlled, while there is a small increase of around 15 °C in $T_{out,R2}$. Moreover, the increase in both $T_{in,R1}$ and $T_{out,R2}$ lead to a rise in u_1 (Figure 5.18) since it is no longer necessary to preheat as much synthesis gas. As expected, W_{C2} decreases as less synthesis gas is present in the loop. To optimize the energy efficiency of the synthesis loop, T_{feed} can be controlled by reducing Q_{HX1}, such that more heat is recovered in the preheater. This would also help stabilize the conversion in the reactor (Figure 5.17), which is reduced from 21 % to 17.7 % due to the rise in T_{feed}.

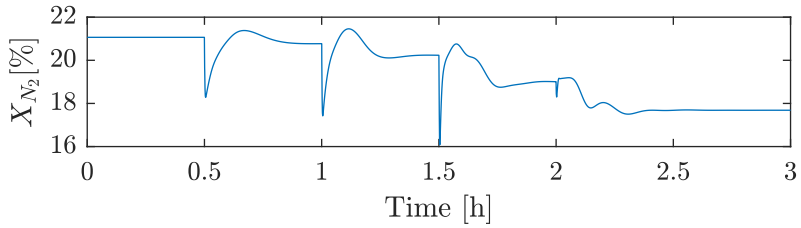

Figure 5.17: Response of conversion X_{N_2} with control structure C to step changes in $\dot{n}_{makeup}$ of -20 % (t = 0.5 h), -40 % (t = 1 h), -60 % (t = 1.5 h) and -70 % (t = 2 h) from nominal value.

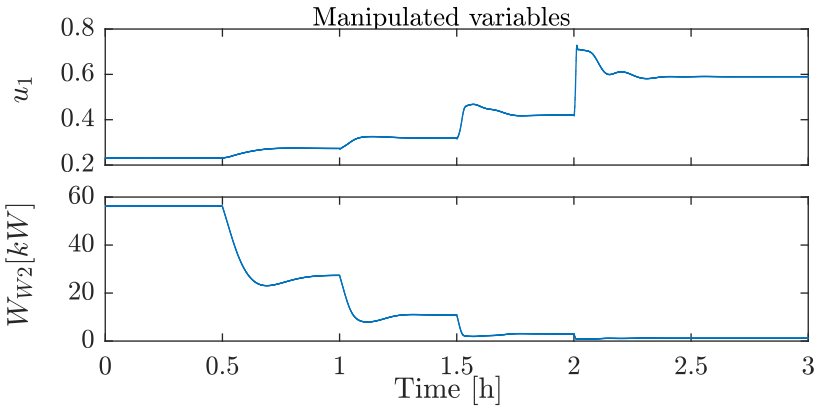

Figure 5.18: Responses of the manipulated variables of control structure C to step changes in $\dot{n}_{makeup}$ of -20 % (t = 0.5 h), -40 % (t =1 h), -60 % (t = 1.5 h) and -70 % (t = 2 h) from nominal value.

From Figure 5.19, it appears as the steady-state compositions in the loop are almost unaffected by the load variations. However, the compositions show interesting dynamic behavior with inverse responses. It seems as the amount of synthesis gas immediately decreases with load reductions, while the amount of inert increases. Eventually the combined effect of an increased purge flow and a decrease in conversion per pass balances out these changes.

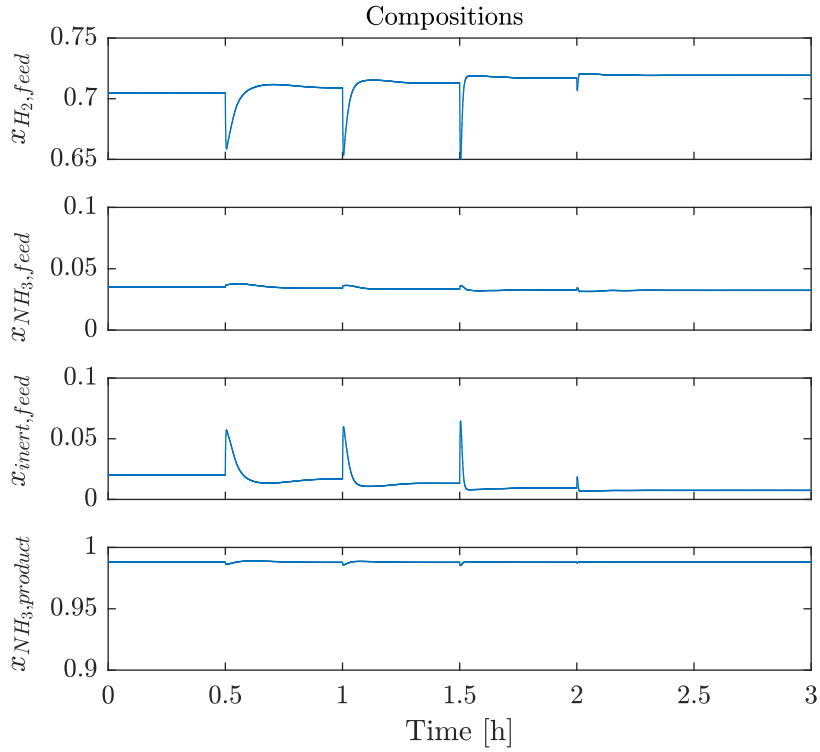

Figure 5.19: Composition responses with control structure C to step changes in $\dot{n}_{makeup}$ of -20 % (t = 0.5 h), -40 % (t = 1 h), -60 % (t = 1.5 h) and -70 % (t = 2 h) from nominal value.

5.4 Optimized Control Structure

The flowsheet with the optimized control structure can be seen in Figure 5.20.

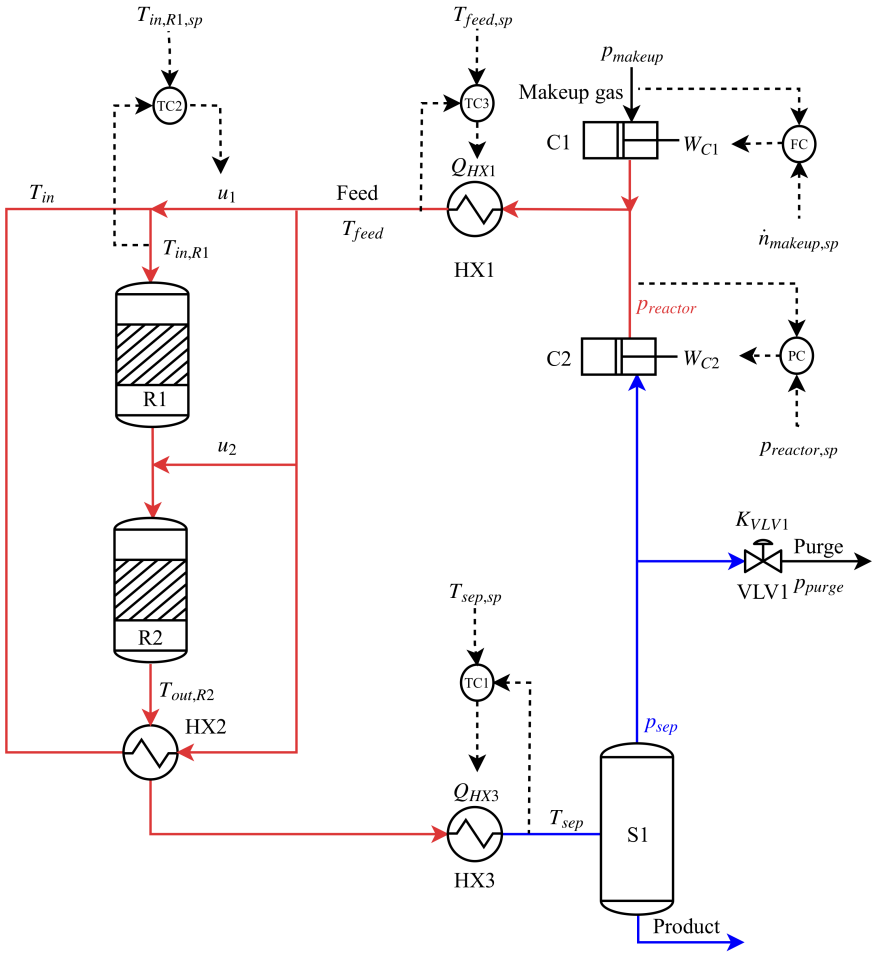

Figure 5.20: Flowsheet of the ammonia synthesis loop with the optimized control structure implementerd.

A third temperature controller, called TC3, was added to control structure C in order to reduce the heat duty Q_{HX1} when less synthesis gas is present in the loop. This controller does not contribute to the stabilization of the loop but is included to optimize the energy efficiency.

5.4.1 Effect of Decrease in Load

Figure 5.21 shows that all the temperatures in the loop are controlled except $T_{out,R2}$, which only shows a slight increase of 5 °C. Furthermore, the overall conversion is stable at 21 % after the ramp down in makeup flow of 70 % from nominal value (Figure 5.22). The main improvement related to the TC3 can be seen in Figure 5.23, which plots the manipulated variables. It is evident that the new temperature controller TC3 improves the energy efficiency of the loop by reducing Q_{HX1}.

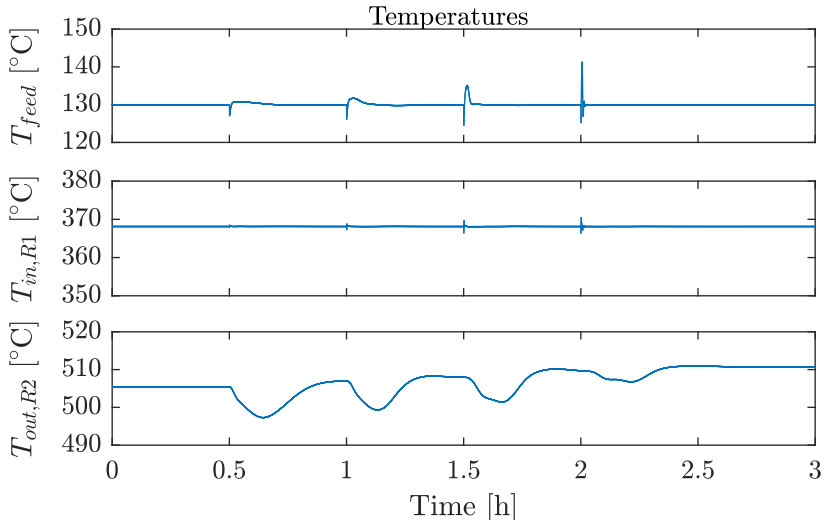

Figure 5.21: Temperature responses with the optimized control structure to step changes in $\dot{n}_{makeup}$ of -20 % (t = 0.5 h), -40 % (t = 1 h), -60 % (t = 1.5 h) and -70 % (t = 2 h) from nominal value.

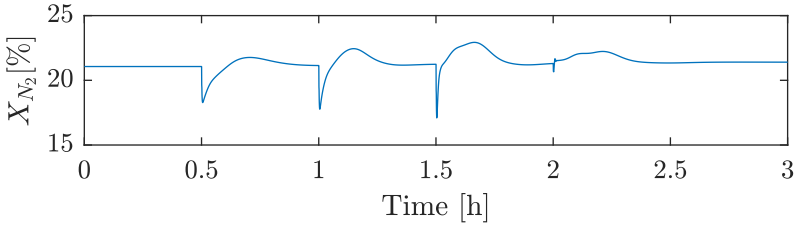

Figure 5.22: Response of conversion X_{N_2} with the optimized control structure to step changes in $\dot{n}_{makeup}$ of -20 % (t = 0.5 h), -40 % (t = 1 h), -60 % (t = 1.5 h) and -70 % (t = 2 h) from nominal value.

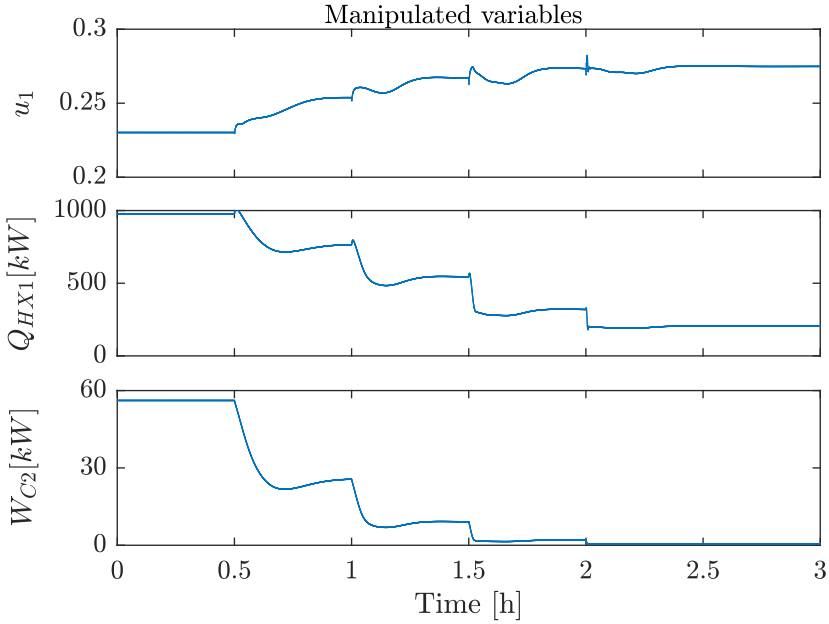

Figure 5.23: Responses of the manipulated variables of the optimized control structure to step changes in $\dot{n}_{makeup}$ of -20 % (t = 0.5 h), -40 % (t = 1 h), -60 % (t = 1.5 h) and -70 % (t = 2 h) from nominal value.

Chapter 6

Conclusions and Recommendations

Several control structures have been investigated that are able to successfully increase the flexibility of the ammonia synthesis loop with respect to load variations. Open-loop simulations demonstrated that dynamic operation can cause unwanted temperature oscillations in the ammonia converter. Two main control strategies have been investigated to avoid limit cycle behavior, which are to either: (1) move into an open-loop unstable operating region with a stabilizing control structure or (2) to keep the system at nominal open-loop stable operating conditions by keeping the pressure stable. Both pathways are able to handle a load range of 30-100 % of nominal capacity. The former strategy is regarded as less complex, since only temperatures are controlled. On the other hand, the latter strategy is considered to be more desirable since it guarantees stable operation. Another benefit of the second control strategy is that the energy efficiency performance of the synthesis loop can easily be optimized. However, open-loop stability comes at the expense of a more complex control structure with the need for more manipulated variables, since both the pressure and temperature are controlled.

6.1 Future Work

Recommendations for further work that can improve the controllability analysis is outlined below.

- Replace perfect control of T_{sep} with an actual feedback controller. Disturbances in T_{sep} may play an important role for the robustness of the control structures.
- Improve the tuning parameters of the controllers and evaluate the speed of the different control structures.
- Further simulations should be performed to compare how fast the control structures can adjust to load variations while still maintaining stable operations.
- Optimize the purge stream with respect to desirable gas composition in the loop. Currently, the purge valve has a constant valve opening, but it can be varied with load changes.
- Perform dynamic simulations that test the effect of other disturbances e.g. synthesis gas composition. In this thesis, the dynamic performance of the control structures are only evaluated based on how they are able to handle disturbances in load. However, it is important that control structures reject as many disturbances as possible.
- Conduct dynamic simulations that investigate how the control structures behave close to the steady-state optimum. As seen in previous studies, the steady-state optimal operating point is even closer to instability.

Appendix A

Data

Table A.1: Input make-up stream parameters.

Symbol	Value	Unit	Description
p	40	bar	Makup gas pressure
T	25	$°C$	Makeup gas temperature
x_{H_2}	0.7479	-	Feed mole fraction of H_2.
x_{N_2}	0.2493	-	Feed mole fraction of N_2.
x_{NH_3}	0	-	Feed mole fraction of NH_3.
x_{inert}	0.0028	-	Feed mole fraction of inert.

Table A.2: Parameters used in the reactor beds R1 and R2.

Symbol	Value	Unit	Description
$C_{p,gas}$[1]	31055	J/(kmol K)	Heat capacity of gas [1]
$C_{p,cat}$	1100	J/(kg K)	Heat capacity of catalyst [1]
-ΔH_{rx}[2]	92·10^6	J/kmol N_2	Heat of reaction [1]
V_{bed}	0.7	m^3	Volume bed reactor R1
V_{bed}	1.3	m^3	Volume bed reactor R2
ρ_{cat}	2200	kg/m^3	Catalyst bulk density [1]
R	8.314	J/(mol K)	Gas constant
ns	20	-	Number of sections

Table A.3: Parameters used in the preheater HX2.

Symbol	Value	Unit	Description
$C_{p,gas}$	31055	J/(kmol K)	Heat capacity of gas
U	536	W/(m^2 K)	Heat-transfer coefficient [1]
A	50	m^2	Heat-transfer area

Table A.4: Parameters used in the cooler HX3.

Symbol	Value	Unit	Description
$C_{p,gas}$	31055	J/(kmol K)	Heat capacity of gas
$\Delta H_{vap,NH_3}$[3]	15150·10^3	J/kmol	Heat of vaporization
Q_{HX3}	-7525248	W	Heat duty

[1] 3500 (J/kg K) · 8.8728 (kg/kmol)
[2] 2.7·10^6(J/kg NH_3)· 17.034 (kg NH_3/kmol NH_3) · 2 (kmol NH_3/kmol N_2)
[3] From Aspen HYSYS simulation at high pressure

Table A.5: Parameters used in the simple heat exchanger HX1.

Symbol	Value	Unit	Description
$C_{p,gas}$	31055	J/(kmol K)	Heat capacity of gas
Q_{HX1}	$9.7651 \cdot 10^5$	W	Heat duty

Table A.6: Parameters used in compressors C1 and C2.

Symbol	Value	Unit	Description
$C_{p,gas}$	31055	J/(kmol K)	Heat capacity of gas
η_c	0.85	W	Isentropic efficiency
R	8314	J/(kmol K)	Gas constant
W_{C1}	$4.1748 \cdot 10^5$	W	Compressor duty
W_{C2}	$5.6155 \cdot 10^4$	W	Compressor duty

Table A.7: Parameters used in the splitter.

Symbol	Value	Unit	Description
u_1	0.2302		Split ratio, quench 1
u_2	0.2659		Split ratio, quench 2

Table A.8: Parameters used in the separator S1.

Symbol	Value	Unit	Description
H_1	[-3.68607, -2.29337, -1.67010]^T	atm	Henry's law parameter [25]
H_2	[0.596736, 0.5294740, 0.440558]$^T \cdot 10^4$	atm K	Henry's law parameter [25]
H_3	[-0.642828, -0.521881, -0.482973]$^T \cdot 10^6$	atm K^2	Henry's law parameter [25]
A	-0.114397$\cdot 10^3$	atm	Antoine equation parameter [25]
B	1.24673	atm/K	Antoine Equation Parameter [25]
C	-0.352266$\cdot 10^{-2}$	atm/K^2	Antoine equation parameter [25]
D	-0.304687$\cdot 10^{-5}$	atm/K^3	Antoine equation parameter [25]
E	-0.186446$\cdot 10^{-7}$	atm/K^4	Antoine equation parameter [25]
V_{sep}	3.474	m^3	Total gas volume
R	0.08314	m^3 bar/(kmol K)	Gas constant
K_{VLV1}	6.7237$\cdot 10^{-4}$	kmol/(s $\sqrt{\text{bar}}$)	Purge valve constant
K_{HX3}	0.121	kmol/(s $\sqrt{\text{bar}}$)	Flow resistance
p_{purge}	10	bar	Purge pressure

Table A.9: Control parameters.

Symbol	Value	Unit	Description
Δt	1	s	Sampling period
$K_{p,FC}$	10^6	-	Control gain of flow controller FC
τ_{FC}	1	s	Time constant of flow controller FC
$K_{p,TC1}$	$1.38{\cdot}10^{-4}$	-	Control gain of temperature controller TC1
τ_{TC1}	0.1	s	Time constant of temperature controller TC1
$K_{p,TC3}$	837	-	Control gain of temperature controller TC3
τ_{TC3}	1	s	Time constant of temperature controller TC3
$K_{p,PC}$	$-1.4255 \cdot 10^3$	-	Control gain of pressure controller PC
τ_{PC}	396	s	Time constant of pressure controller PC
K_i	10^4	-	Integral gain of VPC

Appendix B

Nominal Process Variables

Table B.1: Nominal process variables.

Variable	Compressed makeup	Feed	Inlet R1	Outlet R2	Product	Purge
$\dot{n}$ [kmol/s]	0.0901	0.4072	0.2989	0.3661	0.0413	0.0077
p [bar]	150.2780	150.2780	150.2780	150.2780	141.1239	10.0000
T [°C]	174.1662	129.9337	368.1226	505.4485	12.5000	12.5000
x_{H_2} [-]	0.7479	0.7050	0.7050	0.6156	0.0088	0.6928
x_{N_2} [-]	0.2493	0.2398	0.2398	0.2105	0.0018	0.2371
x_{NH_3} [-]	0	0.0351	0.0351	0.1514	0.9880	0.0450
x_{inert} [-]	0.0028	0.0202	0.0202	0.0225	0.0014	0.0251

Appendix C

Model Verification of Dynamic Mass Balance

From Figure C.1 and Figure C.1, it is clear that the model with the dynamic mass balance approaches the behavior of the model with the steady-state mass balance when V_{sep} is reduced. The "pseudo-volume" of accumulated gas V_{sep} has been reduced from 3.474 m^3 in the original model to 0.5 m^3.

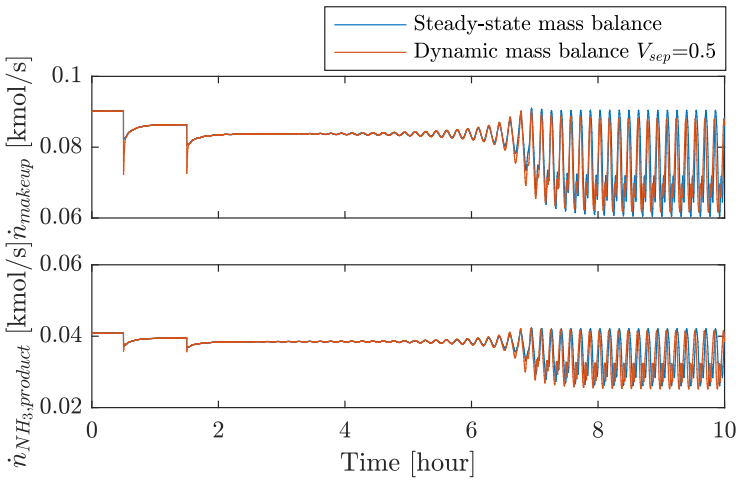

Figure C.1: Makeup flow $\dot{n}_{makeup}$ and product flow of NH_3 $\dot{n}_{NH_3,product}$ responses to step changes in W_{C1} of -20% (t=0.5 hour) and -33% (t=1.5 hour) from reference.

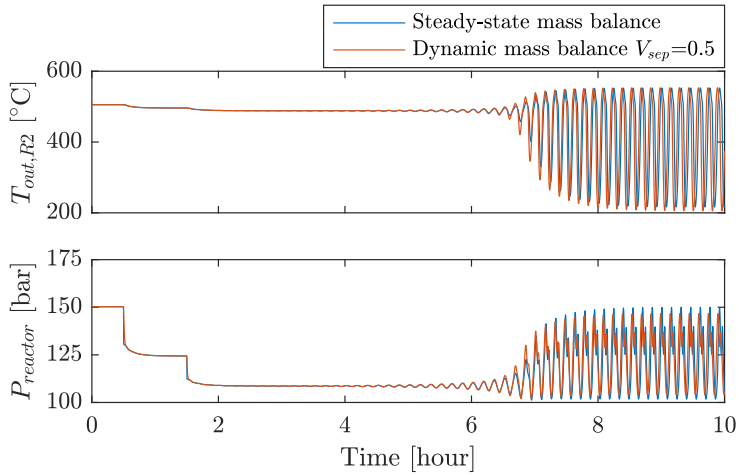

Figure C.2: Reactor outlet temperature $T_{out,R2}$ and reactor pressure $p_{reactor}$ responses to step changes in W_{C1} of -20% (t=0.5 hour) and -33% (t=1.5 hour) from reference.

Appendix D

MATLAB Code

This chapter contains the MATLAB code used in the developed model. The separate units are modeled independently and thereafter interconnected in the main code to simulate the performance of the entire loop.

D.1 Main Code

This section contains the main code which interconnects the different process units and simulates the model. The file *ammonia.m* defines the symbolic variables. First, the DAE system is solved at steady-state with the Newton rootfinder of CasADi. Next, the steady-state values are used to initialize the IDAS integrator. The input parameters can be found in the file *parAmmoniaLoop.m*. In the file *ammoniaLoop.m* the different unit operations are interconnected.

D.1.1 ammonia.m

```
% This script runs the ammonia loop function
% Clear workspace and close windows
clc; clear; close all;

% Definition of the current path folder
FileName = mfilename('fullpath');
[directory,~,~] = fileparts(FileName);
[dirmain,~,~] = fileparts(directory);


% Import of CASADI
addpath([dirmain '/Util1_Casadi'])
addpath([dirmain '/Util2_Functions'])
addpath([dirmain '/matlab2tikz/src'])
import casadi.*

% Load parameters
parAmmoniaLoop;

% Definition of decision variables
dec.reactor = false;                % Run only the reactor section
dec.wo_recycle = false;             % Run without material recycle
dec.dynamicPressure = true;         % Include dynamic pressure
                                    % in separator
dec.dynamic = true;                 % Run dynamic simulations
dec.vanHeerden = true*dec.reactor;  % Van Heerden analysis.
                                    % Note: Requires that
                                    % dec.reactor = true
dec.makeupController = true;        % Makeup flow controller
dec.tempController1 = true;         % Control inlet temperature to 1st
    bed
dec.VPC = false*dec.tempController1;% Valve position control
dec.tempController2 = true;         % Control cooler outlet temperature
dec.Tsep = 12.5*dec.tempController2;%Set separator temperature
dec.tempController3 = true;         % Control heater outlet temperature
```

```
dec.pressureController = true;      % Controller pressure
dec.plot = true;                    % Make plots

% Make-up stream variables:
% Note: The make-up flow is calculated in the model.
f = zeros(7,1);
f(1) = 0;                   % Make-up flow [kmol/s]
f(2) = 40;                  % Pressure [bar]
f(3) = 25;                  % Temperature [C]
f(4) = 0.7479;              % Molar fraction H2 [-]
f(5) = 0.2493;              % Molar fraction N2 [-]
f(6) = 0;                   % Molar fraction NH3 [-]
f(7) = 0.0028;              % Molar fraction inert [-]

% Recycle stream variables:
% Note: This stream is used if you run the loop without material
    recycle
% (dec.wo_recycle = true)
r = zeros(7,1);
r(1) = 0.3213;              % Recycle flow [kmol/s]
r(2) = 150.1169;            % Pressure [bar]
r(3) = 22.7665;             % Temperature [C]
r(4) = 0.6976;              % Molar fraction H2 [-]
r(5) = 0.2325;              % Molar fraction N2 [-]
r(6) = 0.0541;              % Molar fraction NH3 [-]
r(7) = 0.0158;              % Molar fraction inert [-]

if dec.reactor == true
    % Definition of reactor feed variables
    % Note: This stream is used if you only run the reactor section
    f = zeros(7,1);
    f(1) = 0.4073;          % Feed flow kmol/s
    f(2) = 150.2717;        % Pressure [bar]
    f(3) = 129.9333;        % Temperature [C]
    f(4) = 0.7050;          % Mass fraction H2 [-]
    f(5) = 0.2398;          % Mass fraction N2 [-]
    f(6) = 0.0351;          % Mass fraction NH3 [-]
    f(7) = 0.0202;          % Mass fraction inert [-]
```

```
    % Define number of algebraic variables in each unit
    nz.makeupComp = 0;
    nz.mix = 0;
    nz.heater = 0;
    nz.split = 21;
    nz.preheat = 20;
    nz.mix1 = 7;
    nz.reactor1 = par{ind.reactor1}.ns*6;
    nz.mix2 = 7;
    nz.reactor2 = (par{ind.reactor2}.ns-1)*6; %
    nz.cooler = 0;
    nz.separator = 0;
    nz.recComp = 0;
    nz.alpha = 0;

    % Define number of differential variables in each unit
    nx.preheat = 1;
    nx.reactor1 = par{ind.reactor1}.ns;
    nx.reactor2 = par{ind.reactor2}.ns-nx.preheat;
    nx.separator = 0;
else
    % Define number of algebraic variables in each unit
    nz.makeupComp = 8;
    nz.mix = 14;
    nz.heater = 7;
    nz.split = 21;
    nz.preheat = 20;
    nz.mix1 = 7;
    nz.reactor1 = par{ind.reactor1}.ns*(itg.k-1);
    nz.mix2 = 7;
    nz.reactor2 = (par{ind.reactor2}.ns-1)*(itg.k-1);
    nz.cooler = 7;
    nz.separator = 21;
    nz.recComp = 0;
    nz.alpha = 1;

    % Define number of differential variables in each unit
    nx.preheat = 1;
    nx.reactor1 = par{ind.reactor1}.ns;
```

```
    nx.reactor2 = par{ind.reactor2}.ns-nx.preheat;
    nx.separator = 0;

    if dec.dynamicPressure == 1
        nz.separator = 20;
        nx.separator = 1;
    end

    if dec.wo_recycle == 1
       nz.mix = 7;
       nz.recComp = 7;
    end
end

% Total number of algebraic variables:
n.z = nz.makeupComp + nz.mix +nz.heater + nz.split+nz.preheat+nz.mix1
    ...
    +nz.reactor1+nz.mix2+nz.reactor2+nz.cooler+nz.separator+nz.recComp
        ...
    + nz.alpha;
% Define algebraic variables:
z = MX.sym('z',n.z);

% Total number of differential state variables:
n.x = nx.preheat + nx.reactor1 + nx.reactor2 + nx.separator;
% Define differential state variables:
x = MX.sym('x',n.x);

% Rearrangement of makeup gas compressor variables:
z_makeupComp = z(1:nz.makeupComp);
variables{ind.makeupComp} = z_makeupComp;
nz.n = nz.makeupComp;

% Rearrangement of mix variables (recycle and make-up gas)
z_mix = z(nz.n+1:nz.n+nz.mix);
variables{ind.mix} = z_mix;
nz.n = nz.n+nz.mix;

% Rearrangement of heater variables
```

```
z_heater = z(nz.n+1:nz.n+nz.heater);
variables{ind.heater} = z_heater;
nz.n = nz.n+nz.heater;

% Rearrangement of split variables
z_split = z(nz.n+1:nz.n+nz.split);
variables{ind.split} = z_split;
nz.n = nz.n+nz.split;

% Rearrangement of preheat variables
z_preheat = z(nz.n+1:nz.n+nz.preheat);
x_preheat = x(nx.reactor1+nx.reactor2+1);
variables{ind.preheat} = [z_preheat(1:2);x_preheat;z_preheat(3:20)];
nz.n = nz.n + nz.preheat;

% Rearrangement of mixing 1 variables
z_mix1 = z(nz.n+1:nz.n+nz.mix1);
variables{ind.mix1} = z_mix1;
nz.n = nz.n +nz.mix1;

% Rearrangement of reactor bed 1 variables
z_reactor1 = z(nz.n+1:nz.n+nz.reactor1);
z_reactor1 = reshape(z_reactor1,6,nx.reactor1);
x_reactor1 = x(1:nx.reactor1);
a_reactor1 = [z_reactor1(1:2,:); x_reactor1'; z_reactor1(3:6,:)];
variables{ind.reactor1} = reshape(a_reactor1,nz.reactor1+nx.reactor1,1)
    ;
nz.n = nz.n + nz.reactor1;
nx.n = nx.reactor1;

% Rearrangement of mixing 2 variables
z_mix2 = z(nz.n+1:nz.n+nz.mix2);
variables{ind.mix2} = z_mix2;
nz.n = nz.n + nz.mix2;

% Rearrangement of reactor bed 2 variables
z_reactor2 = z(nz.n+1:nz.n+nz.reactor2);
z_reactor2 = reshape(z_reactor2,6,nx.reactor2);
x_reactor2 = x(nx.n+1:nx.n+nx.reactor2);
```

```
a_reactor2 = [z_reactor2(1:2,:); x_reactor2'; z_reactor2(3:6,:)];
variables{ind.reactor2} = reshape(a_reactor2,nz.reactor2+nx.reactor2,1)
    ;
nz.n = nz.n + nz.reactor2;
nx.n = nx.n + nx.reactor2+nx.preheat;

% Rearrangement of cooler variables
z_cooler = z(nz.n+1:nz.n+nz.cooler);
variables{ind.cooler} = z_cooler;
nz.n = nz.n + nz.cooler;

% Rearrangement of separator variables
z_separator = z(nz.n+1:nz.n+nz.separator);
x_separator = x(nx.n+1:nx.n+nx.separator);
if dec.reactor == 1
    variables{ind.separator} = [];
elseif dec.dynamicPressure == 1
    variables{ind.separator} = [z_separator(1);x_separator;z_separator
        (2:end)];
else
    variables{ind.separator} = z_separator;
end
nz.n = nz.n + nz.separator;
nx.n = nx.n + nx.separator;
alpha = z(nz.n+1:nz.n+nz.alpha);
nz.n = nz.n + nz.alpha;

% Rearrangement of recycle compressor variables
z_recComp = z(nz.n+1:nz.n+nz.recComp);
variables{ind.recComp} = z_recComp;
nz.n = nz.n + nz.recComp;

% Definition of feed disturbances
d_f = MX.sym('d_f',7);
% Definition of disturbances in unit operations
d = cell(def.sizeMat);
d_Pressure = MX.sym('d_Pressure',1);% Reactor pressure disturbance[bar]
d{ind.mix}.d_P = d_Pressure;
```

```
d_Wmake = MX.sym('d_Wmake',1);      % Makeup compressor duty
    disturbance[W]
d{ind.makeupComp}.d_W= d_Wmake;
d_Wrec = MX.sym('d_Wrec',1);        % Recycle compressor duty
    disturbance[W]
d{ind.recComp}.d_W= d_Wrec;
d_u1 = MX.sym('d_u1',1);            % Split factor u1 disturbance [-]
d{ind.split}.d_u1 = d_u1;
d_u2 = MX.sym('d_u2',1);            % Split factor u2 disturbance [-]
d{ind.split}.d_u2 = d_u2;
d_Q1 = MX.sym('d_Q1',1);            % Heater duty disturbance[W]
d{ind.heater}.d_Q1 = d_Q1;
d_Q2 = MX.sym('d_Q2',1);            % Cooler duty disturbance [W]
d{ind.cooler}.d_Q2 = d_Q2;
d_Kvlv = MX.sym('d_Kvlv',1);        % Purge valve opening disturbance
    [%]
d{ind.separator}.d_Kvlv = d_Kvlv;

% Input: feed + feed disturbance
in = f+d_f;

% Independent parameters
p = [d_f; d{ind.mix}.d_P; d{ind.makeupComp}.d_W ; d{ind.recComp}.d_W
    ;...
    d{ind.split}.d_u1;d{ind.split}.d_u2; d{ind.heater}.d_Q1; ...
    d{ind.cooler}.d_Q2; d{ind.separator}.d_Kvlv];

% Load the model
dec.startVanHeerden = false;
[alg,ode] =ammoniaLoop(in,r,variables,ind,def,par,itg,d,dec,0,0, alpha)
    ;
% Differential equations
ode_i = vertcat(ode{:});
% Algebraic equations
alg_i = vertcat(alg{:});

% Initial values
[x0,z0]=initAmmoniaLoop(dec);
w0 = [x0; z0];
```

```
% Solve at steady-state without disturbances:
g = [ode_i;alg_i];
g_root = substitute(g,p,0); %Set the independent parameters to zero
w_root = [x; z];
g_fun = Function('g_fun',{w_root},{g_root});
G = rootfinder('G','newton',g_fun);
[root] = full(G(w0));

root0.x = root(1:size(x));
root0.z = root(size(x)+1:end);
% Rearrangement steady-state solution
i = 0;
if dec.reactor == false
    root0.dynamicPressure = root0.x(end);
    root0.makeupComp = root0.z(i+1:nz.makeupComp); i = nz.makeupComp;
    if dec.wo_recycle == true
        root0.mix = root0.z(i+1:i+nz.mix); i = i+nz.mix;
    else
        root0.mix = root0.z(i+1:i+nz.mix); i = i+nz.mix;
    end
    root0.heater = root0.z(i+1:i+nz.heater); i = i+nz.heater;
end
    root0.temperature = root0.x(1:nx.reactor1+nx.reactor2+nx.preheat);
    root0.split = root0.z(i+1:i+nz.split); i = i+nz.split;
    root0.preheat = root0.z(i+1:i+nz.preheat); i = i+nz.preheat;
    root0.mix1 = root0.z(i+1:i+nz.mix1); i = i+nz.mix1;
    root0.reactor1 = root0.z(i+1:i+nz.reactor1); i = i+nz.reactor1;
    root0.mix2 = root0.z(i+1:i+nz.mix2); i = i+nz.mix2;
    root0.reactor2 = root0.z(i+1:i+nz.reactor2); i = i+nz.reactor2;
if dec.reactor == false
    root0.cooler = root0.z(i+1:i+nz.cooler); i = i+nz.cooler;
    if dec.dynamicPressure == 1
        root0.separator = root0.z(i+1:i+nz.separator); i = i + nz.
            separator;
    else
        root0.separator = root0.z(i+1:i+nz.separator); i = i + nz.
            separator;
    end
```

```
    root0.alpha = root0.z(i+1:i+nz.alpha); i = i + nz.alpha;
    if dec.wo_recycle == true
        root0.recComp = root0.z(i+1:i+nz.recComp); i = i+nz.recComp;
        % Calculate conversion
        root0.conv = (root0.mix(1)*root0.mix(4)-root0.preheat(1)*root0.
            preheat(3))/(root0.mix(1)*root0.mix(4));
        root0.conv1 = (root0.mix1(1)*root0.mix1(5)-root0.reactor1(par{
            ind.reactor1}.ns*6-5)*root0.reactor1(par{ind.reactor1}.ns
            *6-2))/(root0.mix1(1)*root0.mix1(5));
        root0.conv2 = (root0.mix2(1)*root0.mix2(5)-root0.preheat(1)*
            root0.preheat(4))/(root0.mix2(1)*root0.mix2(5));
    else
        root0.conv = (root0.mix(8)*root0.mix(12)-root0.preheat(1)*root0
            .preheat(4))/(root0.mix(8)*root0.mix(12));
        root0.conv1 = (root0.mix1(1)*root0.mix1(5)-root0.reactor1(par{
            ind.reactor1}.ns*6-5)*root0.reactor1(par{ind.reactor1}.ns
            *6-2))/(root0.mix1(1)*root0.mix1(5));
        root0.conv2 = (root0.mix2(1)*root0.mix2(5)-root0.preheat(1)*
            root0.preheat(4))/(root0.mix2(1)*root0.mix2(5));
    end
end

if dec.reactor == true
  % Calculate conversion
   root0.conv = (f(1)*f(5)-root0.preheat(1)*root0.preheat(4))/(f(1)*f
       (5));
   root0.conv1 = (f(1)*f(5)-root0.reactor1(par{ind.reactor1}.ns*6-5)*
       root0.reactor1(par{ind.reactor1}.ns*6-2))/(f(1)*f(5));
   root0.conv2 = (root0.mix2(1)*root0.mix2(5)-root0.preheat(1)*root0.
       preheat(4))/(root0.mix2(1)*root0.mix2(5));
end
%% Integration
if dec.dynamic == 1
    % Define time variables:
    t0 = 1;                  % start [s]
    ts = 1;                  % time step [s]
    tf = 5*60*60;           % final [s]
    tsamp = (t0:ts:tf)/ts;
    N = length(tsamp);
```

```
% Predefinition of solution vectors
solution.x = zeros(length(root0.x),N+1);
solution.x(:,1) = root0.x;
solution.z = zeros(length(root0.z),N+1);
solution.z(:,1) = root0.z;
solution.temperature = zeros(length(root0.temperature),N+1);
solution.temperature(:,1) = root0.temperature;
if dec.dynamicPressure == true && dec.reactor == false
    solution.dynamicPressure = zeros(length(root0.dynamicPressure),
        N+1);
    solution.dynamicPressure(:,1) = root0.dynamicPressure;
end
if dec.reactor == false
    solution.makeupComp = zeros(length(root0.makeupComp),N+1);
    solution.makeupComp(:,1) = root0.makeupComp;
    solution.mix = zeros(length(root0.mix),N+1);
    solution.mix(:,1) = root0.mix;
    solution.heater = zeros(length(root0.heater),N+1);
    solution.heater(:,1) = root0.heater;
end
solution.split = zeros(length(root0.split),N+1);
solution.split(:,1) = root0.split;
solution.preheat = zeros(length(root0.preheat),N+1);
solution.preheat(:,1) = root0.preheat;
solution.mix1 = zeros(length(root0.mix1),N+1);
solution.mix1(:,1) = root0.mix1;
solution.reactor1 = zeros(length(root0.reactor1),N+1);
solution.reactor1(:,1) = root0.reactor1;
solution.mix2 = zeros(length(root0.mix2),N+1);
solution.mix2(:,1) = root0.mix2;
solution.reactor2 = zeros(length(root0.reactor2),N+1);
solution.reactor2(:,1) = root0.reactor2;
if dec.reactor == false
    solution.cooler = zeros(length(root0.cooler),N+1);
    solution.cooler(:,1) = root0.cooler;
    solution.separator= zeros(length(root0.separator),N+1);
    solution.separator(:,1) = root0.separator;
    solution.alpha = zeros(1,N+1);
```

```
    solution.alpha(1) = root0.alpha;
end
solution.conv = zeros(1,N+1);
solution.conv(1) = root0.conv;
solution.conv1 = zeros(1,N+1);
solution.conv1(1) = root0.conv1;
solution.conv2 = zeros(1,N+1);
solution.conv2(1) = root0.conv2;

% PI flow controller FC settings:
tuning.Kc_f = 1000000;
tuning.tau_I_f = 1;
tuning.ys_f = root0.makeupComp(1)*ones(1,N+1);
tuning.e_f = zeros(1,N+1);
delta_u_f = zeros(1,N+1);

% PI temperature controller TC2 settings:
% Control inlet temperature to 1st bed
tuning.Kc_T = -1.3800e-04;
tuning.tau_I_T = 0.1;
tuning.ys_T = root0.mix1(3)*ones(1,N+1);
tuning.e_T = zeros(1,N+1);
delta_u_T = zeros(1,N+1);

% I-only Valve position controller (VPC)
tuning.Ki_VPC = 10000;
tuning.e_VPC = zeros(1,N+1);
delta_u_VPC =  zeros(1,N+1);

% PI temperature controller TC3 settings: heater outlet temperature
tuning.Kc_T3 = 837;
tuning.tau_I_T3 = 1;
tuning.ys_T3 = root0.heater(3)*ones(1,N+1);
tuning.e_T3 = zeros(1,N+1);
delta_u_T3 = zeros(1,N+1);

% PI pressure controller PC settings:
tuning.Kc_P =  -1.4255e+03;
tuning.tau_I_P = 396;
```

```
tuning.ys_P = root0.mix(2)*ones(1,N+1); %Pressure at mixing point
    setpoint
tuning.e_P = zeros(1,N+1);
delta_u_P = zeros(1,N+1);

% Define DAE system
dae = struct('x',x,'z',z,'p',p,'ode',ode_i,'alg',alg_i);

% Define integrator
opts = struct('tf',ts); %integrating with time step ts
func = integrator('func','idas',dae,opts);

% Define disturbance in feed stream
p0 = zeros(15,N+1);

tic
for j = 2:N+1
res = func('x0', solution.x(:,j-1), 'z0', solution.z(:,j-1),'p', p0
    (:,j-1));
solution.x(:,j) = full(res.xf);
solution.z(:,j) = full(res.zf);

% Rearrangement of solution:
i = 0;
solution.temperature(:,j) = solution.x(1:nx.reactor1+nx.reactor2+nx
    .preheat,j);
if dec.reactor == false
    solution.dynamicPressure(:,j) = solution.x(end,j);
    solution.makeupComp(:,j) = solution.z(i+1:nz.makeupComp,j); i =
         nz.makeupComp;
    if dec.wo_recycle == true
        solution.mix(:,j) = solution.z(i+1:i+nz.mix,j); i = i+nz.
            mix;
    else
        solution.mix(:,j) = solution.z(i+1:i+nz.mix,j); i = i+nz.
            mix;
    end
    solution.heater(:,j) = solution.z(i+1:i+nz.heater,j); i = i+nz.
        heater;
```

```
end
    solution.split(:,j) = solution.z(i+1:i+nz.split,j); i = i+nz.
        split;
    solution.preheat(:,j) = solution.z(i+1:i+nz.preheat,j); i = i+
        nz.preheat;
    solution.mix1(:,j) = solution.z(i+1:i+nz.mix1,j); i = i+nz.mix1
        ;
    solution.reactor1(:,j) = solution.z(i+1:i+nz.reactor1,j); i = i
        +nz.reactor1;
    solution.mix2(:,j) = solution.z(i+1:i+nz.mix2,j); i = i+nz.mix2
        ;
    solution.reactor2(:,j) = solution.z(i+1:i+nz.reactor2,j); i = i
        +nz.reactor2;
if dec.reactor == false
    solution.cooler(:,j) = solution.z(i+1:i+nz.cooler,j); i = i+nz.
        cooler;
    solution.conv(j) = (solution.mix(8,j)*solution.mix(12,j)-
        solution.preheat(1,j)*solution.preheat(4,j))/(solution.mix
        (8,j).*solution.mix(12,j));
    solution.conv1(j) = (solution.mix1(1,j)*solution.mix1(5,j)-
        solution.reactor1(par{ind.reactor1}.ns*6-5,j)*solution.
        reactor1(par{ind.reactor1}.ns*6-2,j))/(solution.mix1(1,j)*
        solution.mix1(5,j));
    solution.conv2(j) = (solution.mix2(1,j)*solution.mix2(5,j)-
        solution.preheat(1,j)*solution.preheat(4,j))/(solution.mix2
        (1,j)*solution.mix2(5,j));
    if dec.dynamicPressure == 1
        solution.separator(:,j) = solution.z(i+1:i+nz.separator,j);
            i = i + nz.separator;
    else
        solution.separator(:,j) = solution.z(i+1:i+nz.separator,j);
            i = i + nz.separator;
    end
    if dec.wo_recycle ==1
        solution.recComp(:,j) = solution.z(i+1:i+nz.recComp,j);
    end
end
```

```
if dec.makeupController == true
    % PI flow controller FC
    tuning.e_f(j) = tuning.ys_f(j) - solution.makeupComp(1,j);
    delta_u_f(j) = PID(tuning.Kc_f, tuning.tau_I_f,ts,tuning.e_f(j)
        ,tuning.e_f(j-1));
end
    p0(9,j+1) = p0(9,j) + delta_u_f(j);

if dec.tempController1 == true
    % PI temperature controller TC2
    tuning.e_T(j) = tuning.ys_T(j) - solution.mix1(3,j);
    delta_u_T(j) =  PID(tuning.Kc_T, tuning.tau_I_T,ts,tuning.e_T(j
        ),tuning.e_T(j-1));
end
    p0(11,j+1) = p0(11,j) + delta_u_T(j);
     % Constraints
    u = par{ind.split}.u1+p0(11,j+1)+par{ind.split}.u2+p0(12,j+1);
    u1 = par{ind.split}.u1+p0(11,j+1);
    u2 = par{ind.split}.u2+p0(12,j+1);
        if (u>1 || u1<0 || u2<0)
           p0(11,j+1) = p0(11,j);
           p0(12,j+1) = p0(12,j);
        end

% Valve position control VPC
if (u1<0.15) && dec.VPC == true
    tuning.e_VPC(j) = 0.15-u1;
    delta_u_VPC(j) = I_controller(tuning.Ki_VPC,tuning.e_VPC(j));
    p0(13,j+1) = p0(13,j) + delta_u_VPC(j);
end

if dec.tempController3 == true
   % PI temperature controller TC3
    tuning.e_T3(j) = tuning.ys_T3(j) - solution.heater(3,j);
    delta_u_T3(j) = PID(tuning.Kc_T3, tuning.tau_I_T3,ts,tuning.
        e_T3(j),tuning.e_T3(j-1));
    p0(13,j+1) = p0(13,j) + delta_u_T3(j);
end
```

```
    if dec.pressureController == true
       % PI pressure controller PC
        tuning.e_P(j) = tuning.ys_P(j) - solution.mix(2,j);
        delta_u_P(j) = PID(tuning.Kc_P, tuning.tau_I_P,ts,tuning.e_P(j)
            ,tuning.e_P(j-1));
        p0(10,j+1) = p0(10,j) + delta_u_P(j);
    end
    end
    toc
end
%% Van Heerden Analysis
if (dec.vanHeerden == true && dec.reactor == true)
   dec.startVanHeerden = true;

   % Independent reactor inlet temperature
   Ti = MX.sym('Ti',1);
   % Independent reactor outlet temperature
   To = MX.sym('To',1);

   %Load the model
   [alg,ode] = ammoniaLoop(f,r,variables,ind,def,par,scl,itg,d,dec,Ti,
       To);
   %Differential equations
   ode_temp = vertcat(ode{:});
   %Algebraic constraints
   alg_temp = vertcat(alg{:});

   % Define inlet and outlet temperature range
   Ti_list = (50:1:600)./scl_T1;
   To_list = Ti_list;
   nsamp = length(Ti_list);

   % Initial values
   [x0, z0] = initVanHeerden(f, itg);
   w0_temp = [x0; z0];

    % Define solver
    g = [ode_temp;alg_temp];
    w_root = [x;z];
```

```
    g_temp = substitute(g, p, 0);
    g_temp1 = substitute(g_temp, Ti, Ti_list(1));
    g_temp1 = substitute(g_temp1, To, To_list(1));
    g_fun = Function('g_fun',{w_root},{g_temp1});
    G = rootfinder('G','newton',g_fun);

    % Predefine solution vector
    root_temp = zeros(length(w_root),nsamp);
    Treactor_out = zeros(1,nsamp);
    Treactor_in = zeros(1,nsamp);

    % Solve at first time step
    root_temp(:,1) = full(G(w0_temp));
    Treactor_out(1) = root_temp(nx.reactor1+nx.reactor2+nx.preheat,1).*
        scl_T1; %reactor outlet temperature
    Treactor_in(1) = root_temp(n.x+nz.split+6+7+3,1).*scl_T1;
    % Solve for remaining time steps
    for j = 2:nsamp
        g_temp2 = substitute(g_temp, Ti, Ti_list(j));
        g_temp2 = substitute(g_temp2, To, To_list(j));
        g_fun = Function('g_fun',{w_root},{g_temp2});
        G = rootfinder('G','newton',g_fun);
        root_temp(:,j) = full(G(root_temp(:,j-1)));
        Treactor_out(j) = root_temp(nx.reactor1+nx.reactor2+nx.preheat,
            j).*scl_T1;
        Treactor_in(j) = root_temp(n.x+nz.split+6+7+3,j).*scl_T1;
    end
end
```

D.1.2 parAmmoniaLoop.m

```
% This scripts defines the parameters of the different unit operations
% Unit operations in the loop
name.ammoniaLoop = {'makeupcompressor';'mix';'heater';...
    'split'; 'preheat';'mix1'; 'reactorbed1'; ...
    'mix2'; 'reactorbed2';'cooler'; 'separator';'recyclecompessor'};
```

```
def.sizeMat = size(name.ammoniaLoop);
par = cell(def.sizeMat);
scl = cell(def.sizeMat);

% Index of each unit operations
ind.makeupComp = 1;
ind.mix = 2;
ind.heater = 3;
ind.split = 4;
ind.preheat = 5;
ind.mix1 = 6;
ind.reactor1 = 7;
ind.mix2 = 8;
ind.reactor2 = 9;
ind.cooler = 10;
ind.separator = 11;
ind.recComp = 12;

% Define intiger values
itg.k = 7; % process variables in each stream
itg.s = 4; % species in each stream
%% ********* Parameters of makeup compressor C1 ***************
par{ind.makeupComp}.R = 8314;                % J/(kmol K)
par{ind.makeupComp}.Cp = 31055;              % J/(kmol K)
par{ind.makeupComp}.Wcomp = 4.1748e+05;      % W
par{ind.makeupComp}.nc = 0.85;
%% ********* Parameters of heater HX1 **************************
par{ind.heater}.Cp = 31055;                  % J/(kmol K)
par{ind.heater}.Q = 9.7651e+05;              % W
%% ********* Parameters of splitter (quench flow)***************
par{ind.split}.u1 = (0.2302);
par{ind.split}.u2 = 0.1389+0.1270;
%% ************ Parameters of preheater HX2  ******************
par{ind.preheat}.U = 536;                   % W/(m2 K)
par{ind.preheat}.A = 50;                    % m2
par{ind.preheat}.Cpc = 31055;               % J/(kmol K)
par{ind.preheat}.Cph = 31055;               % J/(kmol K)
%% ********** Parameters of reactor bed R1 **********************
par{ind.reactor1}.ns = 20;                % number of sections ns
```

```
par{ind.reactor1}.stoi = [-3 -1 2 0];
par{ind.reactor1}.Vbed = 0.7;              % m3
par{ind.reactor1}.rhocat = 2200;           % kg/m3
par{ind.reactor1}.Cp = 31055;              % J/(kmol K)
par{ind.reactor1}.Cpcat = 1100;            % J/(kg K)
par{ind.reactor1}.dHrx = 91.9836e6;        % J/kmol
%kinetics:
par{ind.reactor1}.Afor = 1.79e4;
par{ind.reactor1}.Abac = 2.57e16;
par{ind.reactor1}.Eafor = 87090;          % J/mol
par{ind.reactor1}.Eabac = 198464;         % J/mol
par{ind.reactor1}.R = 8.314;              % J/(mol K)
%% ********** Parameters of Reactor bed R2 *********************
par{ind.reactor2}.ns = 20;                % number of sections ns
par{ind.reactor2}.stoi = [-3 -1 2 0];
par{ind.reactor2}.Vbed = 1.3;             % m3
par{ind.reactor2}.rhocat = 2200;          % kg/m3
par{ind.reactor2}.Cp = 31055;             % J/(kmol K)
par{ind.reactor2}.Cpcat = 1100;           % J/(kg K)
par{ind.reactor2}.dHrx = 91.9836e6;       % J/kmol
%kinetics:
par{ind.reactor2}.Afor = 1.79e4;
par{ind.reactor2}.Abac = 2.57e16;
par{ind.reactor2}.Eafor = 87090;          % J/mol
par{ind.reactor2}.Eabac = 198464;         % J/mol
par{ind.reactor2}.R = 8.314;              % J/(mol K)
%% *********** Cooler HX3 ************************************
par{ind.cooler}.Q =  (-7.8388e+06)*0.96; % W
par{ind.cooler}.Cp = 31055;               % J/(kmol K)
par{ind.cooler}.Hvap = 1.515e7;           % J/(kmol)
%% *********** Separator S1 **********************************
par{ind.separator}.Ppurge = 10;           % bar
par{ind.separator}.Kvlv = 6.7237e-04;     % kmol/(s bar)
par{ind.separator}.Khx = 0.1210;          % kmol/(s bar)
par{ind.separator}.Vtot = 3.4740;         % m3
par{ind.separator}.R = 0.08314;           % m3 bar/(kmol K)
par{ind.separator}.H1 = [-3.68607;-2.29337;-1.67010];
par{ind.separator}.H2 = [0.596736;0.5294740;0.440558]*10^4;
par{ind.separator}.H3 = [-0.642828;-0.521881;-0.482973]*10^6;
```

```
par{ind.separator}.A = -0.114397*10^3;
par{ind.separator}.B = 1.24673;
par{ind.separator}.C = -0.353366*10^(-2);
par{ind.separator}.D = -0.304684*10^(-5);
par{ind.separator}.E = 0.186446*10^(-7);
%% *********** Compressor C2 *********************************
par{ind.recComp}.R = 8314;              % J/(kmol K)
par{ind.recComp}.Cp = 31055;            % J/(kmol K)
par{ind.recComp}.Wcomp = 5.6155e+04;    % W
par{ind.recComp}.nc = 0.85;
```

D.1.3 ammoniaLoop.m

```
function [alg,ode] = ammoniaLoop(f,r,v,ind,def,par,itg,d,dec,Ti,To,
    alpha)
% This function defines the flowsheet of the ammonia synthesis loop.
%
% The input of this function is defined as
%       f:      Feed stream
%       r:      Recycle stream
%       v:      Structure of algebraic and differential state variables
%       ind:    Index of unit operations
%       def:    Definition of.
%               .sizeMat    Number of unit operations
%       par:    Structure of parameters used in unit operations
%       itg:    Intiger values
%               .k      Total number of variables per stream
%       d       Structure of disturbances in unit operations
%       dec     Decision variables
%       Ti      Reactor inlet temperature (van Heerden analysis)
%       To      Reactor outlet temperature (van Heerden analysis)

% The structures used in this function are
%       into:   Structure containing the input vector for the unit
%       operations.
```

```
% Reassignment of solution vector
into = cell(def.sizeMat);
alg = cell(def.sizeMat);
ode = cell(def.sizeMat);

% Definition of multiples of itg.k
k1 = itg.k;
k2 = 2*itg.k;
k3 = 3*itg.k;
%% ************* Make-up gas compressor C1*******************
k = ind.makeupComp;
if size(v{k},1) ~= 0
    into{k} = [v{k}(1);f(2:7);       % inlet: make-up stream
               v{k}(2:8)];           % outlet: compressed make-up
                   stream
    [alg{k},ode{k}] = compressor(into{k},par{k},itg,d{k}) ;
end
%% ************* Mix of recycle and makeup ******************
k = ind.mix;
if size(v{k},1) ~= 0
    if dec.wo_recycle == 1
        into{k} = [v{k-1}(2:8);     % inlet: compressed make-up stream
                   r;               % inlet: defined recycle stream
                   v{k}(1:k1)];     % outlet: reactor feed
    else
        into{k} = [v{k-1}(2:8);     % inlet: compressed makeup stream
                   v{k}(1:k1)       % inlet: recycle stream
                   v{k}(k1+1:k2)];  % outlet: reactor feed
    end
    [alg{k},ode{k}] = makeupMixer(into{k},itg,d{k});
end
%% ************* Simple HEX HX1 *****************************
k = ind.heater;
if size(v{k},1) ~= 0
    into{k} = [into{k-1}(k2+1:k3);  % inlet
               v{k}(1:k1)];         % outlet
    [alg{k},ode{k}] = simpleHEX(into{k},par{k},itg, d{k});
end
%% *************Split function ******************************
```

```
k = ind.split;
if size(v{k},1) ~= 0
    if dec.reactor == true
        into{k} = [f;                    % inlet: defined reactor inlet
                   v{k}(1:k1)            % outlet: quench 1
                   v{k}(k1+1:k2)         % outlet: quench 2
                   v{k}(k2+1:k3)];       % outlet: preheater cold inlet
    else
        into{k} = [v{k-1}(1:k1);         % inlet: reactor inlet
                   v{k}(1:k1)            % outlet: quench 1
                   v{k}(k1+1:k2)         % outlet: quench 2
                   v{k}(k2+1:k3)];       % outlet: preheater cold inlet
    end
    [alg{k},ode{k}] = splitter(into{k}, par{k}, itg, d{k});
end
%% ************* Preheater HX2 ******************************
k = ind.preheat;
if size(v{k},1) ~= 0
   if dec.startVanHeerden == true
       into{k} = [v{k}(1:2);To;v{k}(4:k1);  % inlet hot stream
               v{k}(k1+1:k2);               % outlet hot stream
               v{k-1}(k2+1:k3)              % inlet cold stream
               v{k}(k2+1:k3)];              % outlet cold stream
   else
        into{k} = [v{k}(1:k1);              % inlet hot stream
                   v{k}(k1+1:k2);           % outlet hot stream
                   v{k-1}(k2+1:k3)          % inlet cold stream
                   v{k}(k2+1:k3)];          % outlet cold stream
   end
    [alg{k},ode{k}] = hexNTU(into{k}, par{k}, itg);
end
 %% ************* Mixing before Reactor Bed R1 ***************
k = ind.mix1;
if size(v{k},1) ~= 0
if dec.startVanHeerden == true
                                              % inlet: preheat cold
                                                  outlet
    into{k} = [v{k-1}(k2+1:k2+2);Ti;v{k-1}(k2+4:k3);
               v{ind.split}(1:k1);           % inlet: quench 1
```

```
                v{k}(1:k1)];                    % outlet: reactor 1 inlet
elseif size(v{k},1) ~= 0
    into{k} = [v{k-1}(k2+1:k3);          % inlet: preheat cold outlet
                v{ind.split}(1:k1);       % inlet: quench 1
                v{k}(1:k1)];              % outlet: reactor 1 inlet
end
    [alg{k},ode{k}] = mixer(into{k}, itg);
end
%% ************* Reactor bed R1 ****************************
k = ind.reactor1;
if size(v{k},1) ~= 0
    into{k} = [v{k-1}(1:k1);           % inlet
                v{k}];    % internal streams + outlet stream
    [alg{k},ode{k}] = reactorBed(into{k}, par{k}, itg);
end
%% ************* Mixing before Reactor Bed R2 ***************
k = ind.mix2;
if size(v{k},1) ~= 0
    into{k} = [v{k-1}(end-k1+1:end);  % inlet: from reactor 1
                v{ind.split}(k1+1:k2); % inlet: quench 2
                v{k}(1:7)];            % outlet: reactor bed 2 inlet
    [alg{k},ode{k}] = mixer(into{k},itg);
end
%% ************* Reactor bed R2 ****************************
k = ind.reactor2;
if size(v{k},1) ~= 0
    into{k} = [v{k-1}(1:k1);          % inlet: from mixer 3
                v{k};                 % internal flows
                v{ind.preheat}(1:k1)]; % outlet flow: preheater hot
                    inlet
    [alg{k},ode{k}] = reactorBed(into{k}, par{k}, itg);
end
%% *************** Cooler HX3 ******************************
k = ind.cooler;
if size(v{k},1) ~= 0
    into{k} = [v{ind.preheat}(k1+1:k2); % inlet: preheater hot outlet
                v{k}(1:7)];              % outlet
    [alg{k},ode{k}] = cooler(into{k}, par{k}, itg,dec, alpha, d{k});
end
```

```
%% *************** Separator S1 ****************************
k = ind.separator;
if size(v{k},1) ~= 0
    into{k} = [v{k-1}(1:k1);      % inlet:  from cooler
               v{k}(1:k1);        % outlet: product stream
               v{k}(k1+1:k2);     % outlet: purge stream
               v{k}(k2+1:k3);     % outlet: stream to recycle
                   compressor
               ];
    [alg{k},ode{k}] = separator(into{k}, par{k},itg,dec, alpha, d{k});
end
%% *************** Recycle compressor C2 *******************
k = ind.recComp;
if size(v{k-1},1) ~= 0
    if dec.wo_recycle == 1
       into{k} = [v{k-1}(k2+1:k3);           % inlet
                  v{k}(1:k1)];               % outlet
    elseif size(v{ind.mix},1) ~= 0
        into{k} = [v{k-1}(k2+1:k3);           % inlet
                  v{ind.mix}(1:7)];          % outlet
    end
    [alg{k},ode{k}] = compressor(into{k}, par{k}, itg, d{k});
end
end
```

D.2 Unit Operations

This section contains the different unit operations used in the file *ammoniaLoop.m*.

D.2.1 Reactor Bed with Heat Accumulation

```
function [alg,ode] = reactorBed(v, par, itg )
% Reactor bed
% The state variables are defined as
%      n =  v(1,:):       Flow [kmol/s]
```

```
%      P =  v(2,:):       Pressure [bar]
%      T =  v(3,:):       Temperature [C]
%      x =  v(4:k1):      Composition [-]
% The necessary structures are defined as
%       par:        Parameters ot the unit, must include:
%                   ns      Number of sections (CSTRs)
%                   stoi    Stochiometric coeff vector
%                   Vbed    Volume of bed [m3]
%                   rhocat  Bulk density of catalyst [kg/m3]
%                   Cp      Heat capacity of gas [J/kmol, K]
%                   Cpcat   Heat capacity of catalyst [J/ kg cat, K]
%                   dHrx    Heat of reaction [J/ kmol ]
%                   + reactionRate parameters (see function
    reactionRate)
%       itg:        Intiger values, which should include
%                   .k      Total number of variables per stream
%                   .s      Total number of species in each stream

% The output structures are
%      ode          Differential equations
%      alg          Algebraic equations

%Reshape input
v = reshape(v,itg.k,par.ns+1);

%Rearrangement of variables
n = v(1,:);
P = v(2,:);
T = v(3,:);
x = v(4:7,:);

%Calculation of catalyst mass in each section
mcat = (par.Vbed/par.ns)*par.rhocat; %m3*kg/m3

%Predefinition of cells
dndt = cell(par.ns,1);
dPdt = cell(par.ns,1);
dxdt_H2 = cell(par.ns,1);
dxdt_N2 = cell(par.ns,1);
```

```
dxdt_NH3 = cell(par.ns,1);
dxdt_inert = cell(par.ns,1);
dTdt = cell(par.ns,1);

for j=1:par.ns
    r = reactionRate(T(j+1),P(j+1),x(1:end,j+1),par);
    dndt{j} = (n(j+1) - (n(j) + sum(par.stoi)*r*mcat));
    dPdt{j} = (P(j+1)- P(j));
    dxdt_H2{j} = (n(j+1)*x(1,j+1)-(n(j)*x(1,j)+mcat*r*par.stoi(1)));
    dxdt_N2{j} = (n(j+1)*x(2,j+1)-(n(j)*x(2,j)+mcat*r*par.stoi(2)));
    dxdt_NH3{j} = (n(j+1)*x(3,j+1)-(n(j)*x(3,j)+mcat*r*par.stoi(3)));
    dxdt_inert{j} = n(j+1)*x(4,j+1)-(n(j)*x(4,j));
    dTdt{j} = (par.Cp*(n(j)*T(j)-n(j+1)*T(j+1)) + r*mcat*par.dHrx)/(
        mcat*par.Cpcat);
end
alg = vertcat(dndt{:}, dPdt{:}, dxdt_H2{:},dxdt_N2{:},dxdt_NH3{:},
    dxdt_inert{:});
ode = vertcat(dTdt{:});
end
```

D.2.1.1 Reaction Rate

```
function r = reactionRate(T,P,x,par)
% This function calculates the reation rate of ammonia in kg NH3/kmol
    cat,s.

% The necessary input structures are defined as
%   T       Temperature of the stage [C]
%   P       Pressure of the stage    [bar]
%   x       Molar fraction of the stage [-]
%   par     Structure containing parameters for the reaction rate
    constants
%                   Afor    Arrhenius factor, forward
%                   Abac    Arrhenius factor, backward
%                   Eafor   Activation Energy, forward [J/mol]
%                   Eabac   Activation Energy, backward [J/mol]
```

```
%                   R       Gas constant [J/mol, K]

% Calculation of the reaction rate constants
k1  = par.Afor*exp(-par.Eafor./(par.R*(T+273.15))); % Forward reaction
    rate constant
k2  = par.Abac*exp(-par.Eabac./(par.R*(T+273.15))); % Backward reaction
     rate constant

pH2 = x(1)*P;
pN2 = x(2)*P;
pNH3 = x(3)*P;

% Calculation of the reaction rate and transformation of it
r = k1*pN2*pH2^1.5/pNH3 - k2*pNH3/pH2^1.5;    % [kmol N2/ m3 cat, h]
r = r/3600/par.rhocat;                        % [kmol N2/ kg cat, s]
r = 4.75*r;                                   % catalyst activity
end
```

D.2.2 Preheater

```
function [alg, ode] = hexNTU(v, par, itg )
% NTU heat exchanger

% The variables are defined as
%       v(1):       Inlet flow hot stream [kmol/s]
%       v(2):       Inlet pressure hot stream [bar]
%       v(3):       Inlet temperature hot stream  [C]
%       v(4:k1):    Inlet composition hot stream [-]

%       v(k1+1):    Outlet flow hot stream [kmol/s]
%       v(k1+2):    Outlet pressure hot stream  [bar]
%       v(k1+3):    Outlet temperature hot stream [C]
%       v(k1+4:k2): Outlet composition hot stream [-]

%       v(k2+1):    Inlet flow cold stream [kmol/s]
%       v(k2+2):    Inlet pressure cold stream [bar]
```

```
%       v(k2+3):    Inlet temperature cold stream [C]
%       v(k2+4:k3): Inlet composition cold stream [-]

%       v(k3+1):    Outlet flow cold stream [kmol/s]
%       v(k3+2):    Outlet pressure cold stream [bar]
%       v(k3+3):    Outlet temperature cold stream [C]
%       v(k3+4:k4): Outlet composition cold stream [-]

% The necessary structures are defined as
%       par:        Parameters ot the unit, must include:
%                   .U:        Heat transfer coefficient [W/m2, K]
%                   .A:        Heat transfer area [m2]
%                   .Cph:      Molar heat capacity hot stream [J/kmol,K
    ]
%                   .Cpc:      Molar heat capacity cold stream [J/kmol,
    K]

% The output structures are
%       ode          Differential equations
%       alg          Algebraic equations

% Definition of multiples of itg.k
k1 = itg.k;
k2 = 2*itg.k;
k3 = 3*itg.k;
k4 = 4*itg.k;

% Rearrangement of the variables
nin_h = v(1);
Pin_h = v(2);
Tin_h = v(3);
xin_h = v(4:itg.k);

nout_h = v(k1+1);
Pout_h = v(k1+2);
Tout_h = v(k1+3);
xout_h = v(k1+4:k2);

nin_c = v(k2+1);
```

```
Pin_c = v(k2+2);
Tin_c = v(k2+3);
xin_c = v(k2+4:k3);

nout_c = v(k3+1);
Pout_c = v(k3+2);
Tout_c = v(k3+3);
xout_c = v(k3+4:k4);

% Heat capacity ratio
Cstar = (nin_c*par.Cpc)/(nin_h*par.Cph);
% Note: the cold stream has the smallest heat capacity rate

% Number of transfer units
NTU = (par.U*par.A)/(nin_c*par.Cpc);

% Effectiveness
E = (1-exp(-NTU*(1-Cstar)))/(1-Cstar*exp(-NTU*(1-Cstar)));

% Maximum heat transfer
Qmax = nin_c*par.Cpc*(Tin_h-Tin_c);

% Actual heat transfer
Q = E*Qmax;

% Mole balance:
dndt{1} = nout_h-nin_h;
dndt{2} = nout_c-nin_c;

% Pressure balance:
dPdt{1} = Pout_h-Pin_h;
dPdt{2} = Pout_c-Pin_c;

% Energy balance:
dTdt{1} = (Q-nin_h*par.Cph*(Tin_h-Tout_h));
dTdt{2} = (Q-nin_c*par.Cpc*(Tout_c-Tin_c));

% Component balance:
dxdt{1} = xout_h-xin_h;
```

```
dxdt{2} = xout_c-xin_c;

alg = vertcat(dndt{:}, dPdt{:}, dTdt{:}, dxdt{:});
ode = [];
end
```

D.2.3 Cooler

```
function [alg, ode] = cooler(v, par,itg,dec, alpha , d )
% Cooler with condensation of ammonia and a fixed duty
% The variables are defined as
%       v(1):       Inlet flow [kmol/s]
%       v(2):       Inlet pressure [bar]
%       v(3):       Inlet temperature [C]
%       v(4:k1):    Inlet composition [-]

%       v(k1+1):    Outlet flow  [kmol/s]
%       v(k1+2):    Outlet pressure [bar]
%       v(k1+3):    Outlet temperature [C]
%       v(k1+4:k2): Outlet composition [-]

% The necessary structures are defined as
%       par:        Parameters of the unit:
%                   .Q:        Heat transfer duty [W]
%                   .Cp:       Heat capacity of gas [J/kmol,K]
%                   .Hvap      Heat of vaporization  [J/kmol]
%       itg:        Intiger values, which should include
%                   .k      Total number of variables per stream
%                   .s      Total number of species in each stream
%       dec:        Decision variable
%                   .tempController2   Activate temperature controller
%                   .dec.Tsep          Perfect control of Tsep
%       alpha       Separation ratio calculated in the separator
%       d:           Disturbances
%                   .d_Q2    Disturbance in heat duty [W]
```

```
% The output structures are
%      ode          Differential equations
%      alg          Algebraic equations

% Definition of multiples of itg.k
k1 = itg.k;

% Rearrangement of the variables
nin = v(1);
Pin = v(2);
Tin = v(3);
xin = v(4:itg.k);

nout = v(k1+1);
Pout = v(k1+2);
Tout = v(k1+3);
xout = v(k1+4:end);

% Mole balance:s
dndt = nout-nin;

% Pressure balance:
dPdt = Pin-Pout;

% Energy balance:
if dec.tempController2 == 1
   dTdt = Tout - dec.Tsep;
else
   dTdt = ((par.Q+d.d_Q2) - nin*par.Cp*(Tout-Tin)-nin*(-par.Hvap)*alpha
       );
end

% Component balance:
dxdt = xout-xin;

alg = vertcat(dndt{:}, dPdt{:}, dTdt{:}, dxdt{:});
ode = [];
end
```

D.2.4 Simple Heater

```
function [alg, ode] = simpleHEX(v, par,itg, d)
% Simple heat-exchanger
% The variables are defined as
%       v(1):       Inlet flow  [kmol/s]
%       v(2):       Inlet pressure [bar]
%       v(3):       Inlet temperature [C]
%       v(4:k1):    Inlet composition [-]

%       v(k1+1):    Outlet flow [kmol/s]
%       v(k1+2):    Outlet pressure [bar]
%       v(k1+3):    Outlet temperature [C]
%       v(k1+4:k2): Outlet composition [-]

% The necessary structures are defined as
%       par:        Parameters ot the unit, must include:
%                   .Q:        Heat duty  [W]
%                   .Cph:      Heat capacity [J/kmol,K]
%       itg:        Intiger values
%                   .k      Total number of variables per stream
%       d:           Disturbances
%                   .d_Q1    Disturbance in heat duty [W]
% The output structures are
%      ode          Differential equations
%      alg          Algebraic equations

% Definition of multiples of itg.k
k1 = itg.k;
k2 = 2*itg.k;

% Rearrangement of the variables
nin = v(1);
Pin = v(2);
Tin = v(3);
xin = v(4:itg.k);
```

```
nout = v(k1+1);
Pout = v(k1+2);
Tout = v(k1+3);
xout = v(k1+4:k2);

%Mole balance:
dndt{1} = nout-nin;

%Pressure balance:
dPdt{1} = Pout-Pin;

%Energy balance:
dTdt{1} = ((par.Q+d.d_Q1)-nin*par.Cp*(Tout-Tin));

%Component balance:
dxdt{1} = xout-xin;

alg = vertcat(dndt{:}, dPdt{:}, dTdt{:}, dxdt{:});
ode = [];
end
```

D.2.5 Separator with Mass Accumulation

```
function [alg, ode] = separator(v, par, itg ,dec, alpha, d)
% Separator
% The variables are defined as
%       v(1):       Inlet flow [kmol/s]
%       v(2):       Inlet pressure [bar]
%       v(3):       Inlet temperature [C]
%       v(4:k1):    Inlet composition [-]

%       v(k1+1):    Product flow [kmol/s]
%       v(k1+2):    Product pressure [bar]
%       v(k1+3):    Product temperature [C]
%       v(k1+4:k2): Product composition [-]
```

```
%       v(k2+1):    Purge flow [kmol/s]
%       v(k2+2):    Purge pressure [bar]
%       v(k2+3):    Purge temperature [C]
%       v(k2+4:k3): Purge composition [-]

%       v(k3+1):    Outlet flow [kmol/s]
%       v(k3+2):    Outlet pressure [bar]
%       v(k3+3):    Outlet temperature [C]
%       v(k3+4:end): Outlet composition [-]
% The necessary structures are defined as
%       par:        Parameters ot the unit, must include:
%                   .Kvlv      Purge valve opening [-]
%                   .Khx       Pressure resistance [kmol/bar]
%                   .Vtot      Total volume of loop [m3]
%                   .R         Gas constant [m3 bar/kmol, K]
%                   .A         Antoine Equation Parameter
%                   .B         Antoine Equation Parameter
%                   .C         Antoine Equation Parameter
%                   .H1        Henry's constant polynomial
%                   .H2        Henry's constant polynomial
%                   .H3        Henry's constant polynomial
%       itg:        Intiger values
%                   .k      Total number of variables per stream
%       dec:        Decision variable
%                   .dynamicPressure
%       alpha       Separation ratio
%       d:           Disturbances
%                   .d_Kvlv    Disturbance in purge valve opening



% The output structures are
%      ode          Differential equations
%      alg          Algebraic equations

% Definition of multiples of itg.k
k1 = itg.k;
k2 = 2*itg.k;
k3 = 3*itg.k;
```

```
% Rearrangement of the variables
nin = v(1);
Pin = v(2);
Tin = v(3)+273.15;
xin = v(4:itg.k);

nprod = v(k1+1);
Pprod = v(k1+2);
Tprod = v(k1+3)+273.15;
xprod = v(k1+4:k2);

npurge = v(k2+1);
Ppurge = v(k2+2);
Tpurge = v(k2+3)+273.15;
xpurge = v(k2+4:k3);

nout = v(k3+1);
Pout = v(k3+2);
Tout = v(k3+3)+273.15;
xout = v(k3+4:end);

% Raoult's law for NH3
P_NH3 = (1.01325)*(par.A + par.B*Tin + par.C*Tin^2 + par.D*Tin^3 + par.
    E*Tin^4);
% Henry's law for H2, N2 and inert:
H = (1.01325)*exp(par.H1 + par.H2/Tin + par.H3/Tin^2);
% Calculation of equilibrium constant:
Keq = [H(1); H(2); P_NH3; H(3)];

% Mole balance:
dndt{1} = nin*xin - nprod*xprod - (nin-nprod)*xpurge;
dndt{2} = npurge - (par.Kvlv+d.d_Kvlv)*sqrt(Pprod-Ppurge);
dndt{3} = alpha - nprod/(nin*xin(3));

% Pressure balance:
dPdt{1} = Ppurge - par.Ppurge;
dPdt{2} = Pout - Pprod;
dPdt{3} = nin-par.Khx*sqrt(Pin-Pprod);
```

```
if dec.dynamicPressure == 1
    ode =(((par.R*Tin)/par.Vtot)...
        *(par.Khx*sqrt(Pin-Pprod)-nprod-npurge-nout));
else
    dndt{4} = nout - (nin-nprod-npurge);
    ode = [];
end

% Energy balance
dTdt{1} = Tprod - Tin;
dTdt{2} = Tpurge - Tin;
dTdt{3} = Tout - Tin;

% Component balance:
dxdt{1} = 1 - sum(xprod);
dxdt{2} = xout - xpurge ;
dxdt{3} = xpurge*Pprod - Keq.*xprod;

alg = vertcat(dndt{:}, dPdt{:}, dTdt{:}, dxdt{:});
end
```

D.2.6 Compressor

```
function [alg, ode] = compressor(v, par,itg, d )
% Piston compressor
% The variables are defined as
%       v(1):       Inlet flow [kmol/s]
%       v(2):       Inlet pressure [bar]
%       v(3):       Inlet temperature [C]
%       v(4:k1):    Inlet composition [-]

%       v(k1+1):    Outlet flow [kmol/s]
%       v(k1+2):    Outlet pressure [bar]
%       v(k1+3):    Outlet temperature [C]
%       v(k1+4:k2): Outlet composition [-]
```

```
% The necessary input structures are defined as
%       par:        Parameters of unit
%                   .Cp     Heat capacity [J/kmol]
%                   .R      Gas constant [J/kmol K]
%                   .W      Compressor duty [W]
%                   .nc     Compressor efficiency [-]

%       itg:        Intiger values
%                   .k      Total number of variables per stream

%       d:           Disturbances
%                   .d_W    Disturbance in compressor duty [W]

% The output structures are
%      ode          Differential equations
%      alg          Algebraic equations



% Definition of multiples of itg.k
k1 = itg.k;

% Rearrangement and scaling of variables
nin = v(1);
Pin = v(2);
Tin = v(3)+273.15;
xin = v(4:itg.k);

nout = v(k1+1);
Pout = v(k1+2);
Tout = v(k1+3)+273.15;
xout = v(k1+4:end);

% Mole balance:
dndt = nout-nin;

% Pressure balance:
```

```
dPdt = ((par.Wcomp+d.d_W)*par.nc - nin*par.Cp*Tin*((Pout/Pin)^(par.R/
    par.Cp)-1));

% Energy balance:
dTdt = (Tout - Tin*(1+((Pout/Pin)^(par.R/par.Cp)-1)/par.nc));

% Component balance:
dxdt = xout - xin;

alg = vertcat(dndt{:}, dPdt{:}, dTdt{:}, dxdt{:});
ode = [];
end
```

D.2.7 Flow Splitter (quench flows)

```
function [Ceq,ddt] = splitter(v, par, itg, d )
% This function split one stream into 3 streams
% The variables are defined as
%       v(1):           Inlet flow [kmol/s]
%       v(2):           Inlet pressure [bar]
%       v(3):           Inlet temperature [C]
%       v(4:k1):        Inlet composition [-]

%       v(k1+1):        Outlet flow [kmol/s]
%       v(k1+2):        Outlet pressure [bar]
%       v(k1+3):        Outlet temperature [C]
%       v(k1+4:k2):     Outlet composition [-]

%       v(k2+1):        Outlet flow [kmol/s]
%       v(k2+2):        Outlet pressure [bar]
%       v(k2+3):        Outlet temperature [C]
%       v(k2+4:k3):     Outlet composition [-]

%       v(k3+1):        Outlet flow [kmol/s]
%       v(k3+2):        Outlet pressure  [bar]
%       v(k3+3):        Outlet temperature [C]
```

```
%       v(k3+4:k4):    Outlet composition [-]

% The necessary structures are defined as
%       par:        Parameters of the unit, must include:
%                   u1      split ratio of nout1
%                   u2      split ratio of nout2
%       scl:        Scaling variables
%       itg:        Intiger values, which should include
%                   .k      Total number of variables per stream
%                   .s      Total number of species in each stream
%       d:           Disturbances
%                   .d_u1    Disturbance in u1 [-]
%                   .d_u2    Disturbance in u2 [-]
% The output structures are
%      ode          Differential equations
%      alg          Algebraic equations

% Definition of multiples of itg.k
k1 = itg.k;
k2 = 2*k1;
k3 = 3*k1;
k4 = 4*k1;

% Rearrangement of variables
nin = v(1);
Pin = v(2);
Tin = v(3);
xin = v(4:itg.k);

nout = v(k1+1);
Pout = v(k1+2);
Tout = v(k1+3);
xout = v(k1+4:k2);

nout2 = v(k2+1);
Pout2 = v(k2+2);
Tout2 = v(k2+3);
xout2 = v(k2+4:k3);
```

```
nout3 = v(k3+1);
Pout3 = v(k3+2);
Tout3 = v(k3+3);
xout3 = v(k3+4:k4);

u1 = par.u1+d.d_u1;
u2 = par.u2+d.d_u2;

% Mole balance
dNdt{1} = nout - u1*nin;
dNdt{2} = nout2 - u2*nin;
dNdt{3} = nout3 - (1-u1-u2)*nin;
% Pressure neutrality
dPdt{1} = (Pout-Pin);
dPdt{2} = (Pout2-Pin);
dPdt{3} = (Pout3-Pin);
% Temperature neutrality
dTdt{1} = (Tout-Tin);
dTdt{2} = (Tout2-Tin);
dTdt{3} = (Tout3-Tin);
% Composition balance
dxdt{1} = xout-xin;
dxdt{2} = xout2-xin;
dxdt{3} = xout3-xin;

Ceq = vertcat(dNdt{:}, dPdt{:}, dTdt{:}, dxdt{:});
ddt = [];
end
```

D.2.8 Flow Mixer

```
function [alg,ode] = mixer(v, itg )
% This function mix two streams into one stream
% The state variables are defined as
%       v(1):          Inlet flow stream [kmol/s]
%       v(2):          Inlet pressure stream [bar]
```

```
%       v(3):           Inlet temperature stream [C]
%       v(4:k1):        Inlet composition stream [-]

%       v(k1+1):        Inlet flow stream [kmol/s]
%       v(k1+2):        Inlet pressure stream [bar]
%       v(k1+3):        Inlet temperature stream [C]
%       v(k1+4:k2):     Inlet composition stream [-]

%       v(k2+1):        Outlet flow stream [kmol/s]
%       v(k2+2):        Outlet pressure stream [bar]
%       v(k2+3):        Outlet temperature stream [C]
%       v(k2+4:end):    Outlet composition stream [-]
% The necessary input structures are defined as
%       itg:         Intiger values, which should include
%                    .k      Total number of variables per stream
% The output structures are
%       ode           Differential equations
%       alg           Algebraic equations

% Definition of multiples of itg.k
k1 = itg.k;
k2 = 2*k1;

% Rearrangement of variables
nin1 = v(1);
Pin1 = v(2);
Tin1 = v(3);
xin1 = v(4:itg.k);

nin2 = v(k1+1);
Pin2 = v(k1+2);
Tin2 = v(k1+3);
xin2 = v(k1+4:k2);

nout = v(k2+1);
Pout = v(k2+2);
Tout = v(k2+3);
xout = v(k2+4:end);
```

```
% Mole fractions:
d_nin1 = nin1/(nout); %stream 1/total stream
d_nin2 = nin2/(nout); %stream 2/total stream

% Mole balance
dndt = nout - (nin1+nin2);
% Pressure neutrality
dPdt = Pout - Pin1;
% Energy balance
dTdt = Tout - (d_nin1*Tin1+ d_nin2*Tin2);
% Component balance
dxdt = xout - (d_nin1*xin1+ d_nin2*xin2);

alg = [dndt; dPdt ; dTdt; dxdt];
ode = [];

end
```

```
function [alg,ode] = makeupMixer(v,itg,d)
% This function mix two streams into one stream
% The variables are defined as
%       v(1):           Inlet flow stream [kmol/s]
%       v(2):           Inlet pressure stream  [bar]
%       v(3):           Inlet temperature stream [C]
%       v(4:k1):        Inlet composition stream [-]

%       v(k1+1):        Inlet flow stream [kmol/s]
%       v(k1+2):        Inlet pressure stream [bar]
%       v(k1+3):        Inlet temperature stream [C]
%       v(k1+4:k2):     Inlet composition stream [-]

%       v(k2+1):        Outlet flow stream [kmol/s]
%       v(k2+2):        Outlet pressure stream [bar]
%       v(k2+3):        Outlet temperature stream [C]
%       v(k2+4:end):    Outlet composition stream [-]
% The necessary input structures are defined as
%       itg:         Intiger values
```

```
%                   .k      Total number of variables per stream
%       d           Disturbances
%                   .d_P    Pressure disturbance
% The output structures are
%       ode         Differential equations
%       alg         Algebraic equations


% Definition of multiples of itg.k
k1 = itg.k;
k2 = 2*k1;

% Rearrangement of variables
nin1 = v(1);
Pin1 = v(2);
Tin1 = v(3)+273.15;
xin1 = v(4:itg.k);

nin2 = v(k1+1);
Pin2 = v(k1+2);
Tin2 = v(k1+3)+273.15;
xin2 = v(k1+4:k2);

nout = v(k2+1);
Pout = v(k2+2);
Tout = v(k2+3)+273.15;
xout = v(k2+4:end);

% Mole fractions:
d_nin1 = nin1/(nout); %stream 1/total stream
d_nin2 = nin2/(nout); %stream 2/total stream

% Mole balance:
dndt = nout - (nin1+nin2);

% Energy balance:
dTdt = Tout - (d_nin1*Tin1+ d_nin2*Tin2);

% Component balance:
```

```
dxdt = (xout - (d_nin1*xin1+ d_nin2*xin2));

% Pressure neutrality:
dPdt{1} = Pout - (Pin1+d.d_P);
dPdt{2} = Pout - (Pin2+d.d_P);

alg = vertcat(dndt, dPdt{:} , dTdt, dxdt{:});
ode = [];
end
```

References

[1] J. C. Morud and S. Skogestad, "Analysis of instability in an industrial ammonia reactor," *AIChE Journal*, vol. 44, no. 4, pp. 888–895, 1998.

[2] M. Reese, C. Marquart, M. Malmali, K. Wagner, E. Buchanan, A. McCormick, and E. L. Cussler, "Performance of a small-scale haber process," *Industrial & Engineering Chemistry Research*, vol. 55, no. 13, pp. 3742–3750, 2016.

[3] C. Van Heerden, "Autothermic processes," *Industrial & Engineering Chemistry*, vol. 45, no. 6, pp. 1242–1247, 1953.

[4] A. D. Stephens and R. Richards, "Steady state and dynamic analysis of an ammonia synthesis plant," *Automatica*, vol. 9, no. 1, pp. 65–78, 1973.

[5] L. Naess, A. Mjaavatten, and J.-O. Li, "Using dynamic process simulation from conception to normal operation of process plants," *Computers & chemical engineering*, vol. 17, no. 5-6, pp. 585–600, 1993.

[6] K. Rabchuk, B. Lie, A. Mjaavatten, and V. Siepmann, "Stability map for ammonia synthesis reactors," in *Proceedings of the 55th Conference on Simulation and Modelling (SIMS 55), Modelling, Simulation and Optimization, 21-22 October 2014, Aalborg, Denmark*, Linköping University Electronic Press, 2014, pp. 159–166.

[7] K. Rabchuk, "Stability map for ammonia synthesis reactors," Master's thesis, Faculty of Technology, Telemark University College, Norway, 2014.

[8] A. Jinasena, B. Lie, and B. Glemmestad, "Dynamic model of an ammonia synthesis reactor based on open information," 2016.

[9] A. Jinasena, "Model of ammonia synthesis reactor for control studies," Master's thesis, University College of Southeast Norway, Faculty of Technology, 2016.

[10] M. Rovaglio, D. Manca, and F. Cortese, "A reliable control for the ammonia loop facing limit-cycle and snowball effects," *AIChE journal*, vol. 50, no. 6, pp. 1229–1241, 2004.

[11] A. Araújo and S. Skogestad, "Control structure design for the ammonia synthesis process," *Computers & Chemical Engineering*, vol. 32, no. 12, pp. 2920–2932, 2008.

[12] C. Zhang, S. Vasudevan, and G. Rangaiah, "Plantwide control system design and performance evaluation for ammonia synthesis process," *Industrial & Engineering Chemistry Research*, vol. 49, no. 24, pp. 12 538–12 547, 2010.

[13] W. L. Luyben, "Plantwide control of a coupled reformer/ammonia process," *Chemical Engineering Research and Design*, 2018.

[14] J. Straus and S. Skogestad, "Economic nmpc for heat-integrated chemical reactors," in *Process Control (PC), 2017 21st International Conference on*, IEEE, 2017, pp. 309–314.

[15] J. A. E. Andersson, J. Gillis, G. Horn, J. B. Rawlings, and M. Diehl, "CasADi – A software framework for nonlinear optimization and optimal control," *Mathematical Programming Computation*, 2018.

[16] A. C. Hindmarsh, P. N. Brown, K. E. Grant, S. L. Lee, R. Serban, D. E. Shumaker, and C. S. Woodward, "Sundials: Suite of nonlinear and differential/algebraic

equation solvers," *ACM Trans. Math. Softw.*, vol. 31, no. 3, pp. 363–396, Sep. 2005.

[17] M. Appl, "Ammonia," *Ullmann's encyclopedia of industrial chemistry*, 2006.

[18] J. R. Jennings, *Catalytic ammonia synthesis: fundamentals and practice*. Springer Science & Business Media, 2013.

[19] H. Liu, *Ammonia synthesis catalysts: innovation and practice*. World Scientific, 2013.

[20] R. Schlögl, *Ammonia synthesis*. Wiley Online Library, 2008.

[21] G. F. Froment, K. B. Bischoff, and J. De Wilde, *Chemical Reactor-Analysis and Design*. 2011.

[22] A. Nielsen, "Ammonia synthesis: Exploratory and applied research," *Catalysis Reviews—Science and Engineering*, vol. 23, no. 1-2, pp. 17–51, 1981.

[23] S. Skogestad, *Chemical and energy process engineering*. CRC press, 2008.

[24] K.-i. Aika, L. Christiansen, I. Dybkjaer, J. Hansen, P. H. Nielsen, A. Nielsen, P. Stoltze, and K. Tamaru, *Ammonia: catalysis and manufacture*. Springer Science & Business Media, 2012.

[25] C. G. Alesandrini, S. Lynn, and J. M. Prausnitz, "Calculation of vapor-liquid equilibria for the system nh3-n2-h2-ar-ch4," *Industrial & Engineering Chemistry Process Design and Development*, vol. 11, no. 2, pp. 253–259, 1972.

[26] C. J. Geankoplis, *Transport processes and separation process principles:(includes unit operations)*. Prentice Hall Professional Technical Reference, 2003.

[27] E. Avallone, I. Baumeister, and A. Sadegh, *Marks' Standard Handbook for Mechanical Engineers, Tenth Edition*. New York: McGraw-Hill, 1998.

[28] D. E. Seborg, D. A. Mellichamp, T. F. Edgar, and F. J. Doyle III, *Process dynamics and control*. John Wiley & Sons, 2010.